Contributions of Upper Mantle Rheology, Afterslip and Poroelasticity to the Viscoelastic Postseismic Deformation of the 2011 Tohoku Earthquake

Yan Hu

Roland Bürgmann (UC Berkeley)

Jeff Freymueller (UA Fairbanks)

Paramesh Banerjee (NTU, Singapore)

Naoki Uchida and Toru Matsuzawa (Tohoku University, Japan)

Kelin Wang (PGC&UVic, Canada)

CIG, 06/25/2014

Outline

1. Background of Earthquake Cycle Deformation
2. Finite Element Model of 2011 Tohoku Earthquake
3. Systematic Tests on Rheological Properties
4. Three-dimensional Heterogeneity of Upper Mantle Rheology
    - Subduction of the Philippine Sea plate
    - Weak lower crust beneath the arc
    - Weak asthenosphere beneath the oceanic lithosphere
5. Poroelastic Rebound of the Top Crust

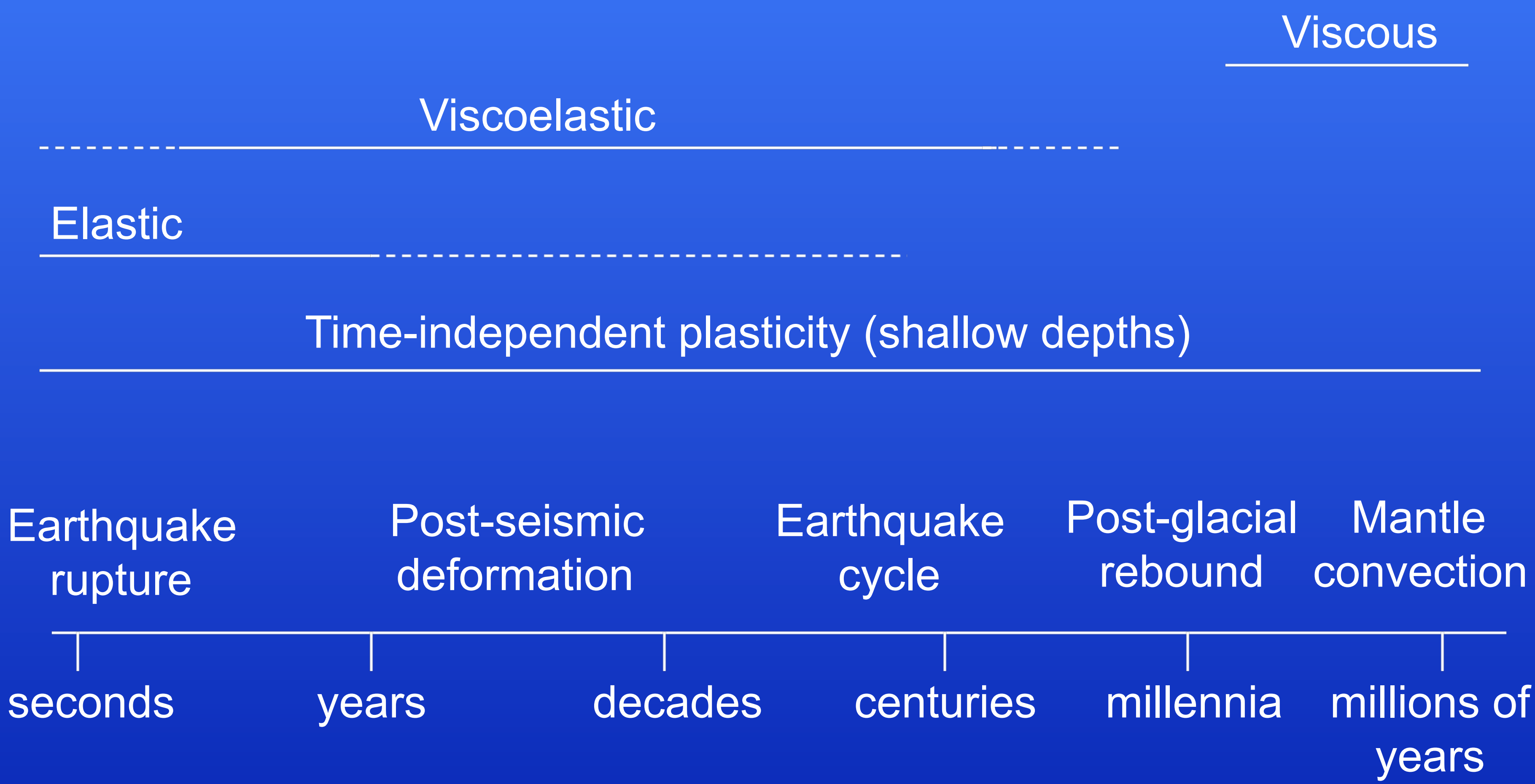
Viscous
Viscoelastic
Elastic
Time-independent plasticity (shallow depths)
Earthquake rupture
Post-seismic deformation
Earthquake cycle
Post-glacial rebound
Mantle convection
seconds
years
decades
centuries
millennia
millions of years

Japan and Sumatra: shortly after a great earthquake

All sites move seaward

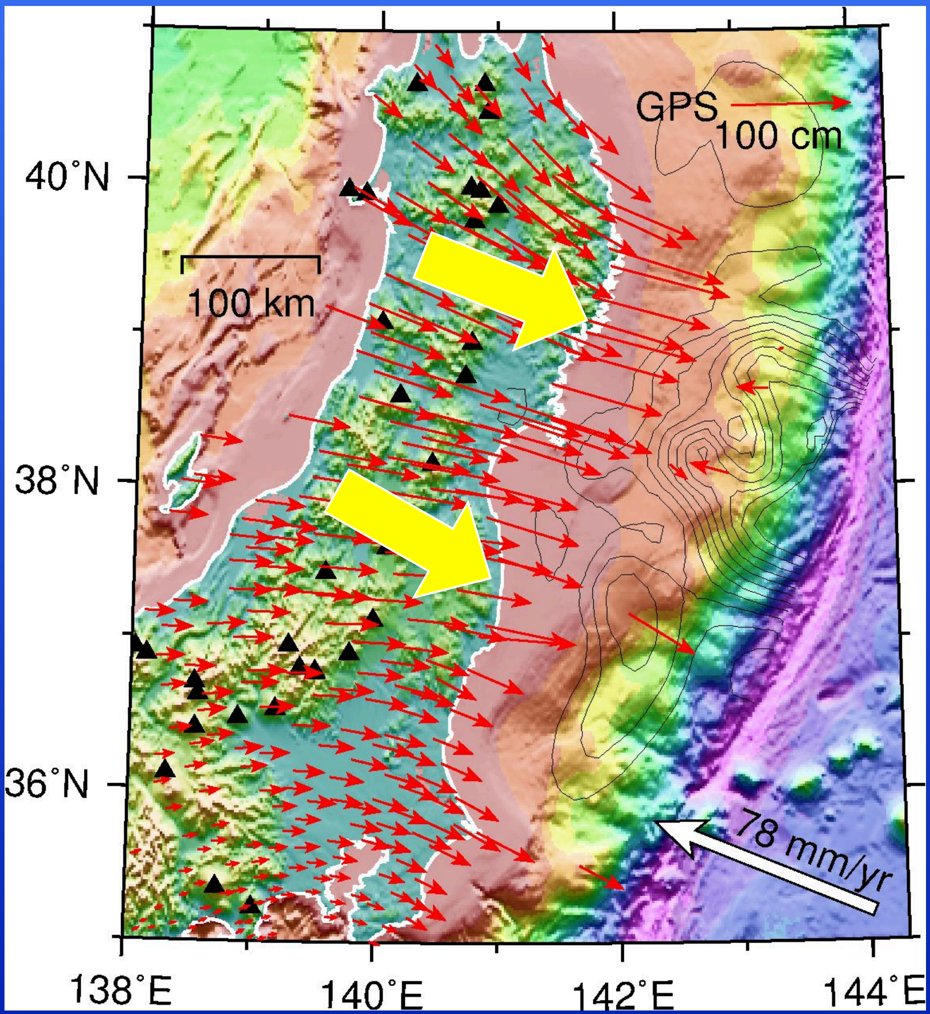

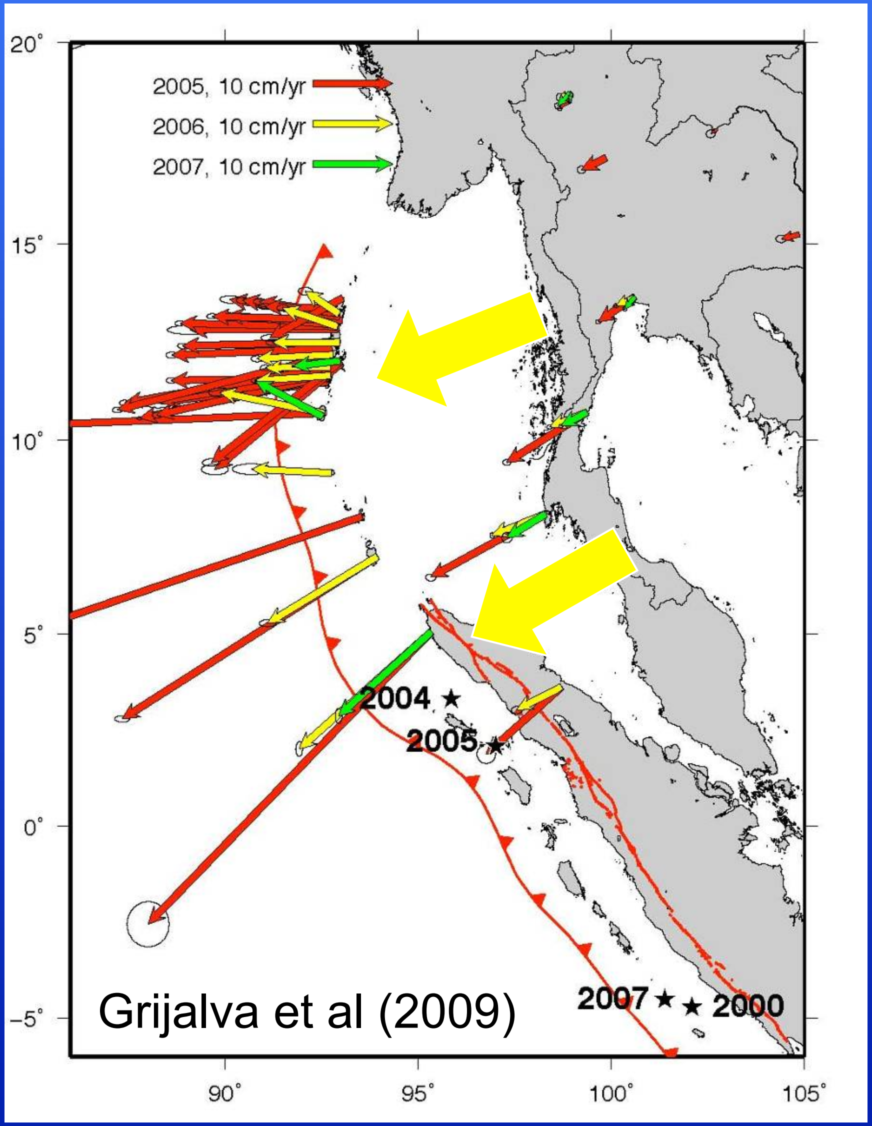

Alaska and Chile: ~ 40 years after a great earthquake:

Opposing motion of coastal and inland sites

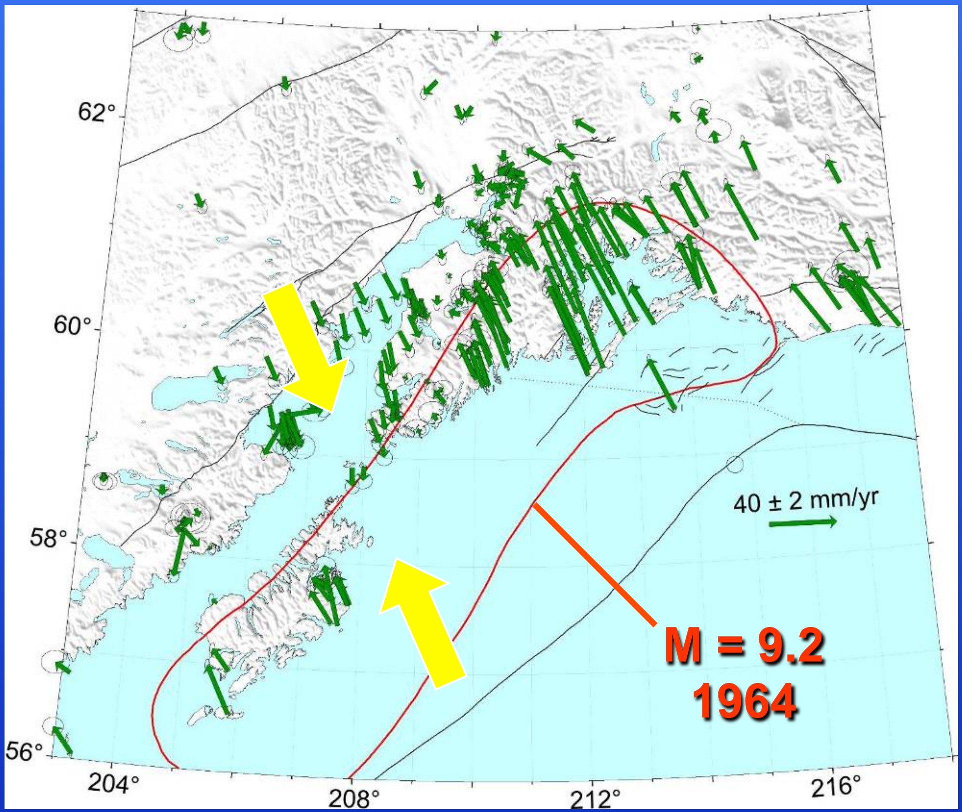

Freymueller et al. (2009)

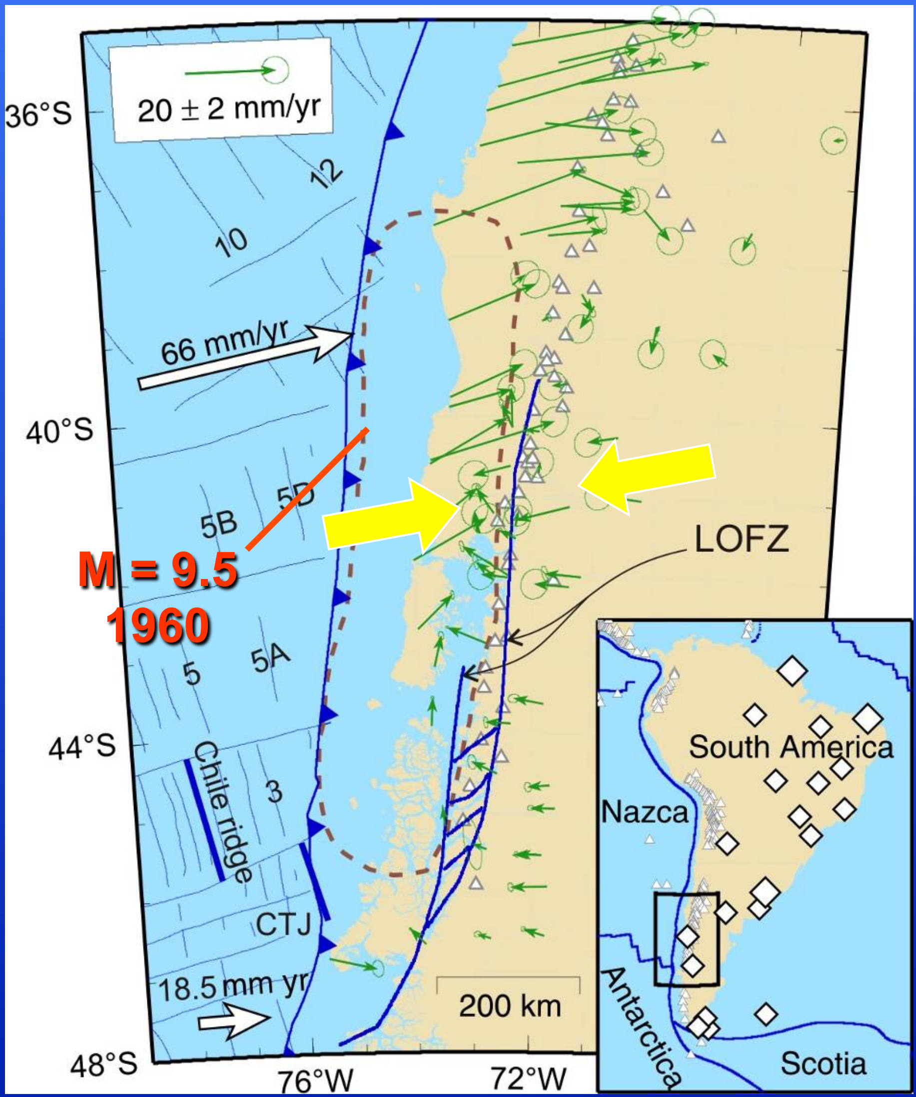

Wang et al. (2007)

Cascadia: ~ 300 years after a M ~ 9 earthquake:

All sites move landward

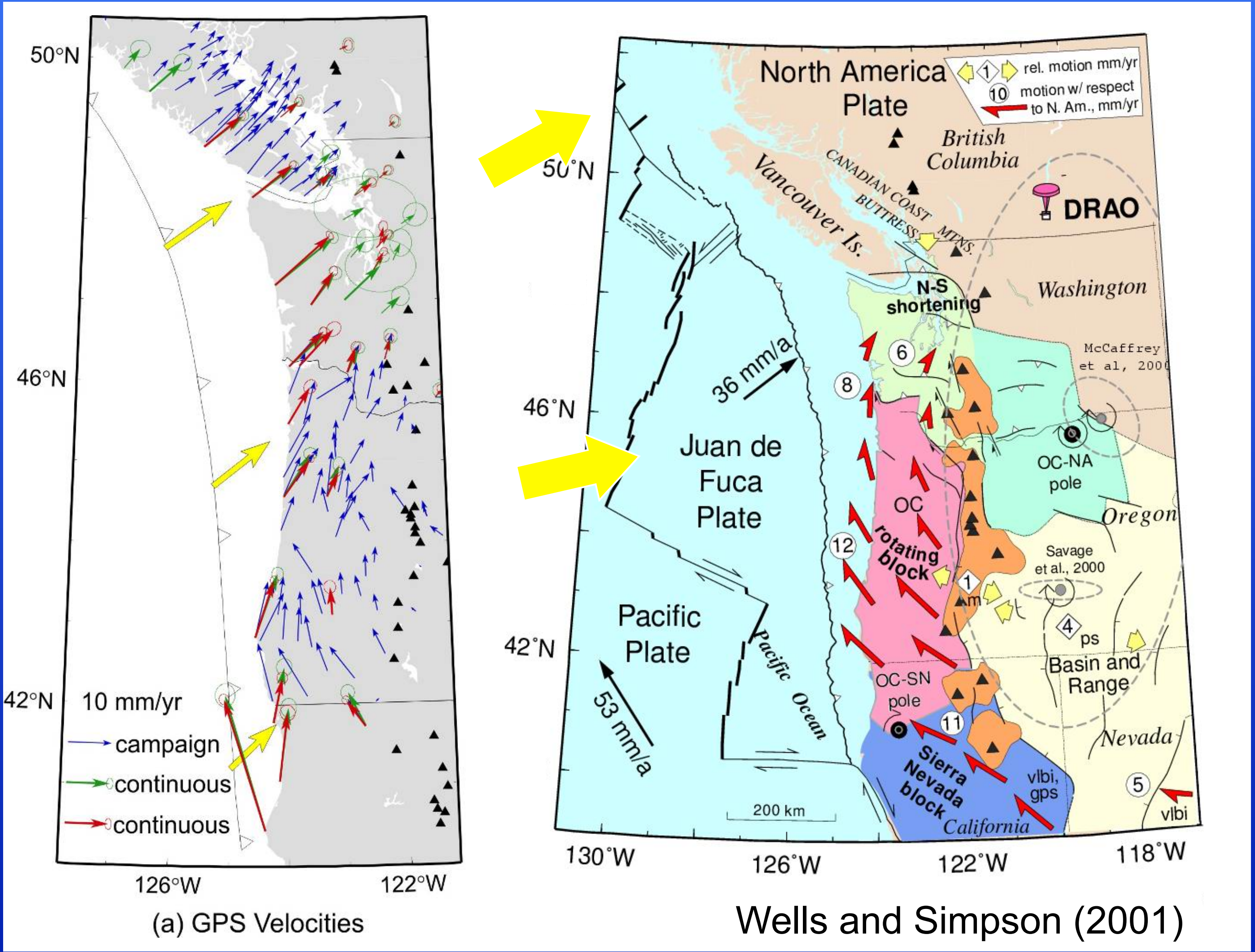

Wells and Simpson (2001)

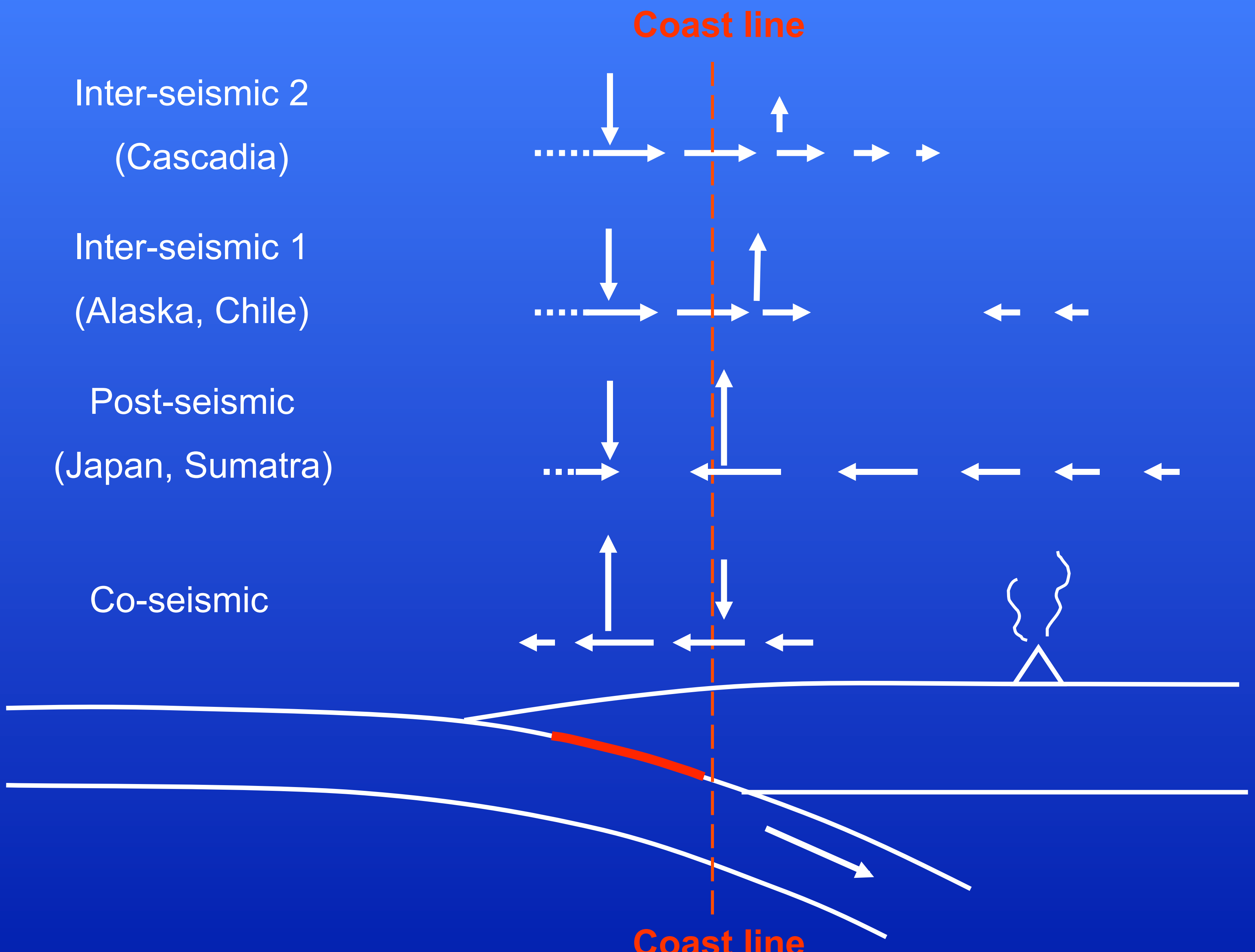
Coast line
Inter-seismic 2
(Cascadia)
Inter-seismic 1
(Alaska, Chile)
Post-seismic
(Japan, Sumatra)
Co-seismic
Coast line

Processes After a Great Earthquake

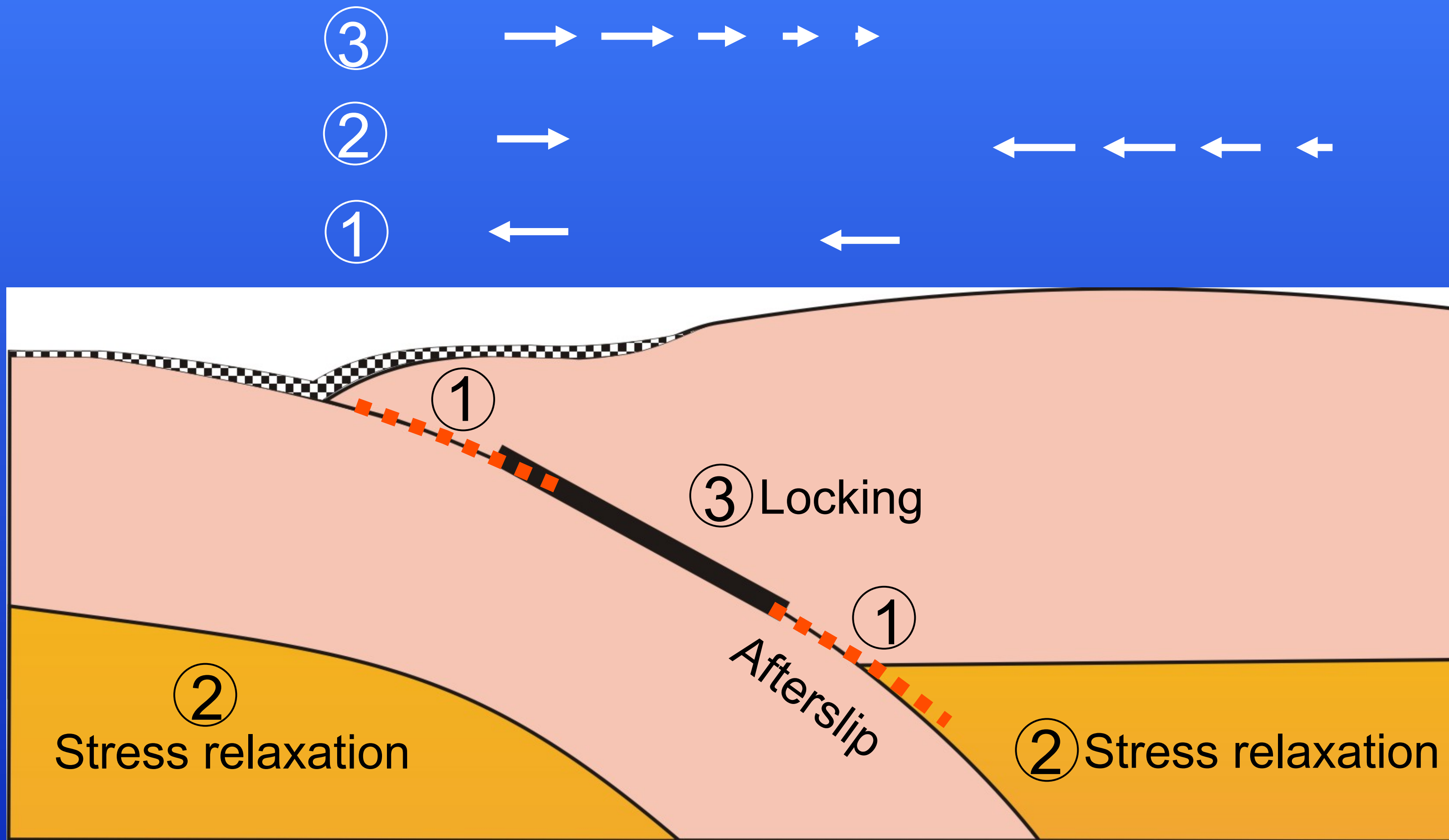

Earthquake Cycle = Rupture + ① + ② + ③

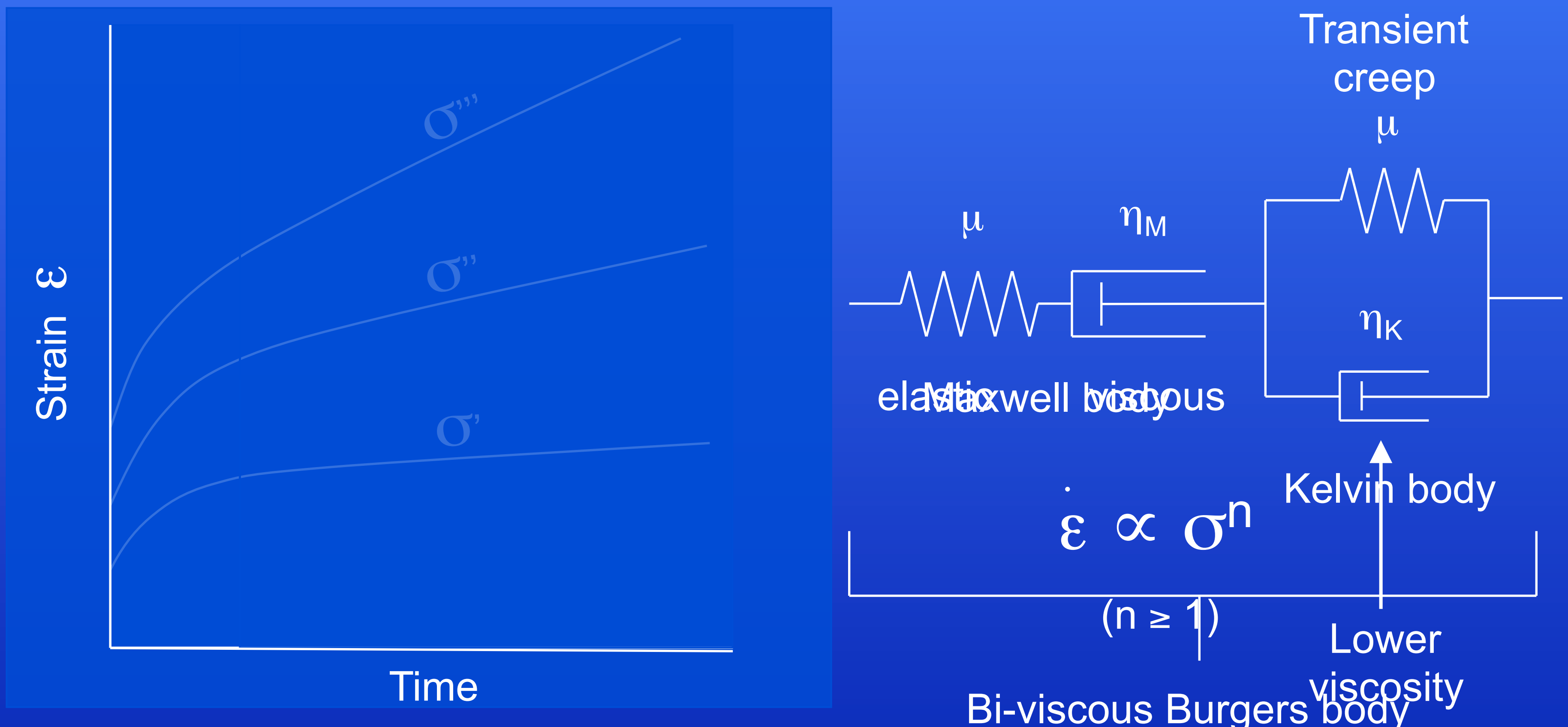
Strain ε
Time
σ'''
σ''
σ'
Transient
creep
μ
μ
ηM
ηK
elastic
Maxwell body
viscous
Kelvin body
ε̇ ∝ σn
(n ≥ 1)
Lower
viscosity
Bi-viscous Burgers body

Postseismic Deformation Following the 2011 Tohoku Earthquake

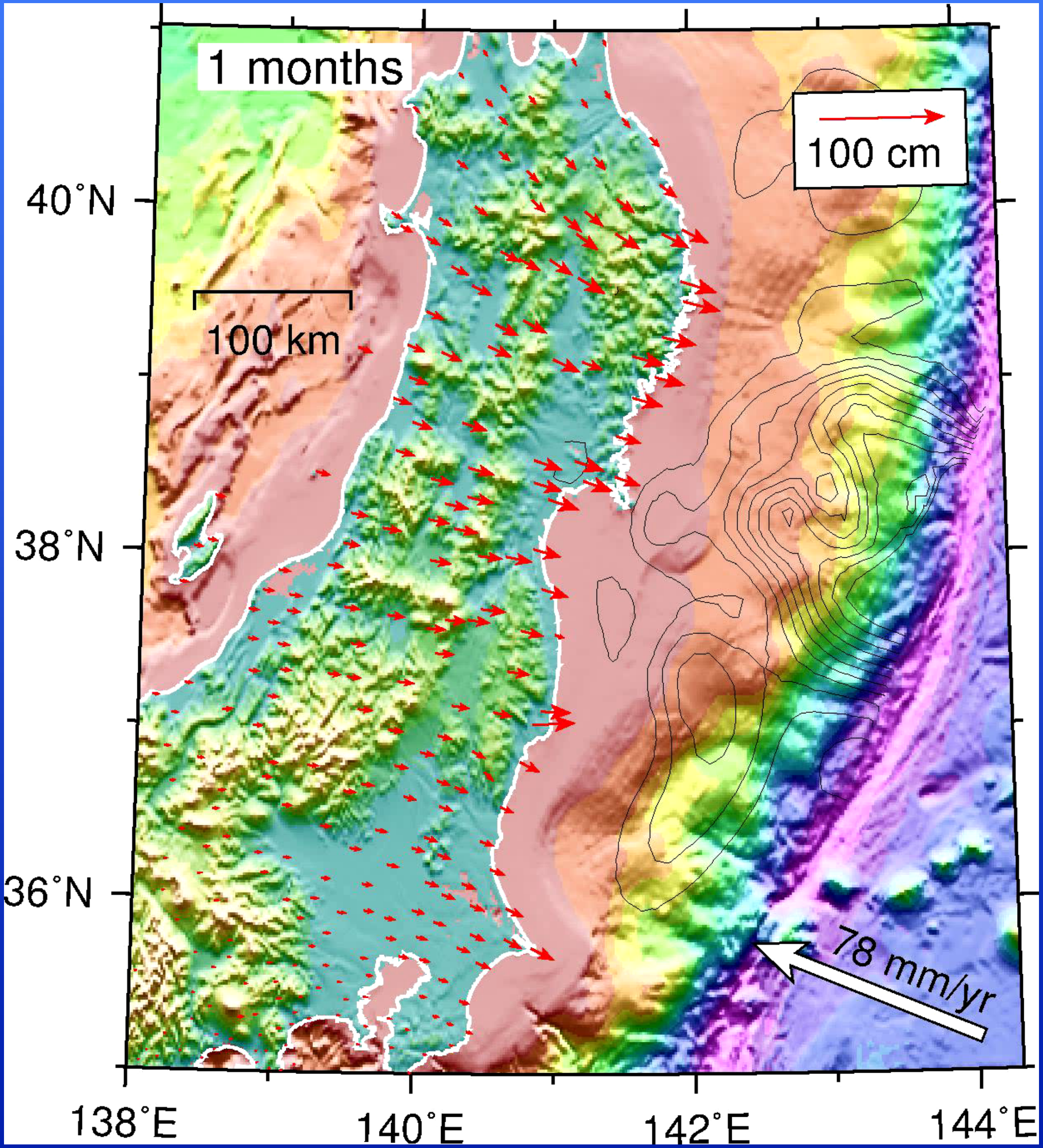

Postseismic Deformation Following the 2011 Tohoku Earthquake

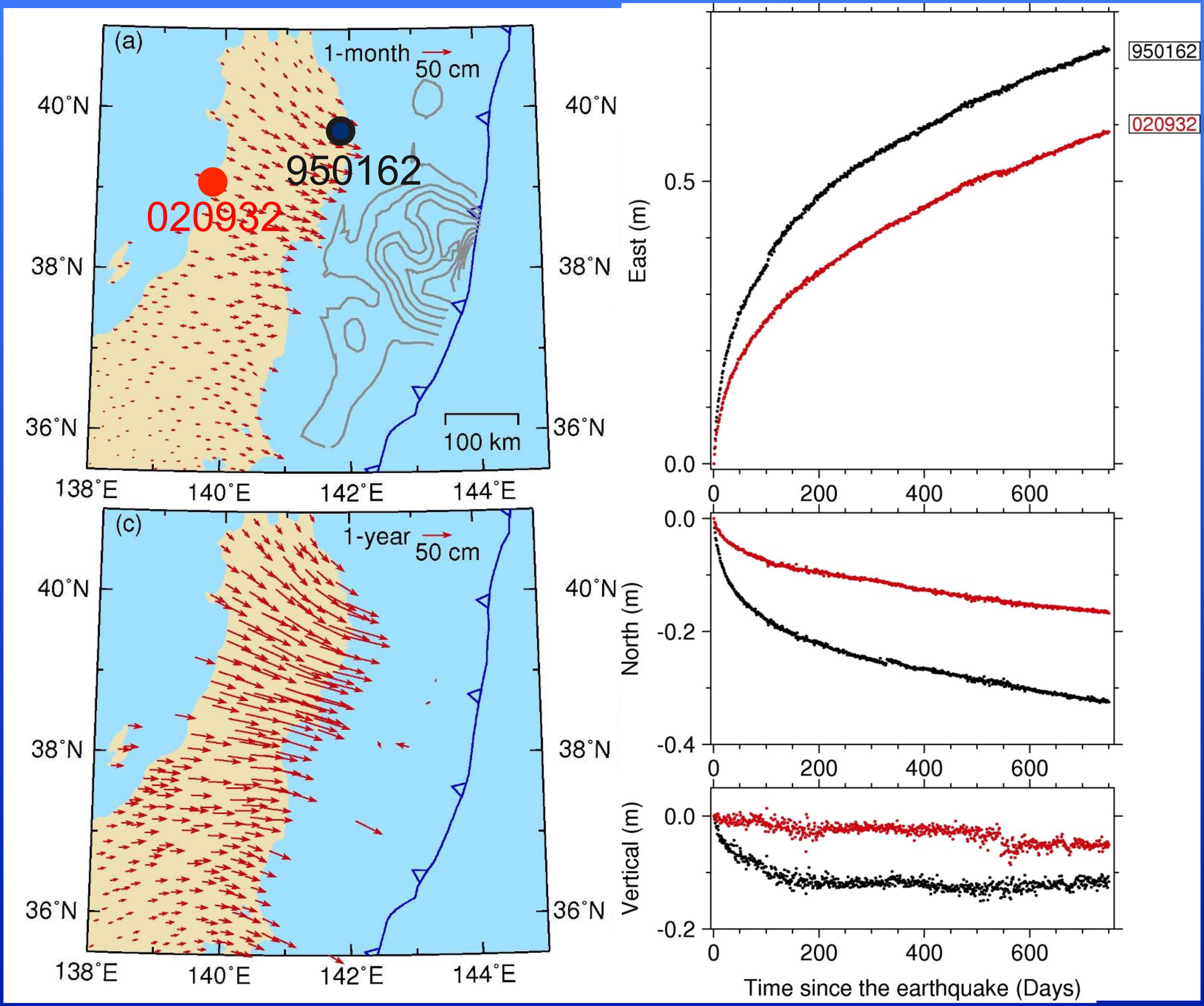

Processes After a Great Earthquake

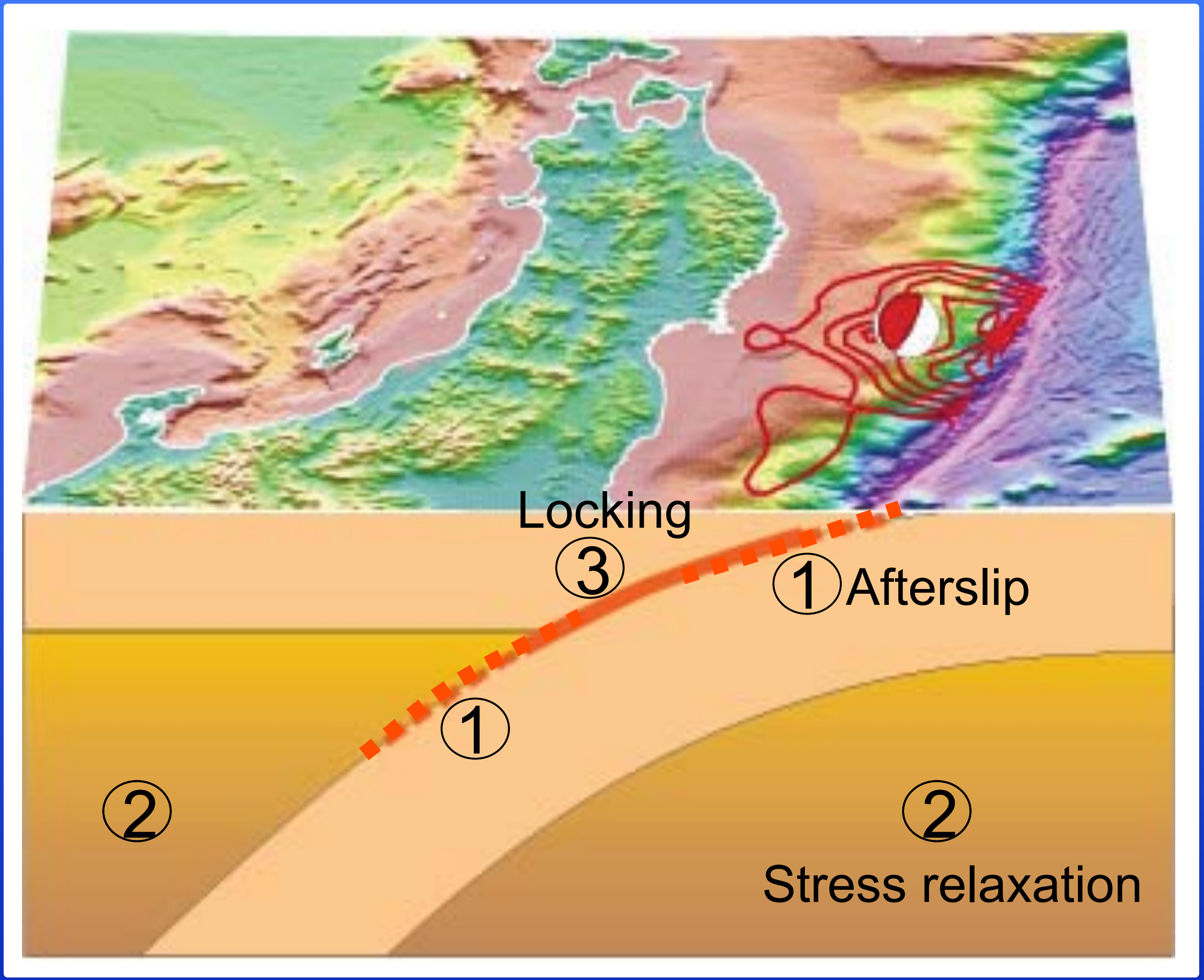

Major Challenges:

1. How do we distinguish the effects of afterslip and transient relaxation of mantle?
2. How do we eliminate the model ambiguities?

Afterslip of the Megathrust

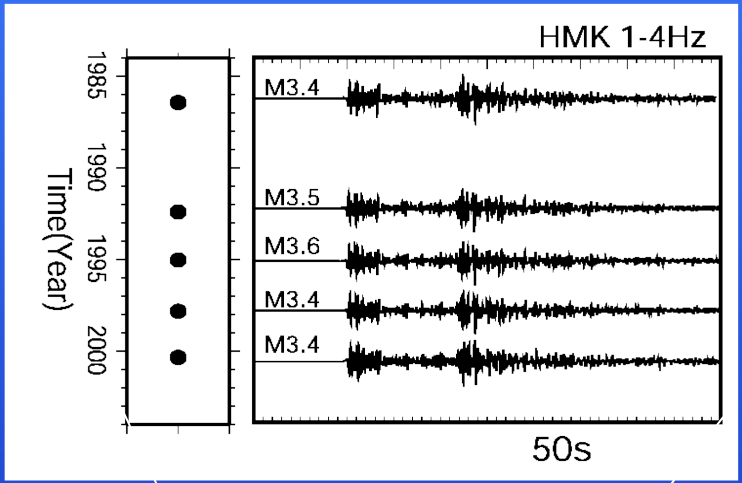

(Uchida, 2012)

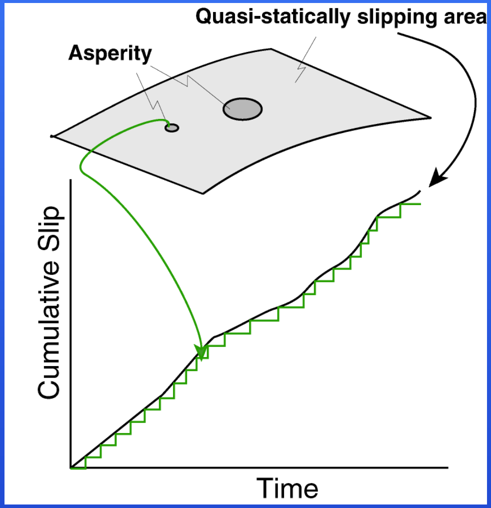

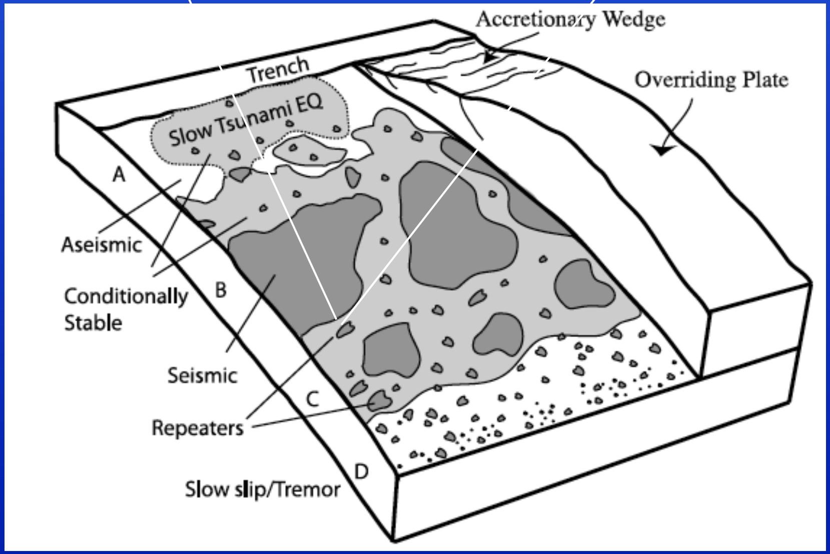

(Lay, 2012)

Afterslip Simulated by Weak Shear Zone

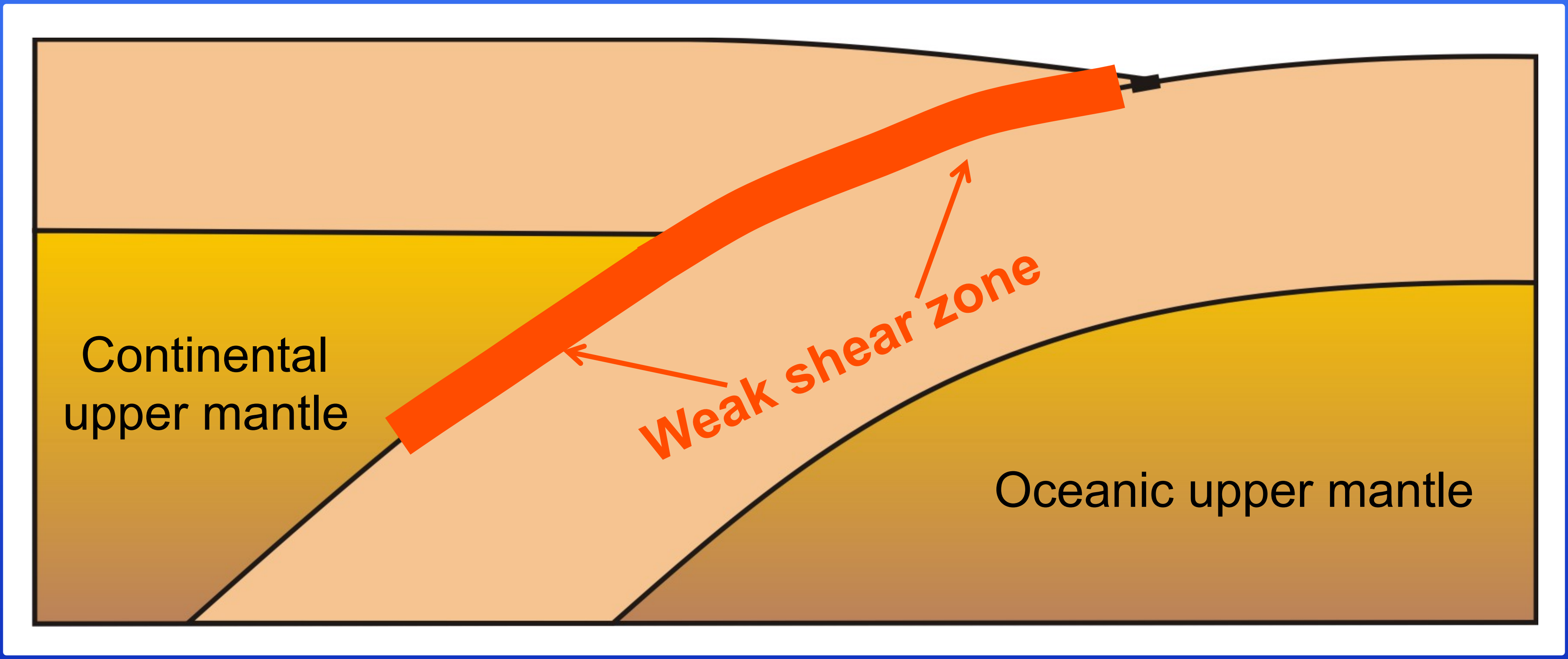

Shear zone viscosity: $10^{17} – 10^{18}$ Pa s

Continental mantle viscosity: $\sim 10^{19}$ Pa s

Locked Regions of the Megathrust

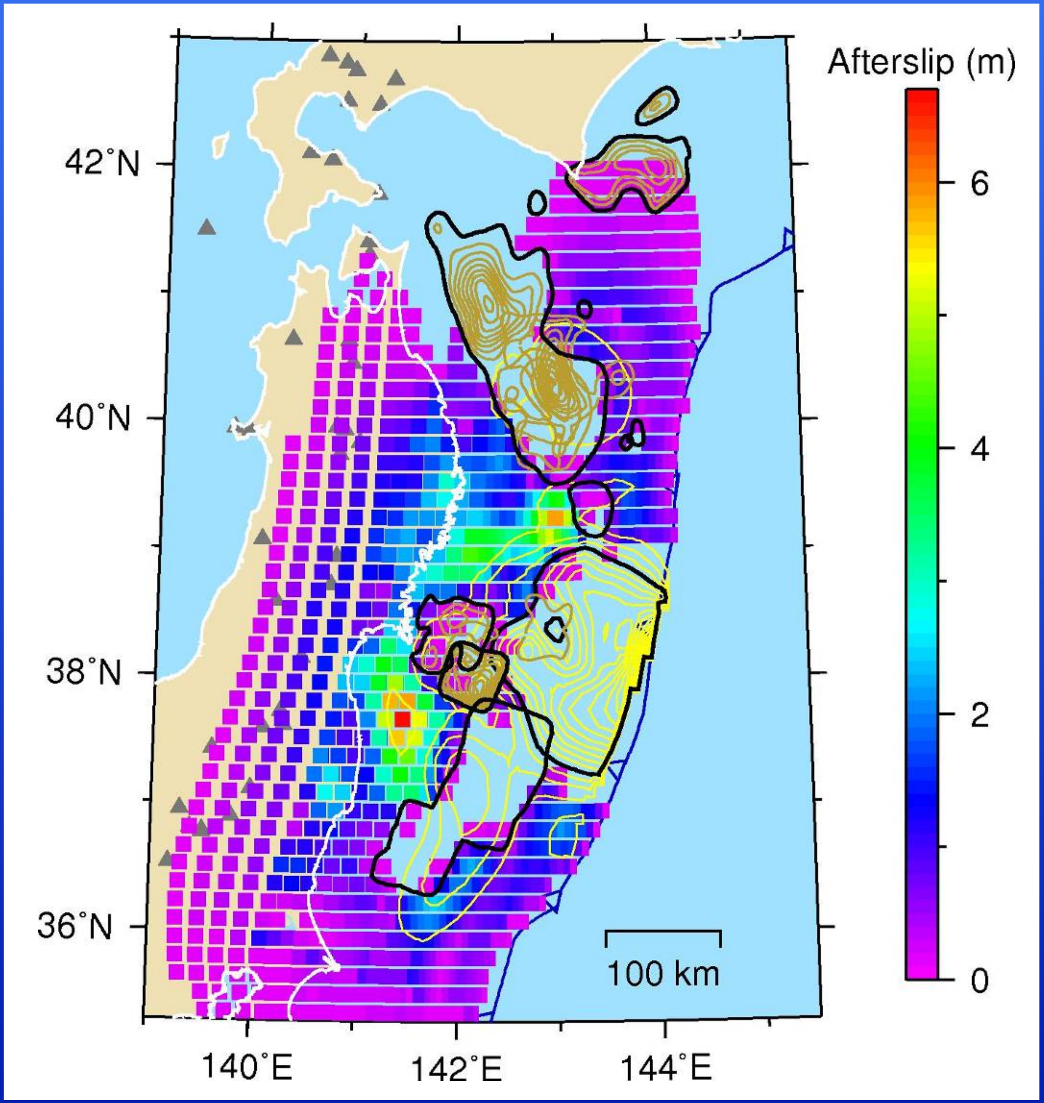

Finite Element Model

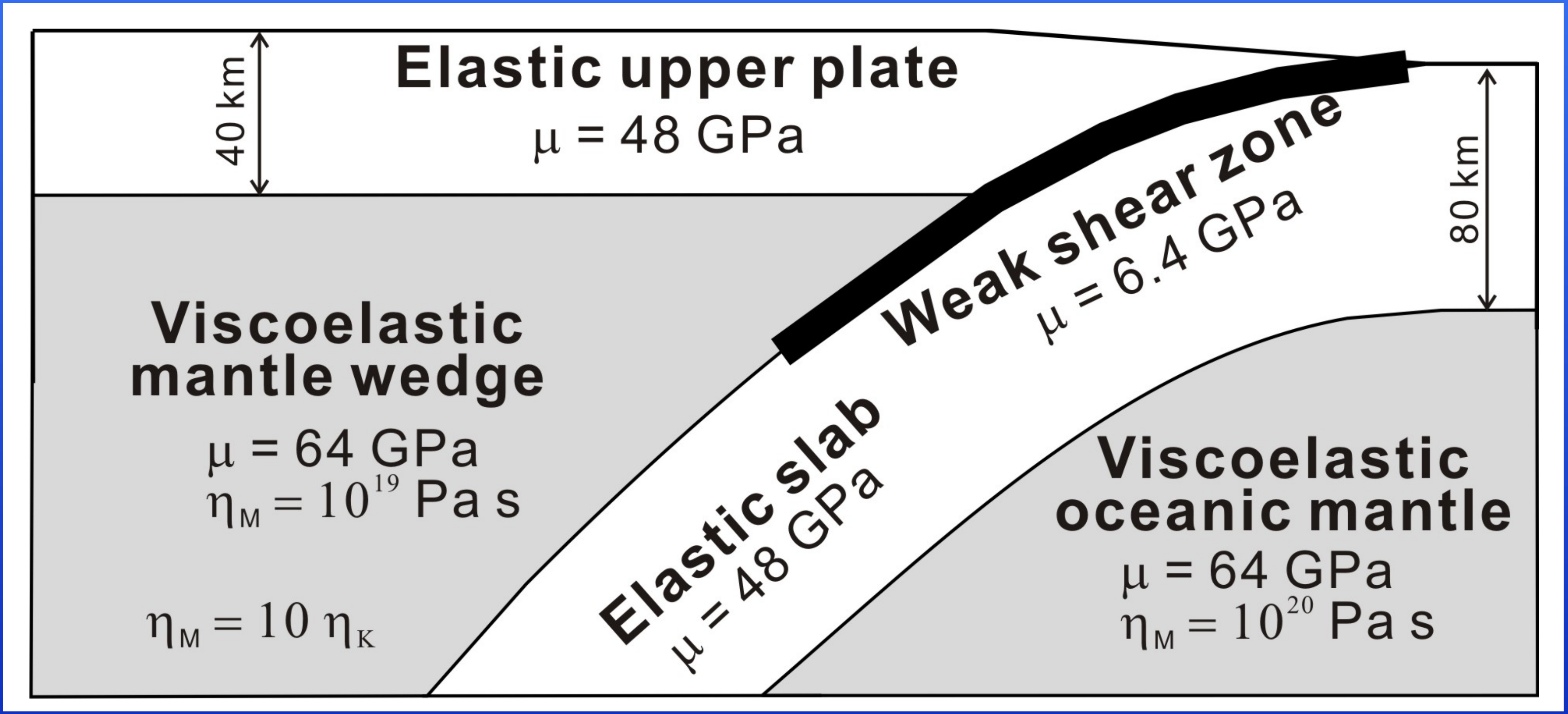

Conceptual representation of the subduction zone model. Modelling code is written by *J. He*, Geological Survey of Canada, Pacific Geoscience Centre, Canada.

Central Part of the Finite Element Mesh and Slip Assignment

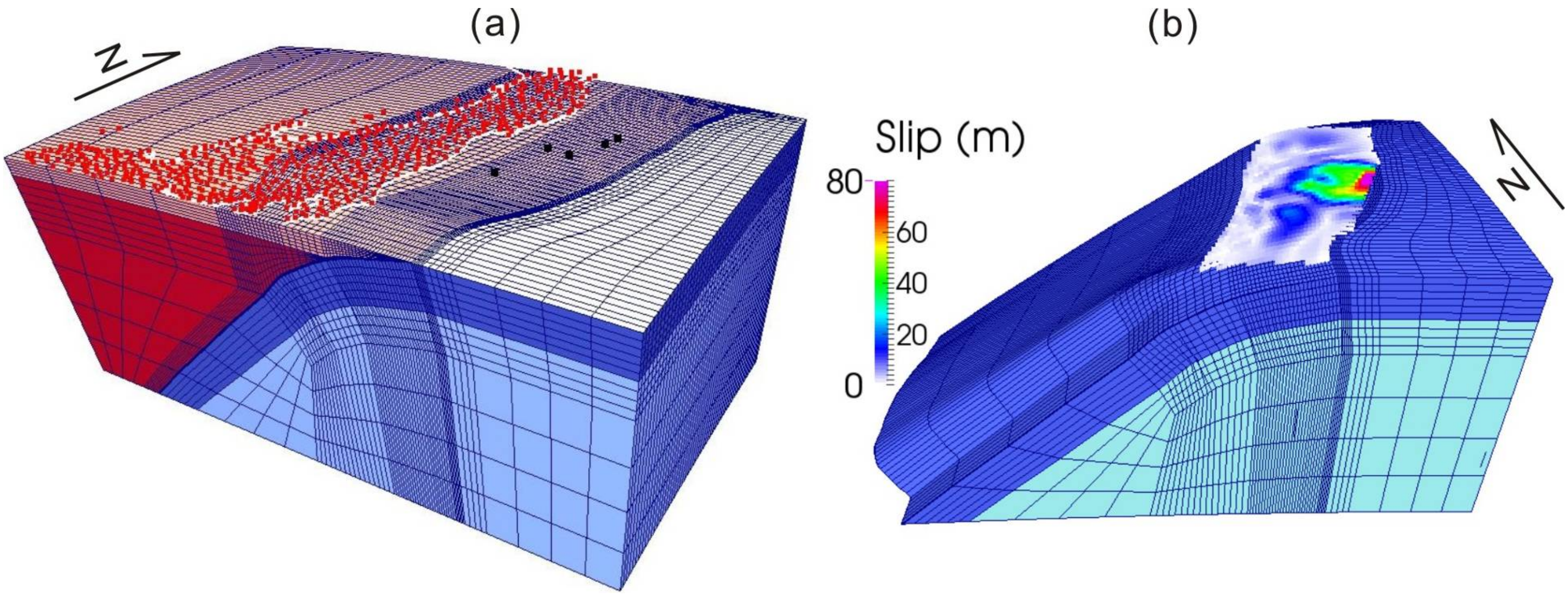

Coastlines: thick white lines
Land GPS sites: red dots
Marine GPS sites: black dots

(Coseismic slip from *Iinuma et al.*, 2012)

Offshore Repeating Earthquakes

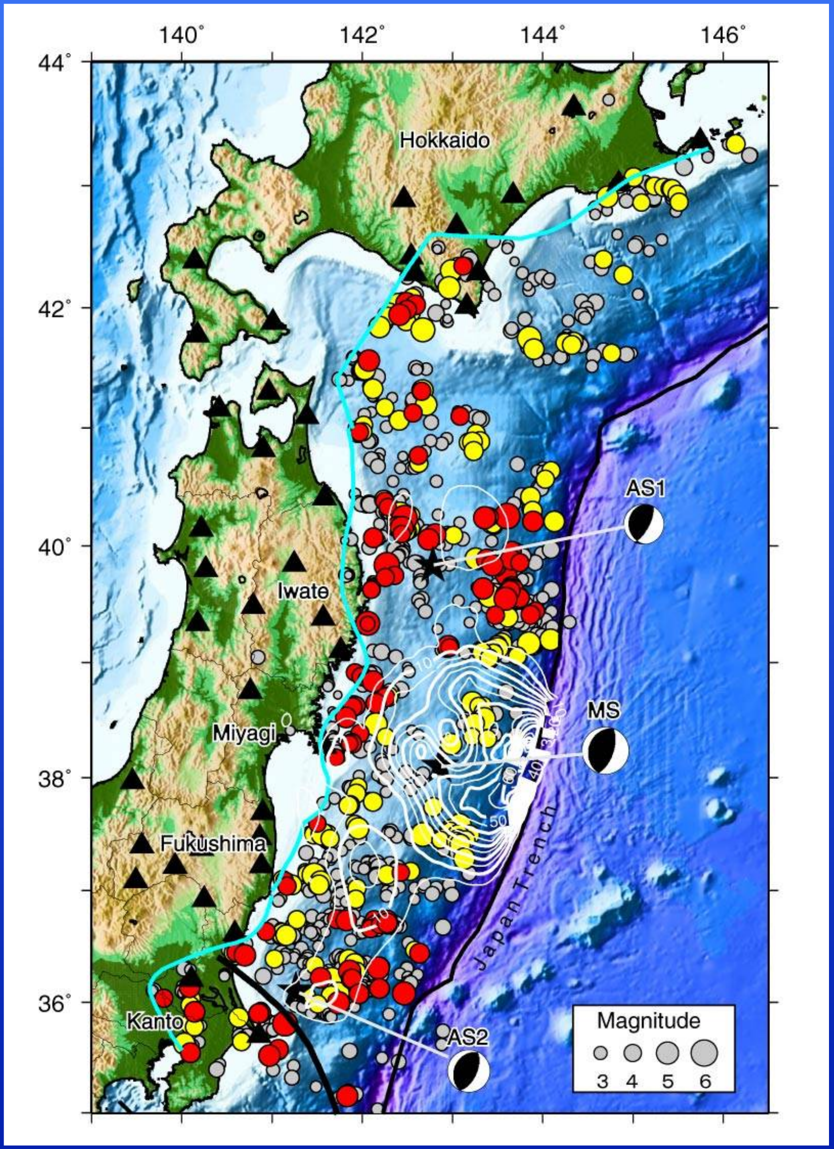

1984- 2011.12.31 repeaters

Red : both before and after M9

Yellow: only before M9

(Uchida & Matsuzawa, 2013)

Shallow Shear Zone Viscosities Constrained From Repeating Earthquakes

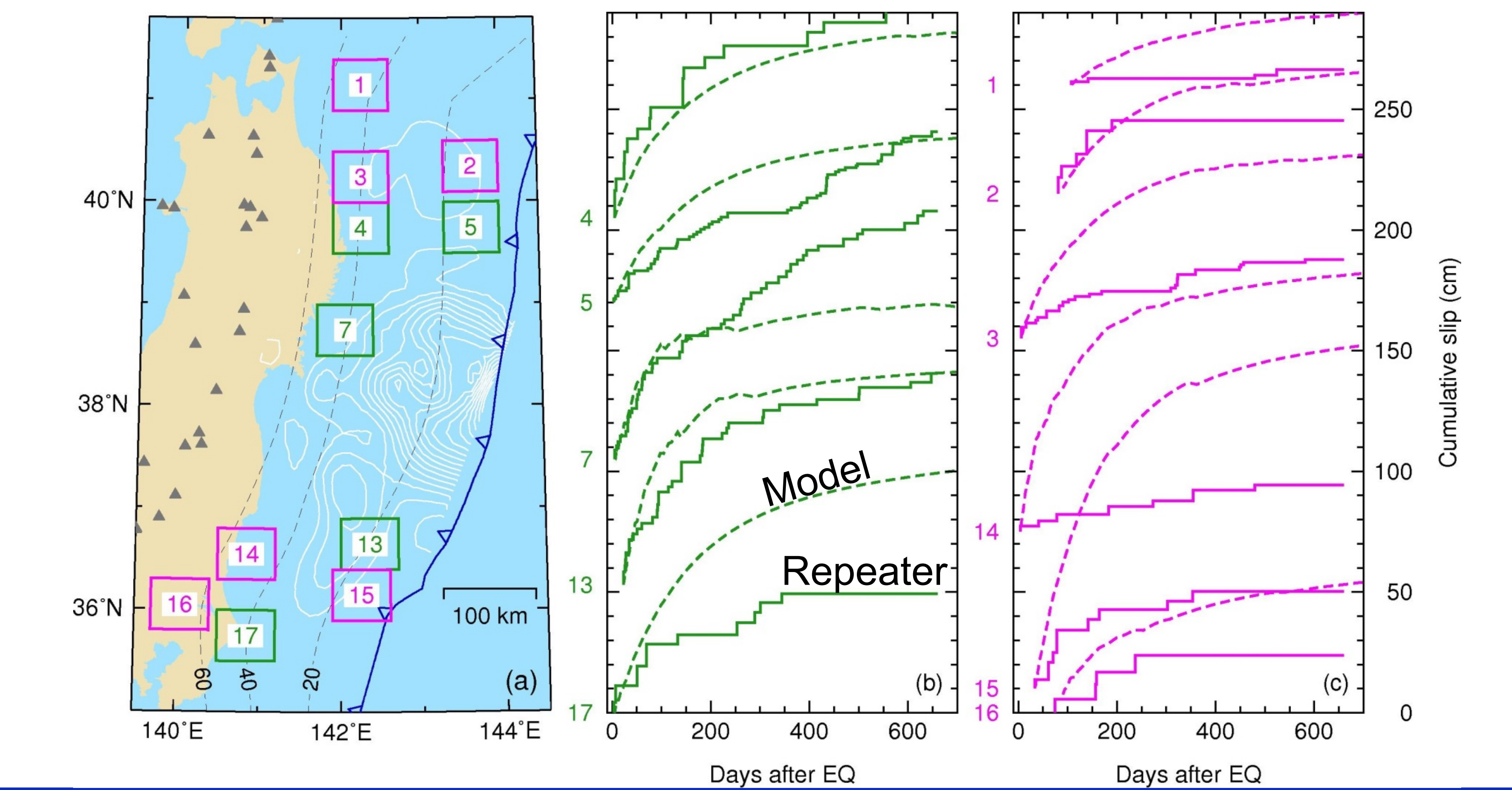

Shallow shear zone (≤50 km):

Steady-state (Maxwell) viscosity: $\eta_M = 10^{17}$ Pa s

Transient (Kelvin) viscosity: $\eta_K = 10^{16}$ Pa s

Variable Model Parameters

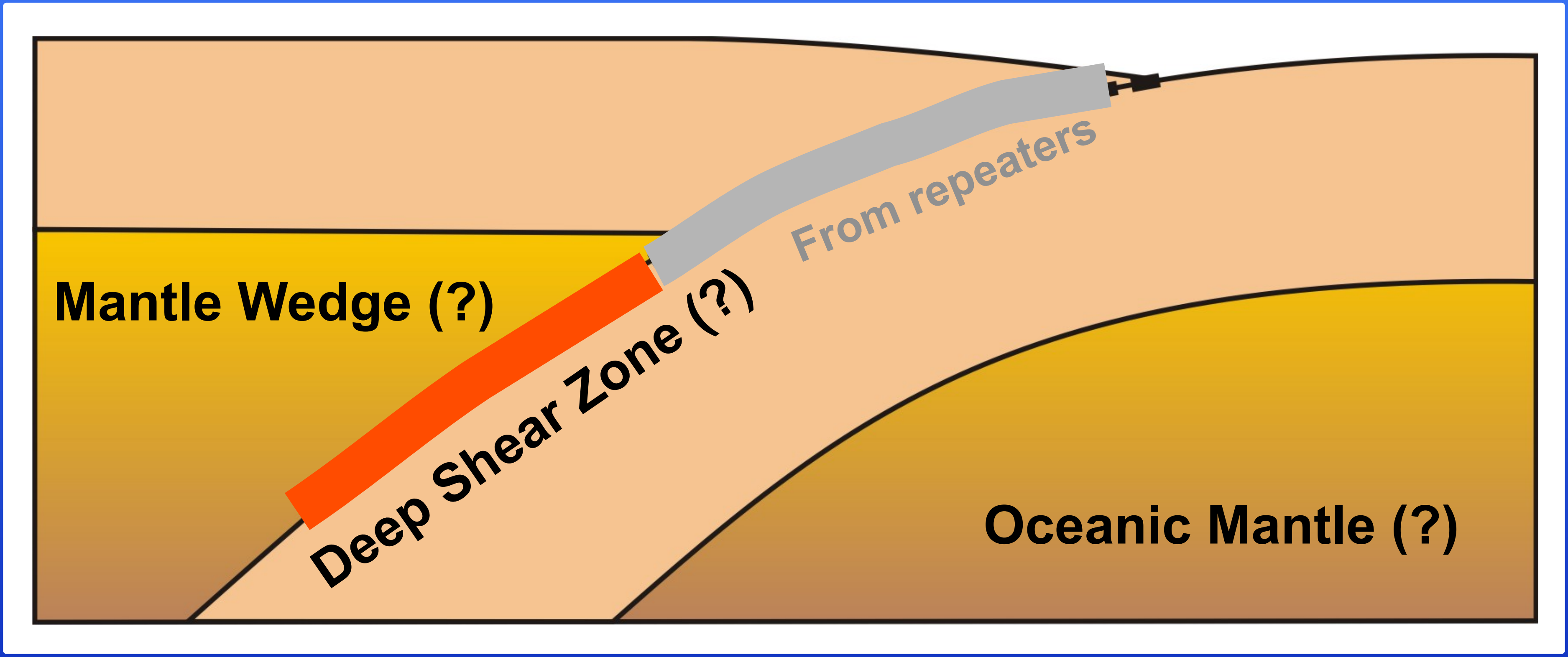

Mantle Wedge: steady-state viscosity η_M $10^{18} - 10^{20}$ Pa s
(transient viscosity $\eta_K = \eta_M/10$)

Oceanic mantle: η_M $10^{18} - 10^{22}$ Pa s ($\eta_K = \eta_M/10$)

Deep shear zone: η_M $10^{17} - 10^{20}$ Pa s ($\eta_K = \eta_M/10$)

Systematic Tests on Rheological Properties

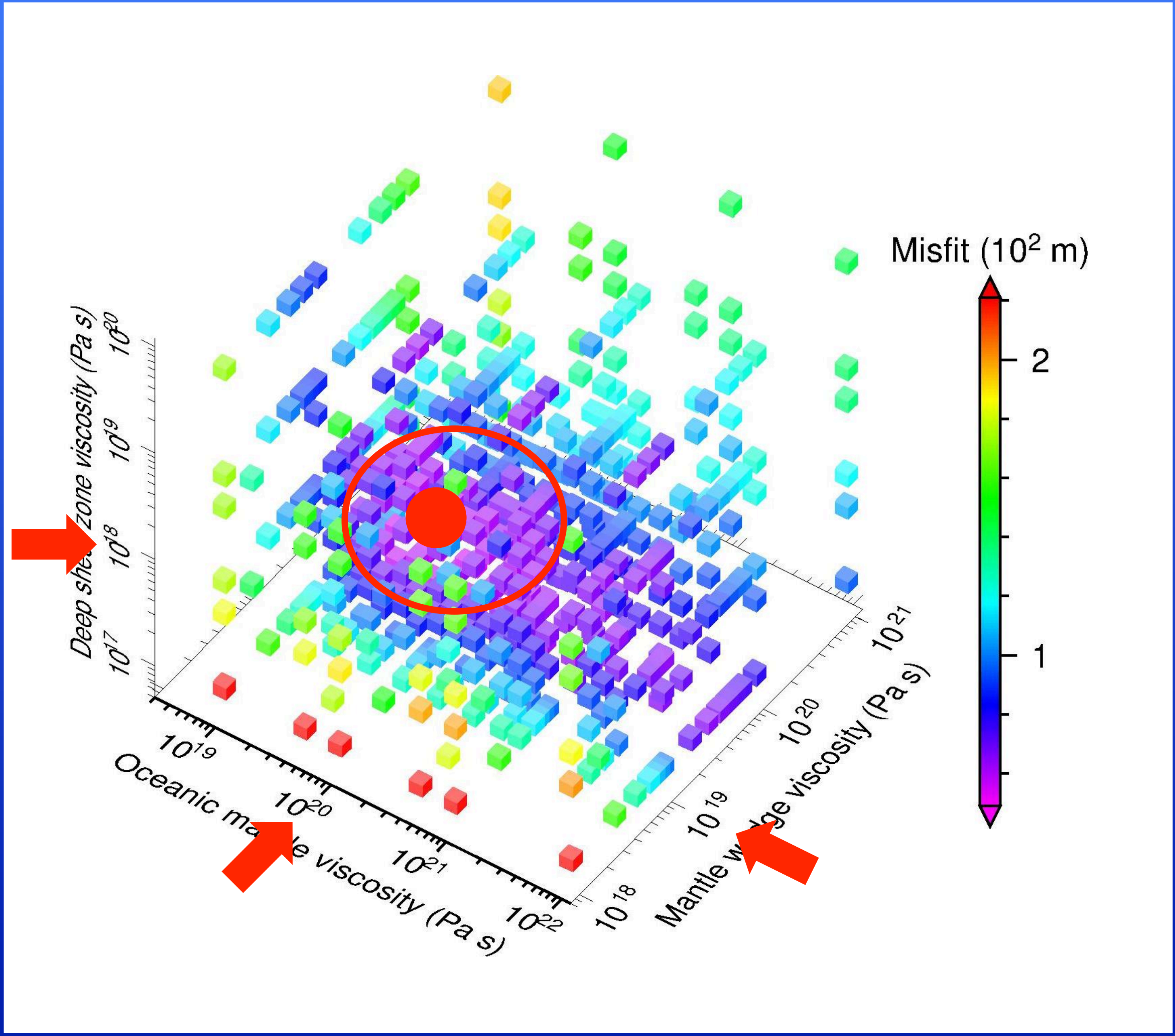

Systematic Tests on Rheological Properties

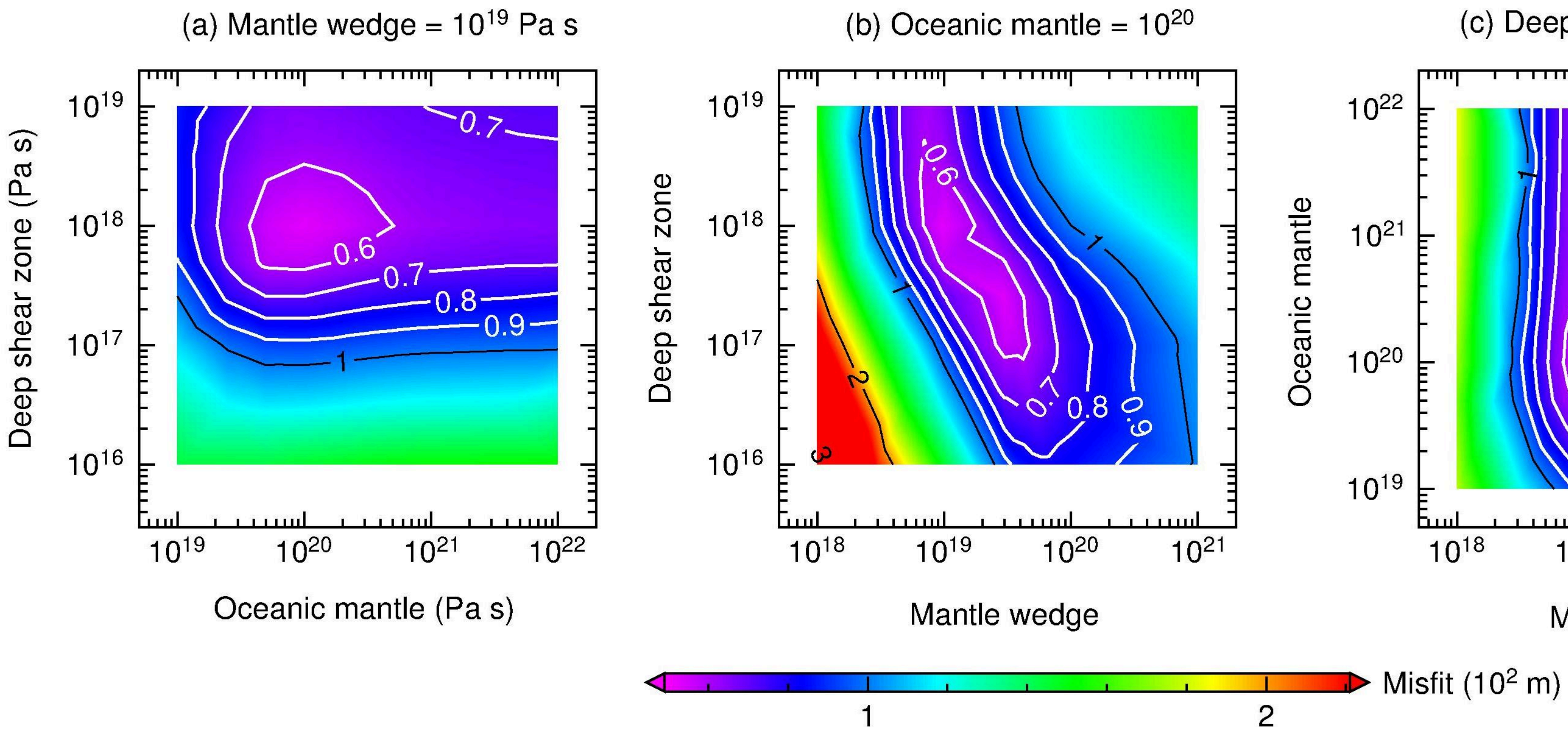

Systematic Tests on Viscosity Range

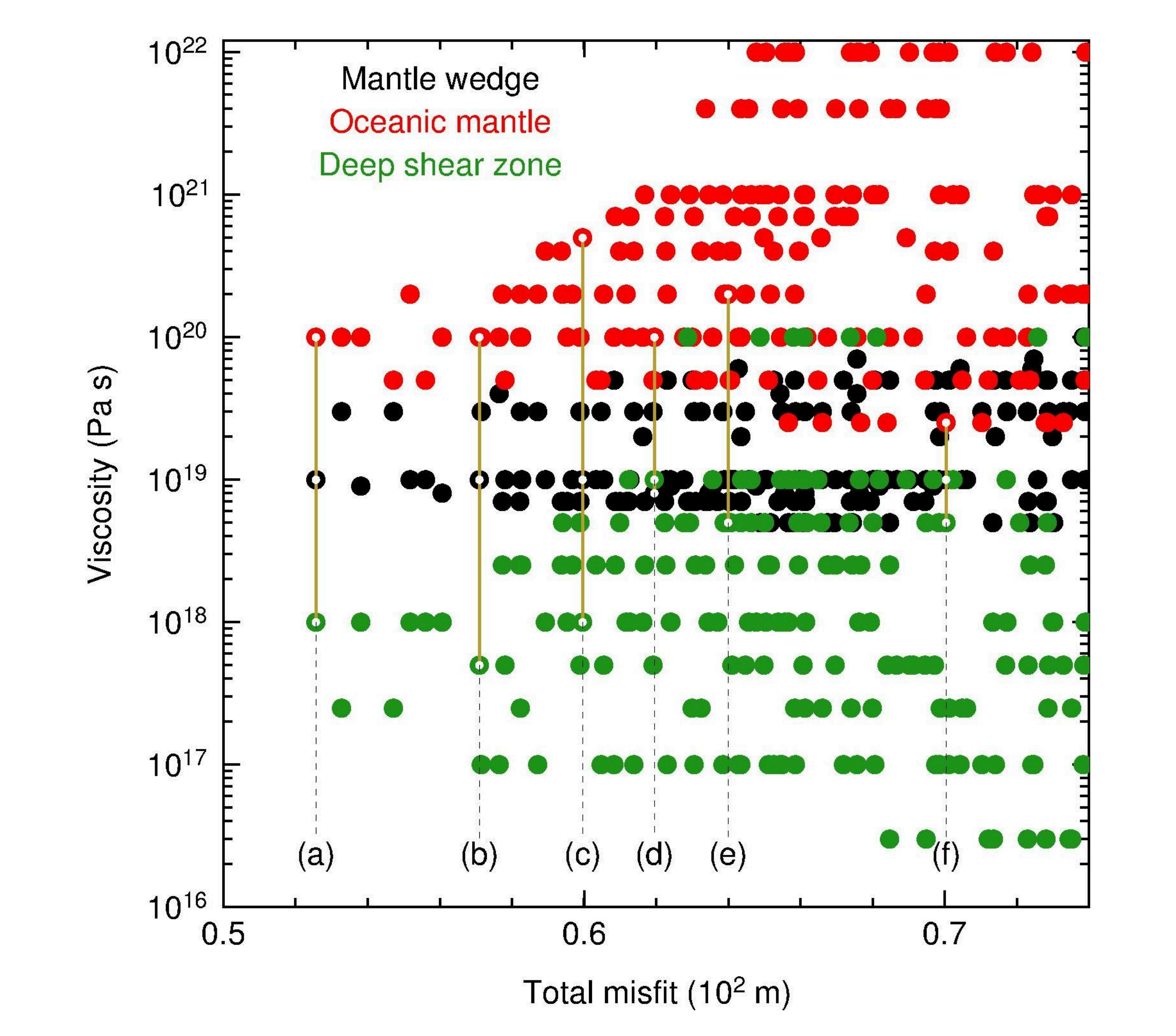

Residual of Selected Test models

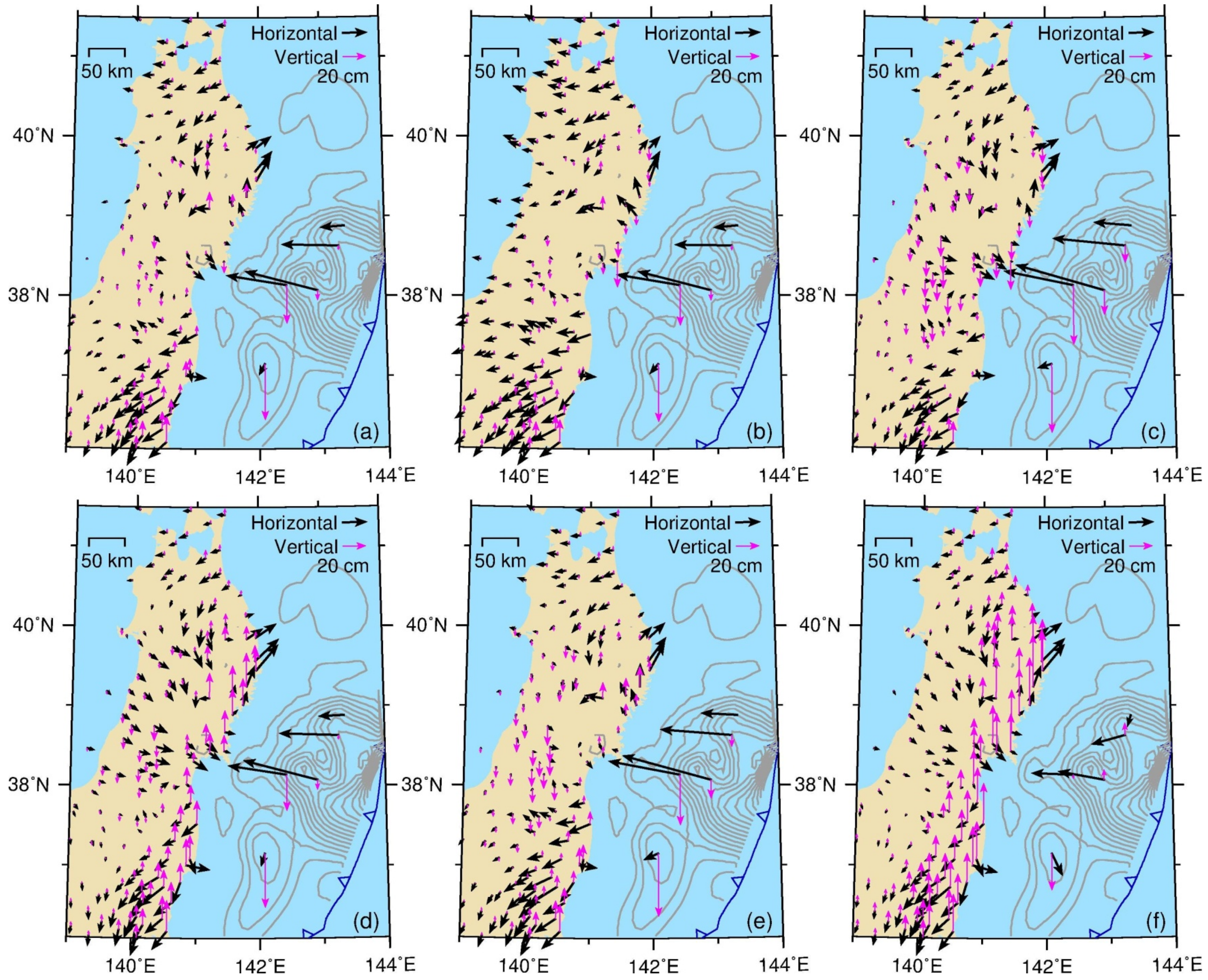

Systematic Tests on Viscosity Range

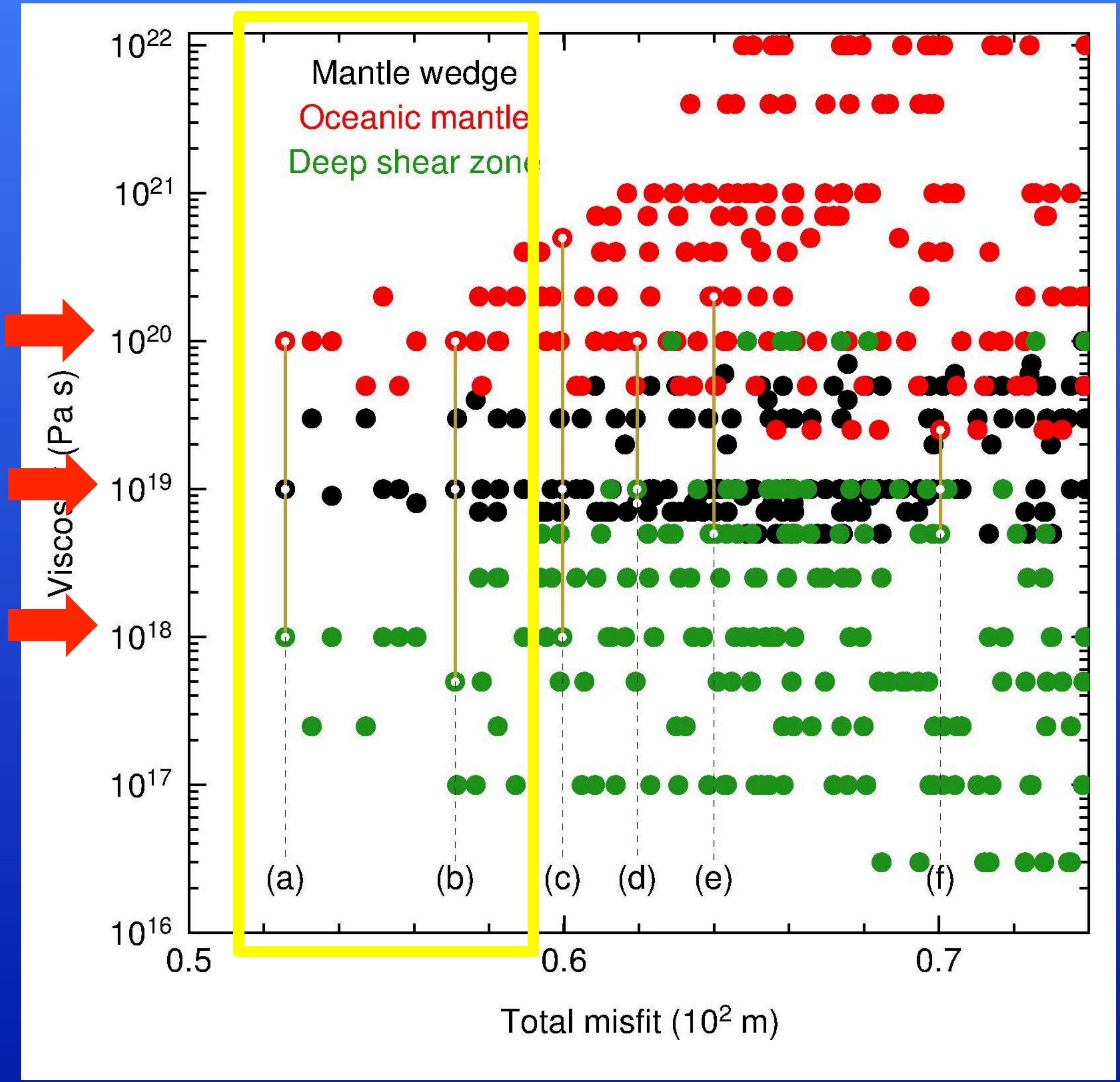

Viscosity Range

Mantle Wedge:

7×10^{18} – 5×10^{19} Pa s

Oceanic Mantle:

5×10^{19} – 5×10^{20} Pa s

Deep shear zone:

10^{17} – 5×10^{18} Pa s

Effects of Deep Shear Zone on Surface Deformation

Surface profile along latitude 38°N

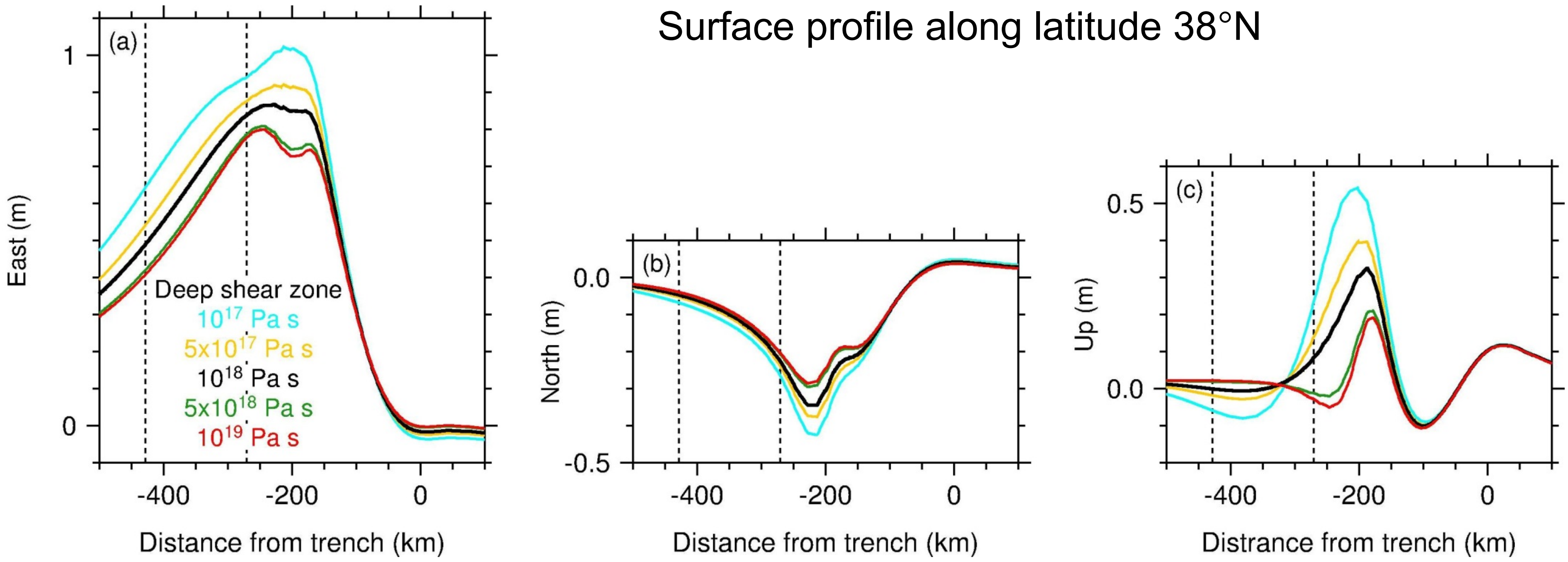

Effects of Mantle Wedge on Surface Deformation

Surface profile along latitude 38°N

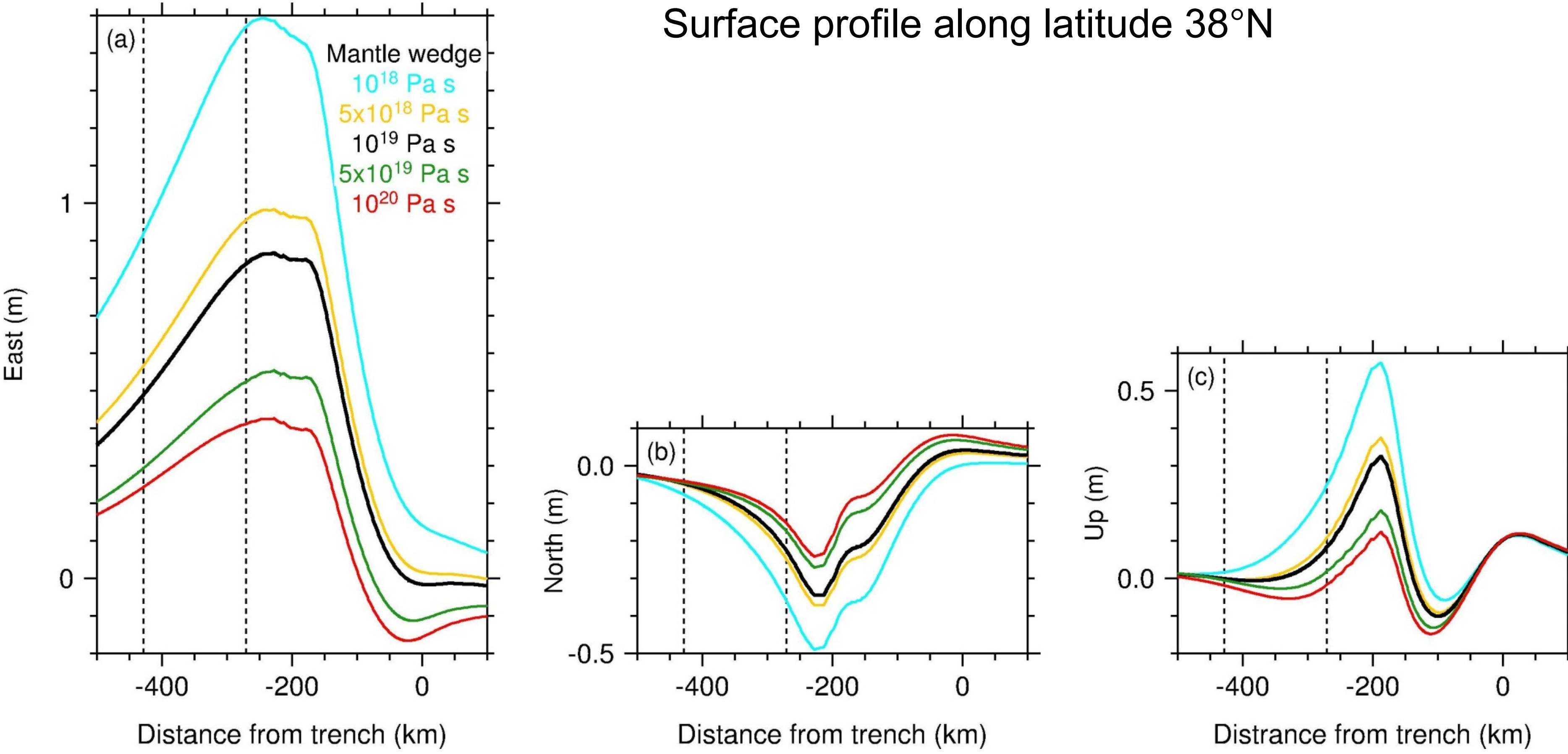

Effects of Oceanic Mantle on Surface Deformation

Surface profile along latitude 38°N

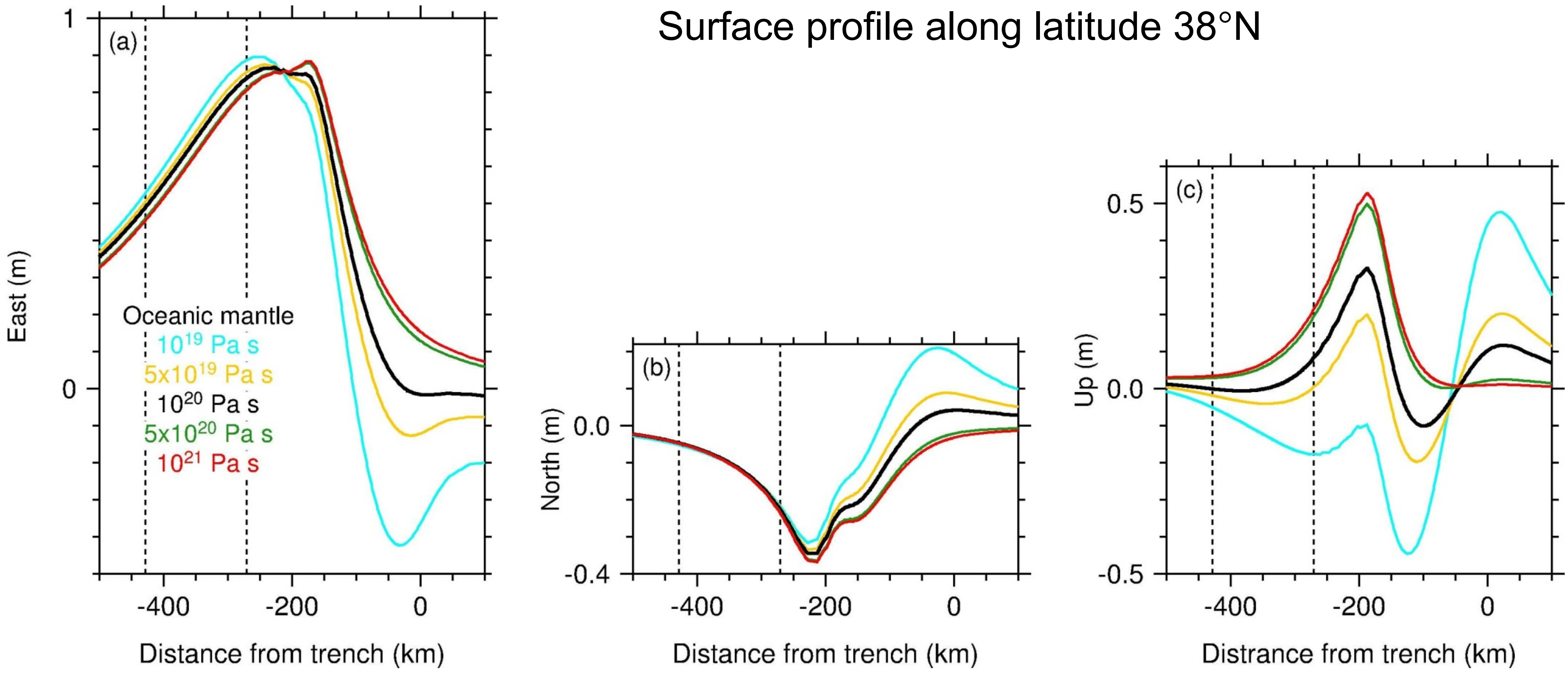

Contributions of Viscoelastic Relaxation and Afterslip

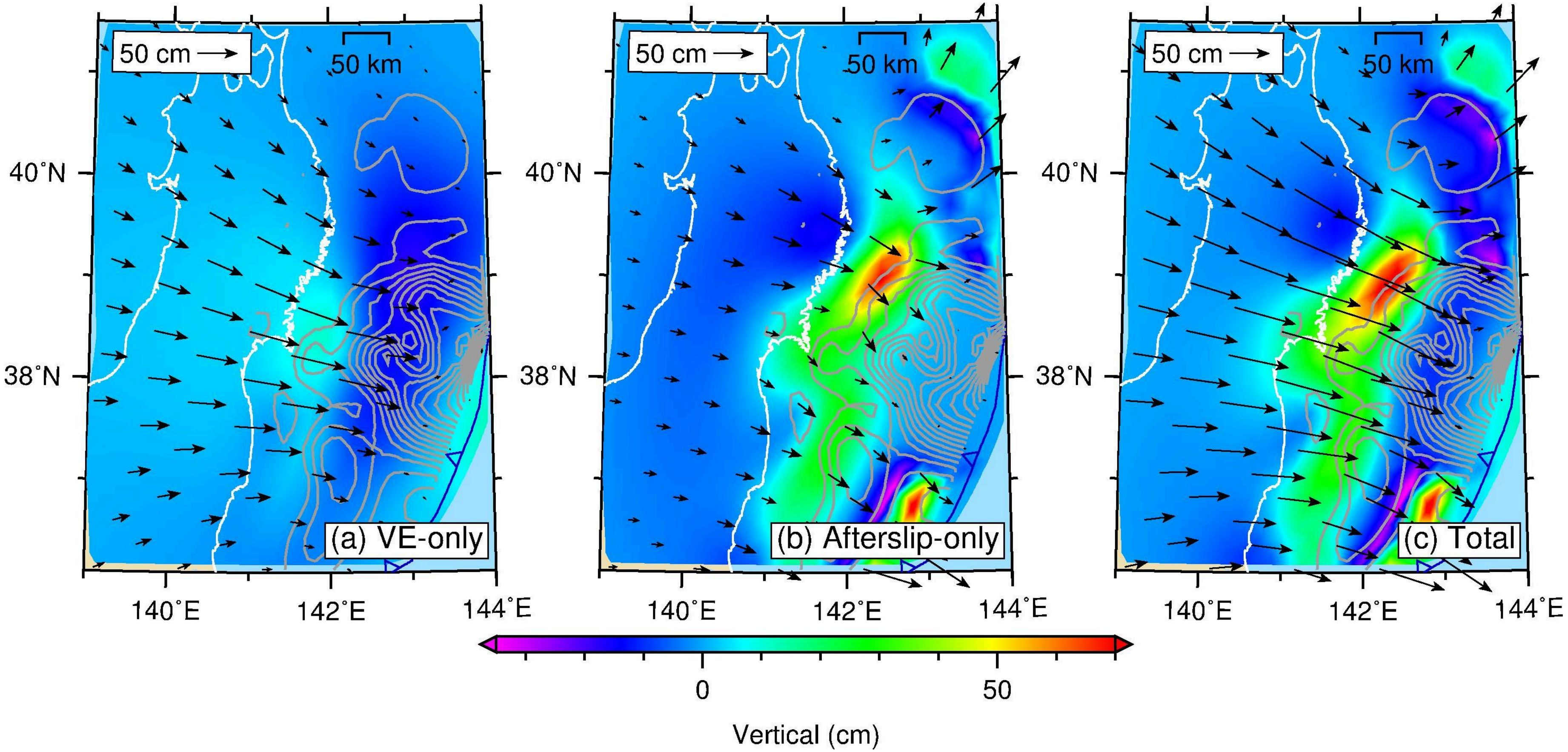

Comparison of GPS With Best-fit Model

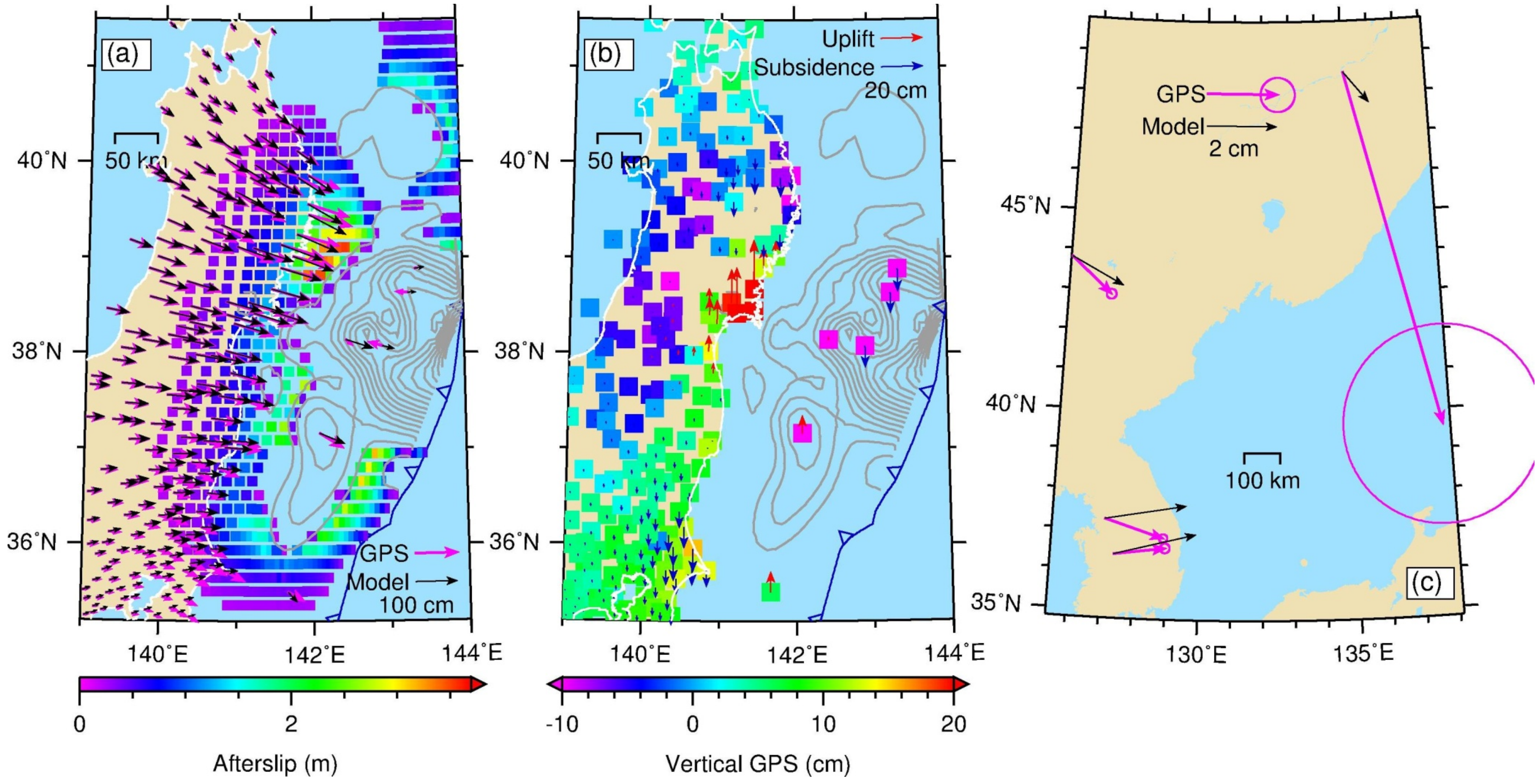

Comparison of GPS Time-series With Best-fit Model

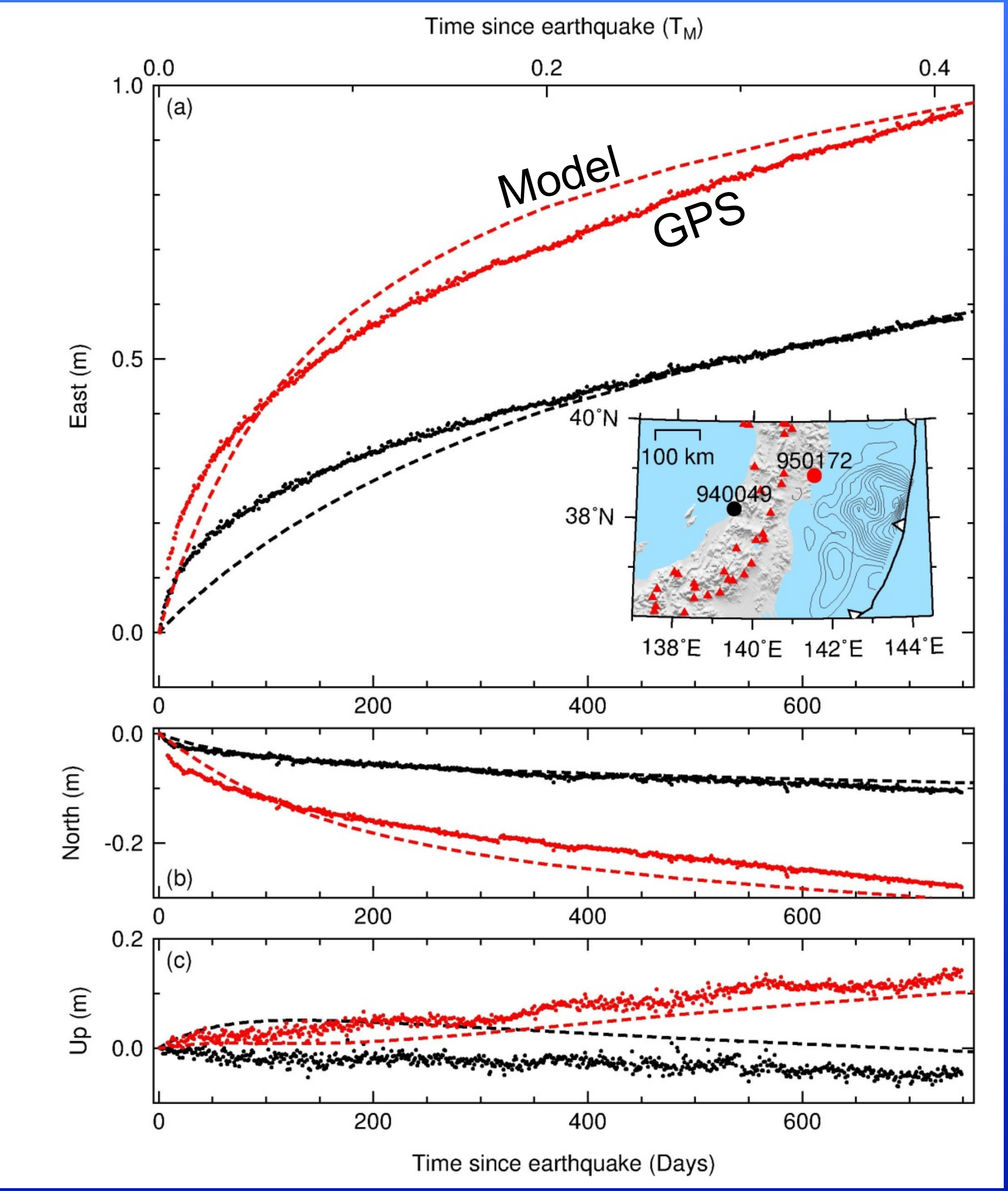

Distribution and Evolution of Afterslip

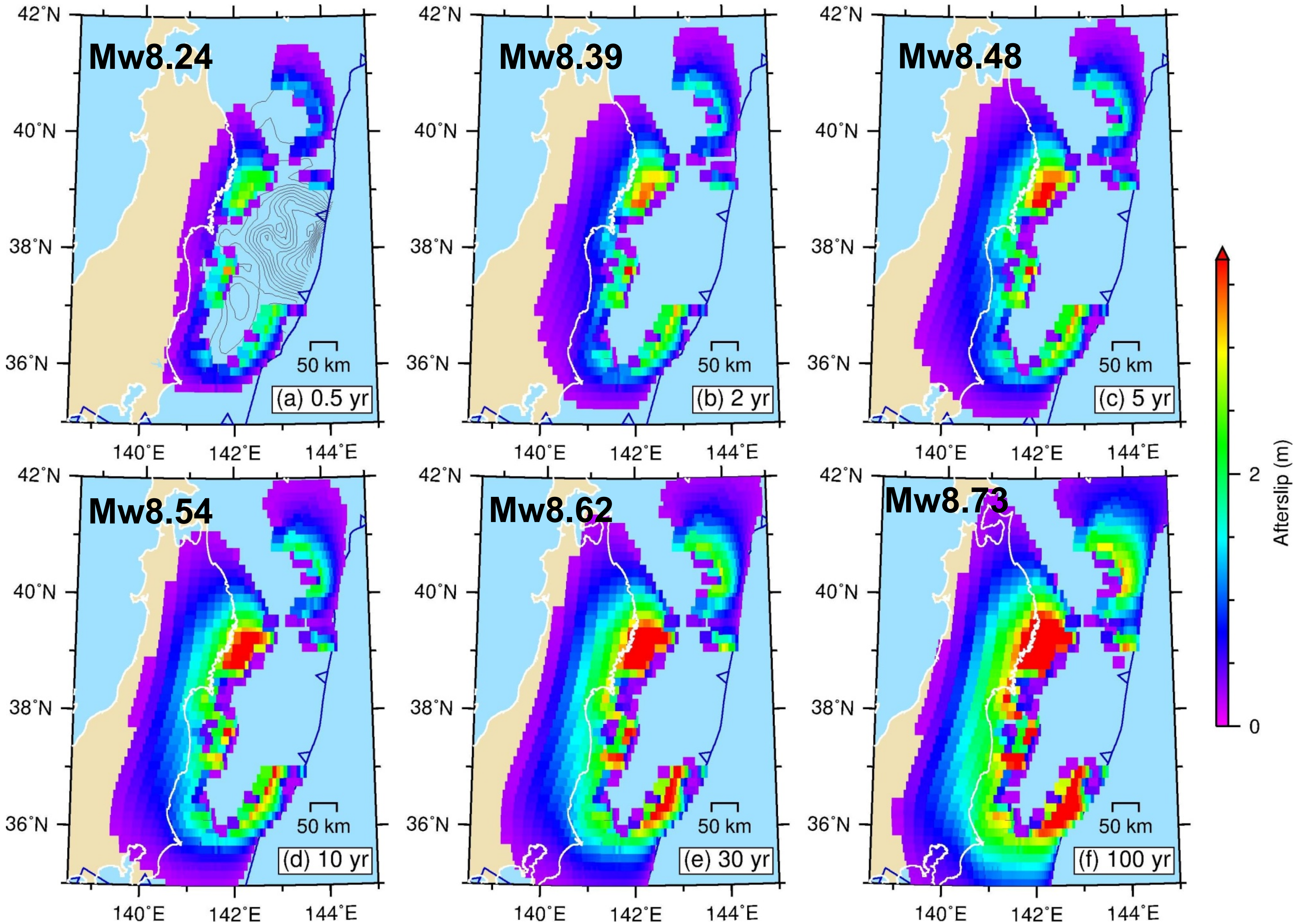

Surface Deformation at Future Times

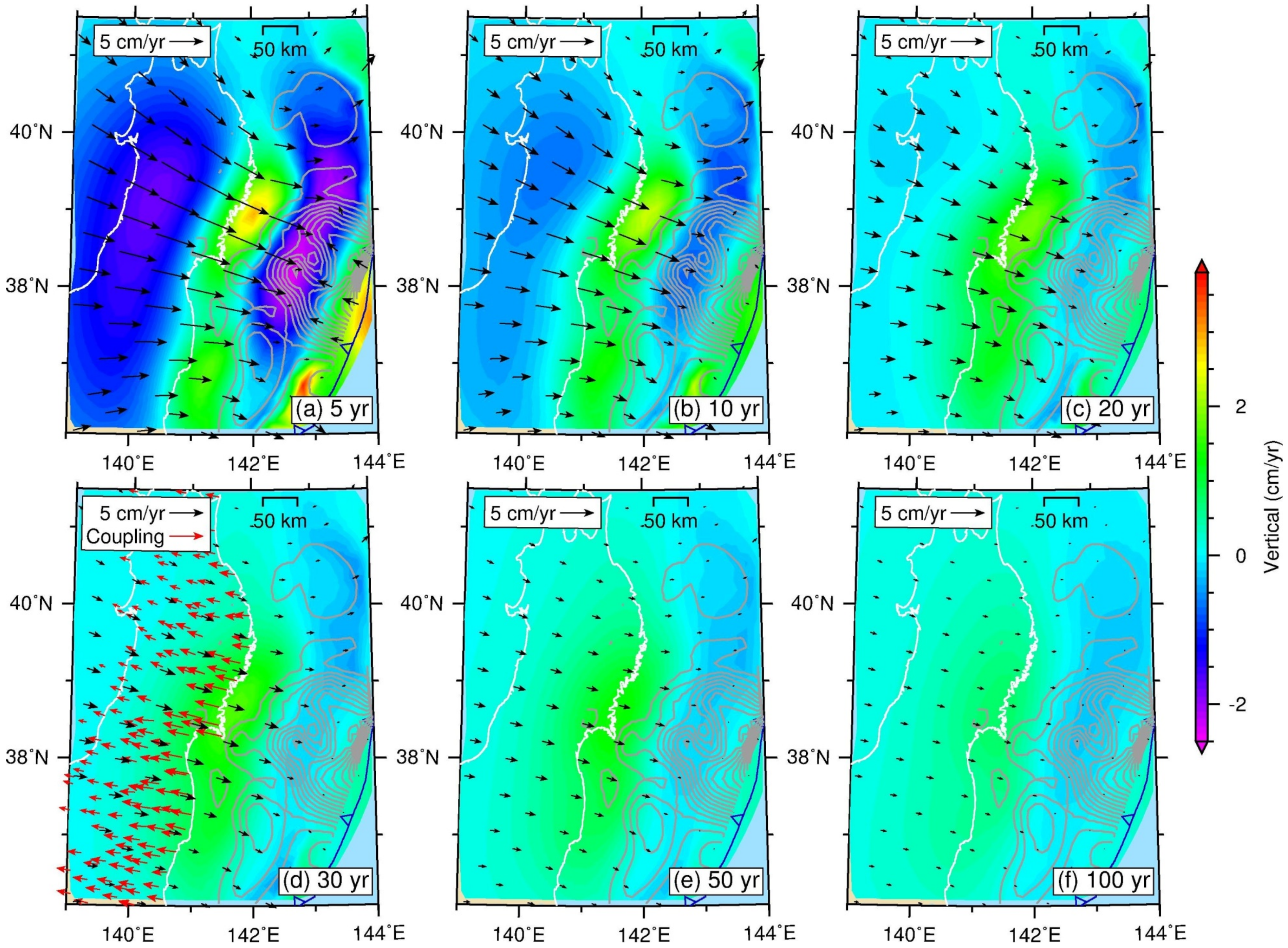

Effects of Different Source Models

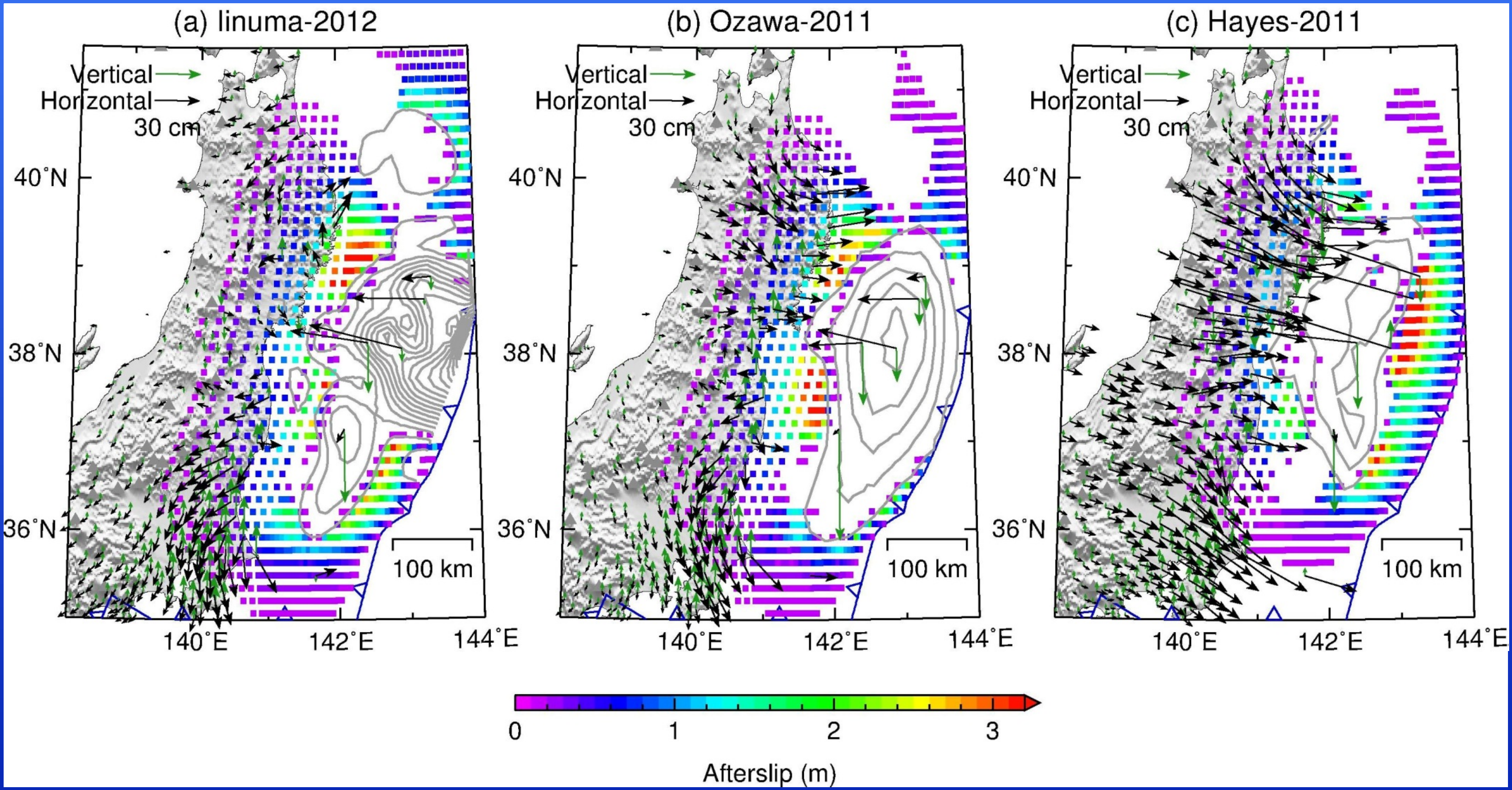

Effects of the Elastic Subducting PHS Slab

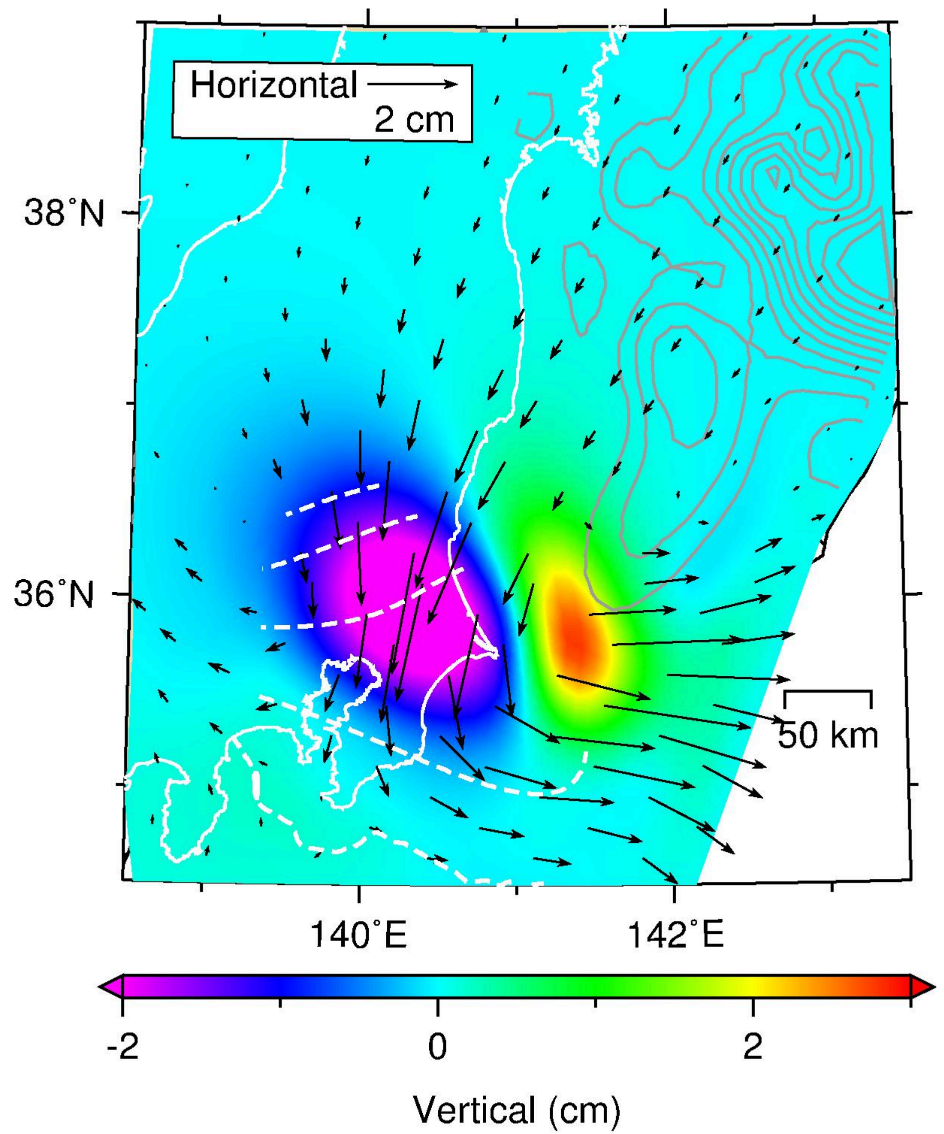

Residual of Best-fit Model

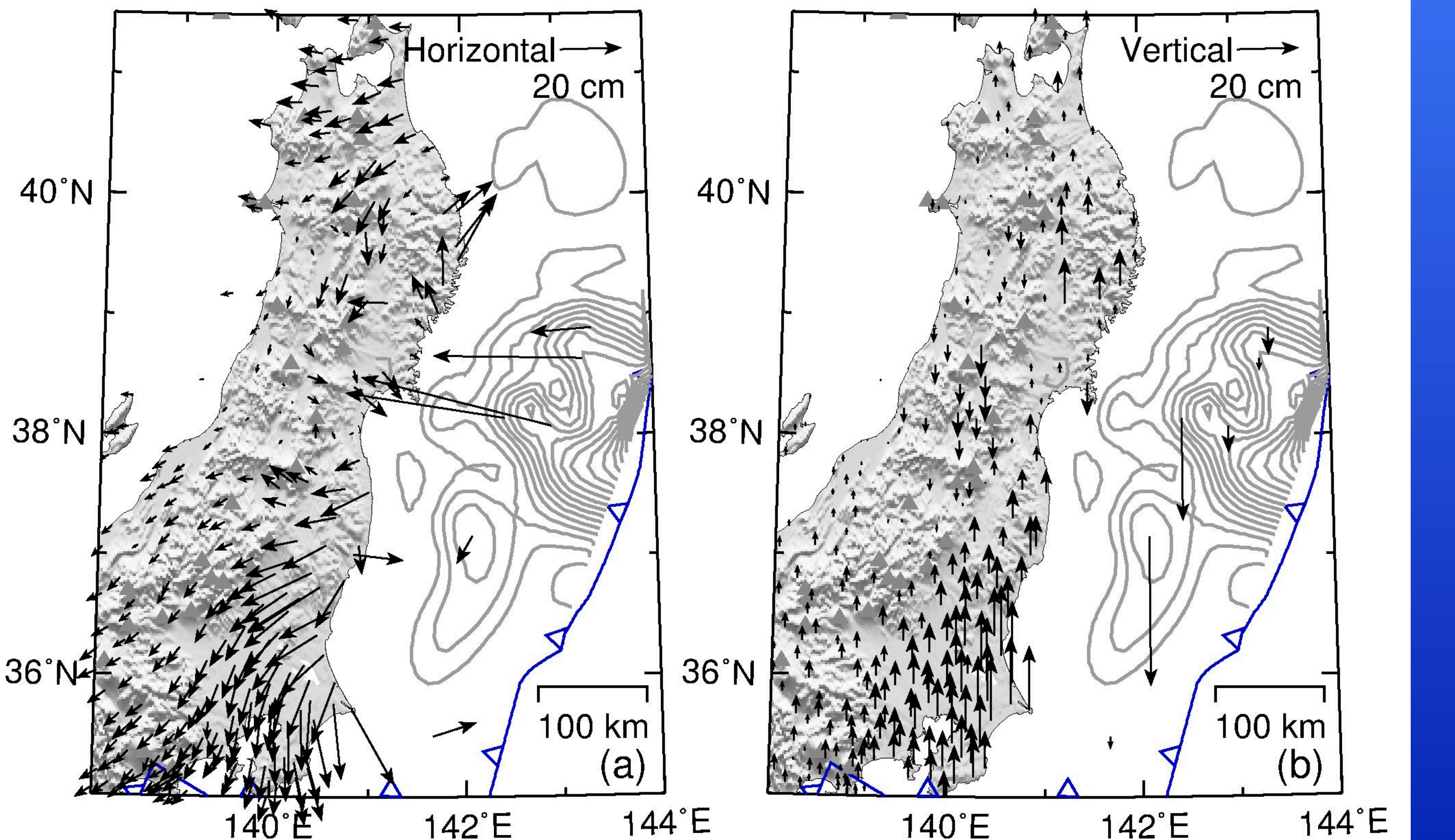

Afterslip of PHS and PAC Derived from Repeating Earthquakes

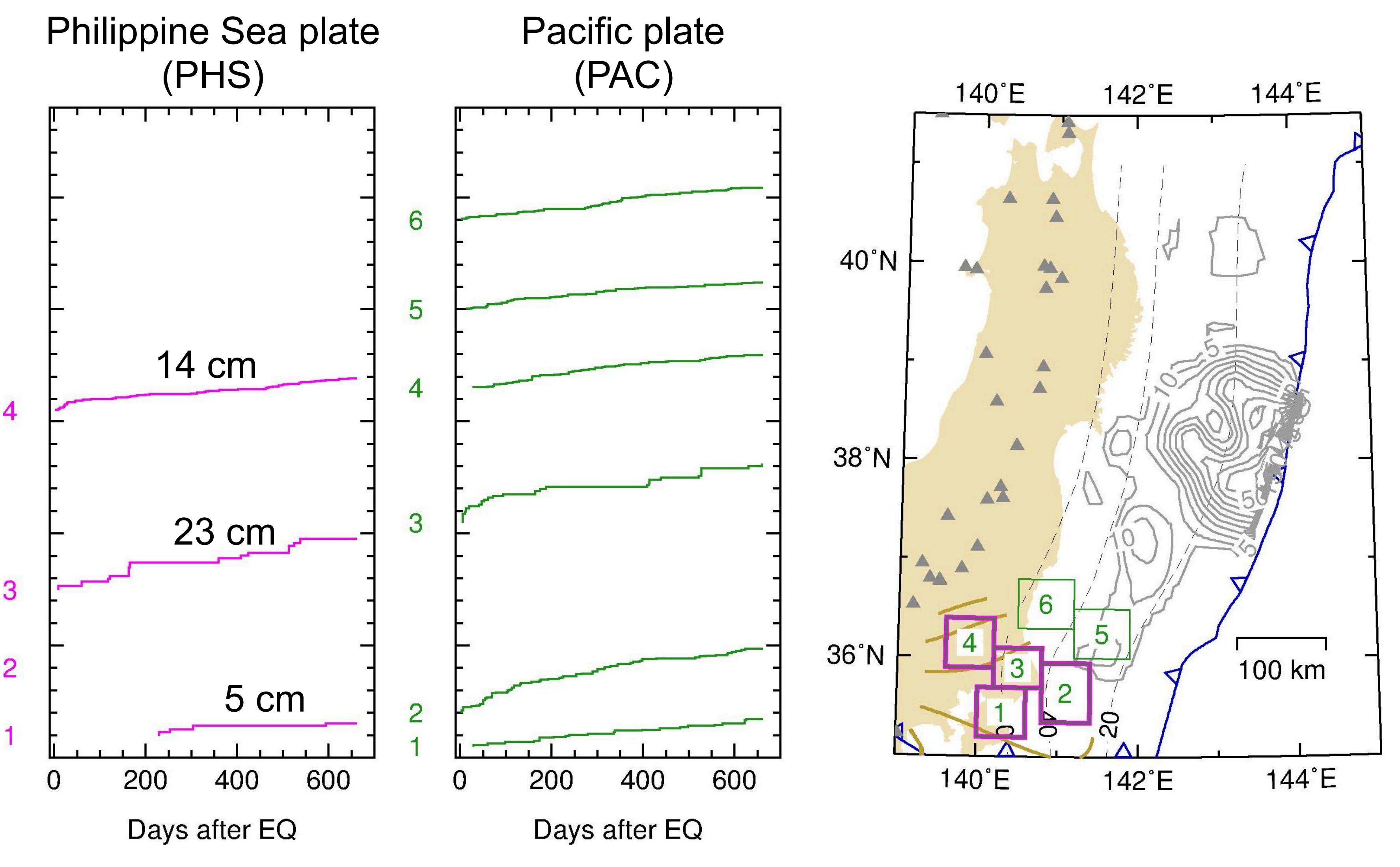

(data courtesy of N. Uchida)

Afterslip of the PHS Slab

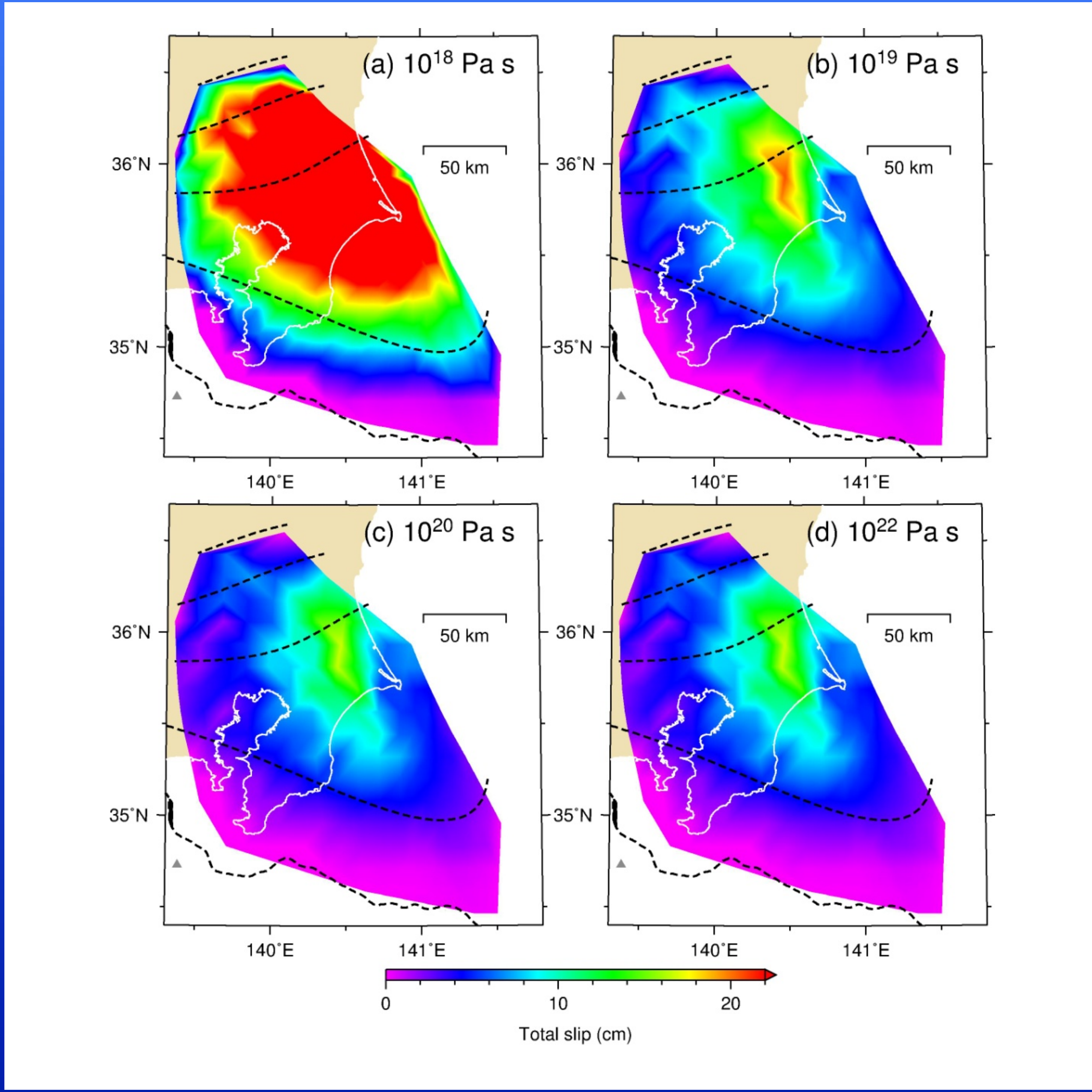

Surface Deformation due to Afterslip of PHS

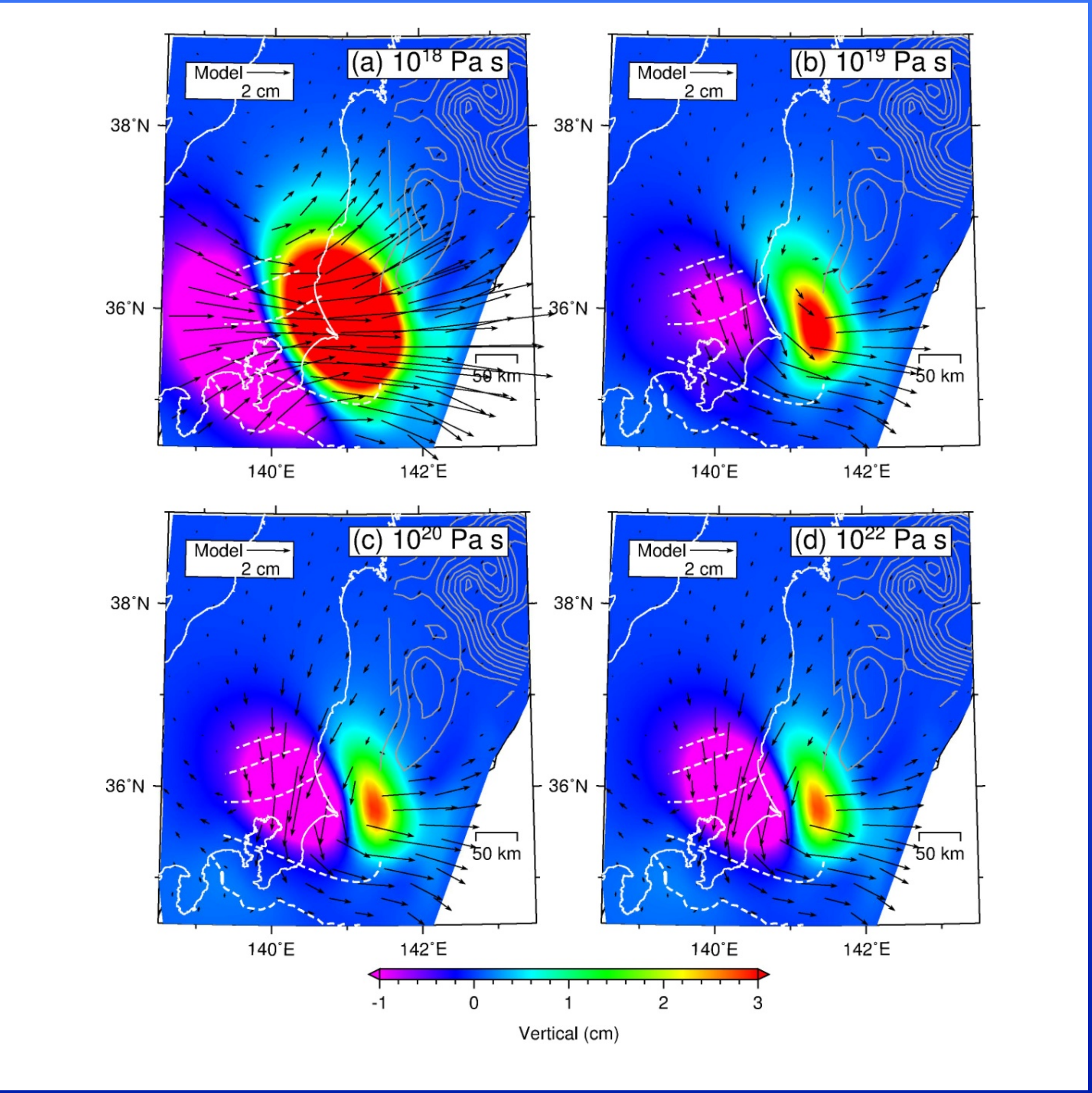

Surface Thermal Gradient in NE Japan

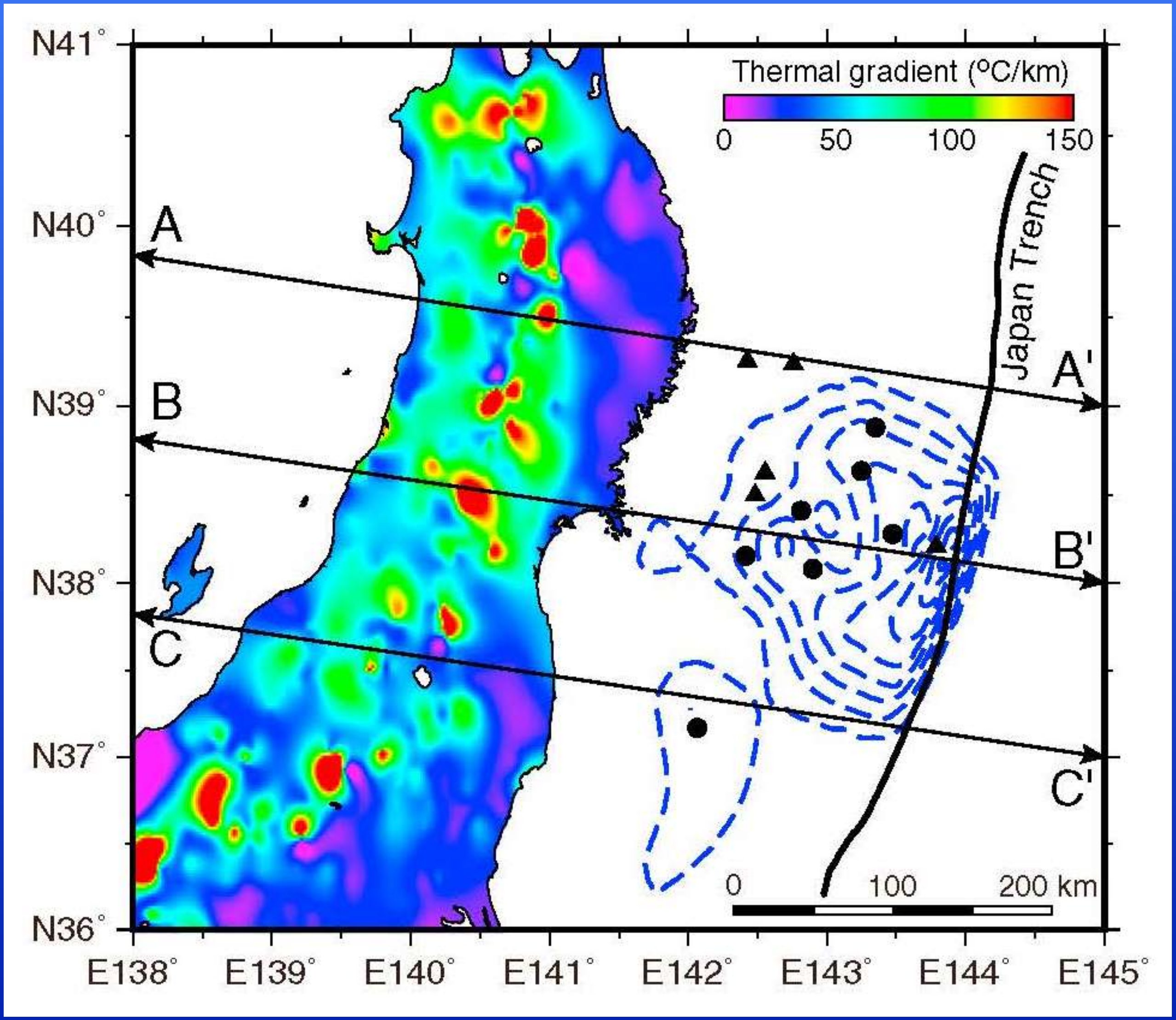

(Muto et al., 2013)

Finite Element Model of Weakened Zone Beneath the Arc

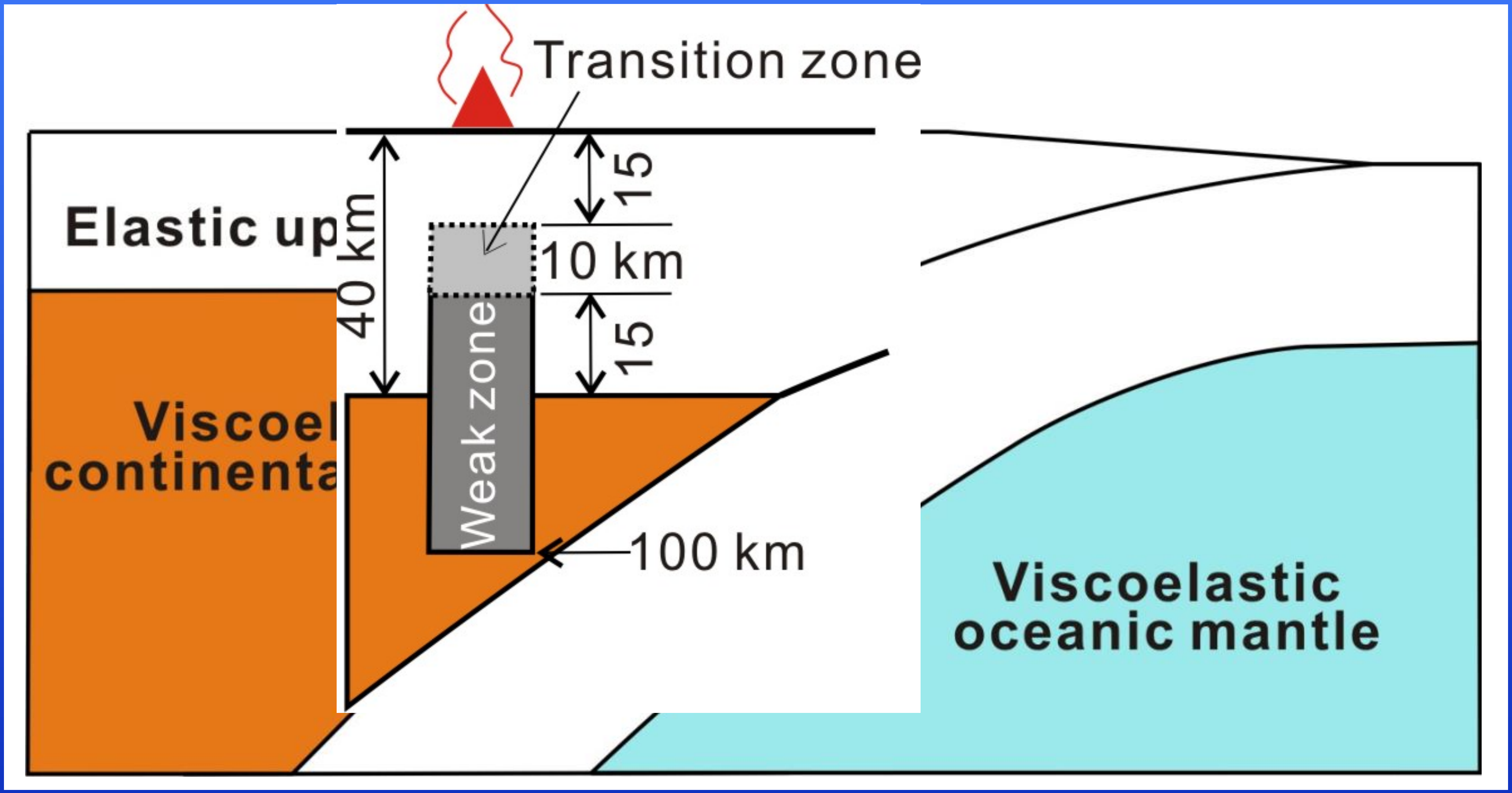

Steady-state viscosity of the weakened zone:

In the transition zone: 10^{23} – 10^{18} Pa s
Weak zone: 10^{18} Pa s

Effects of Weak Sub-arc Zone

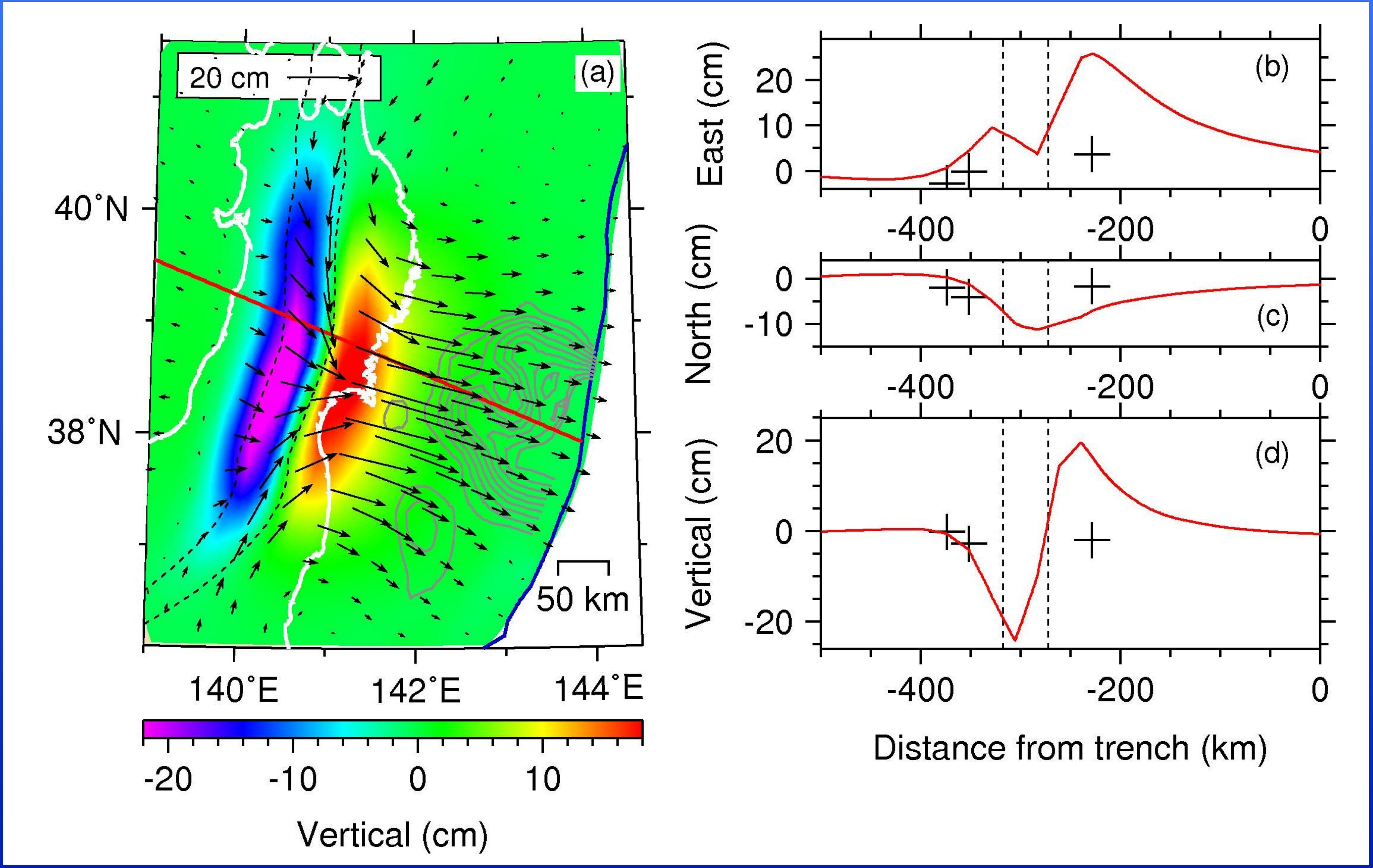

Structure of the Oceanic Mantle

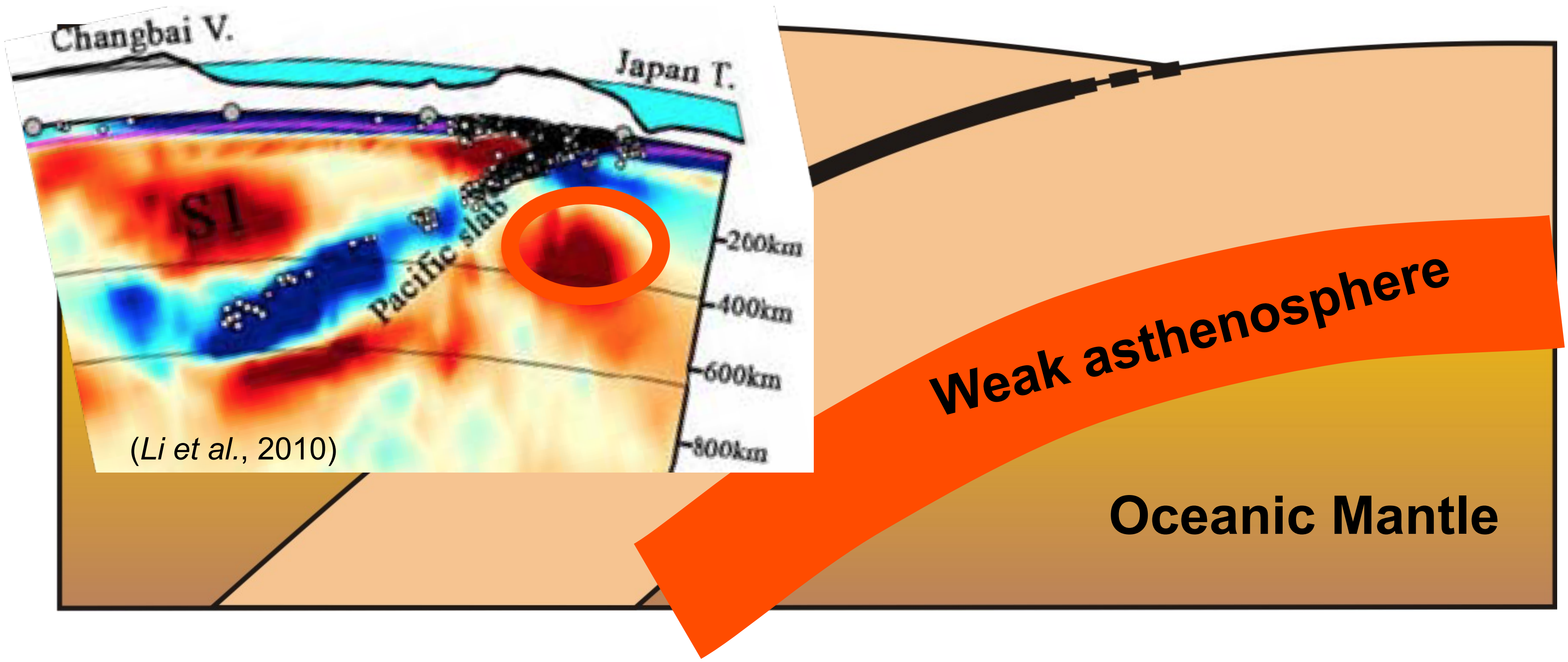

Effects of Weak Asthenosphere

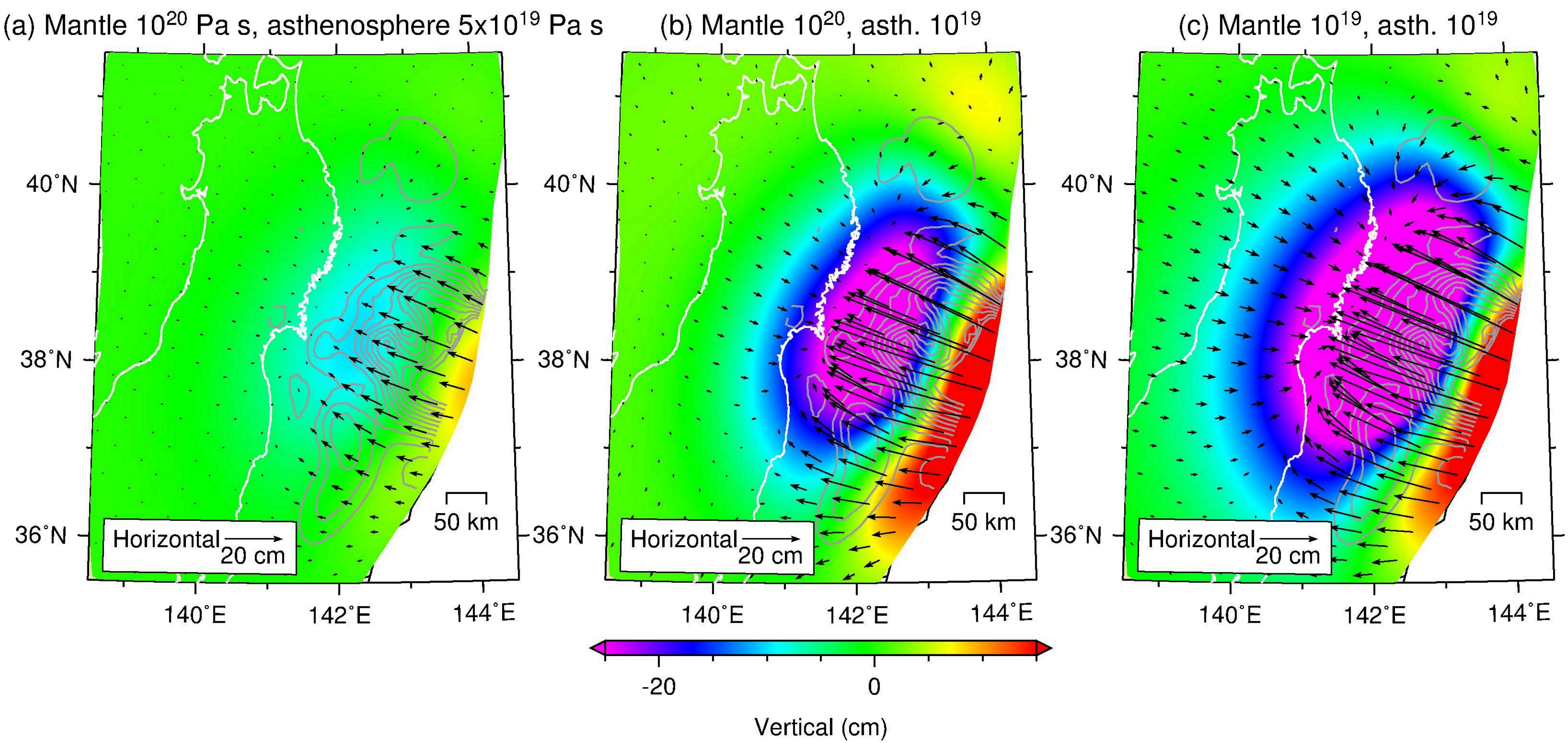

Poroelastic Rebound

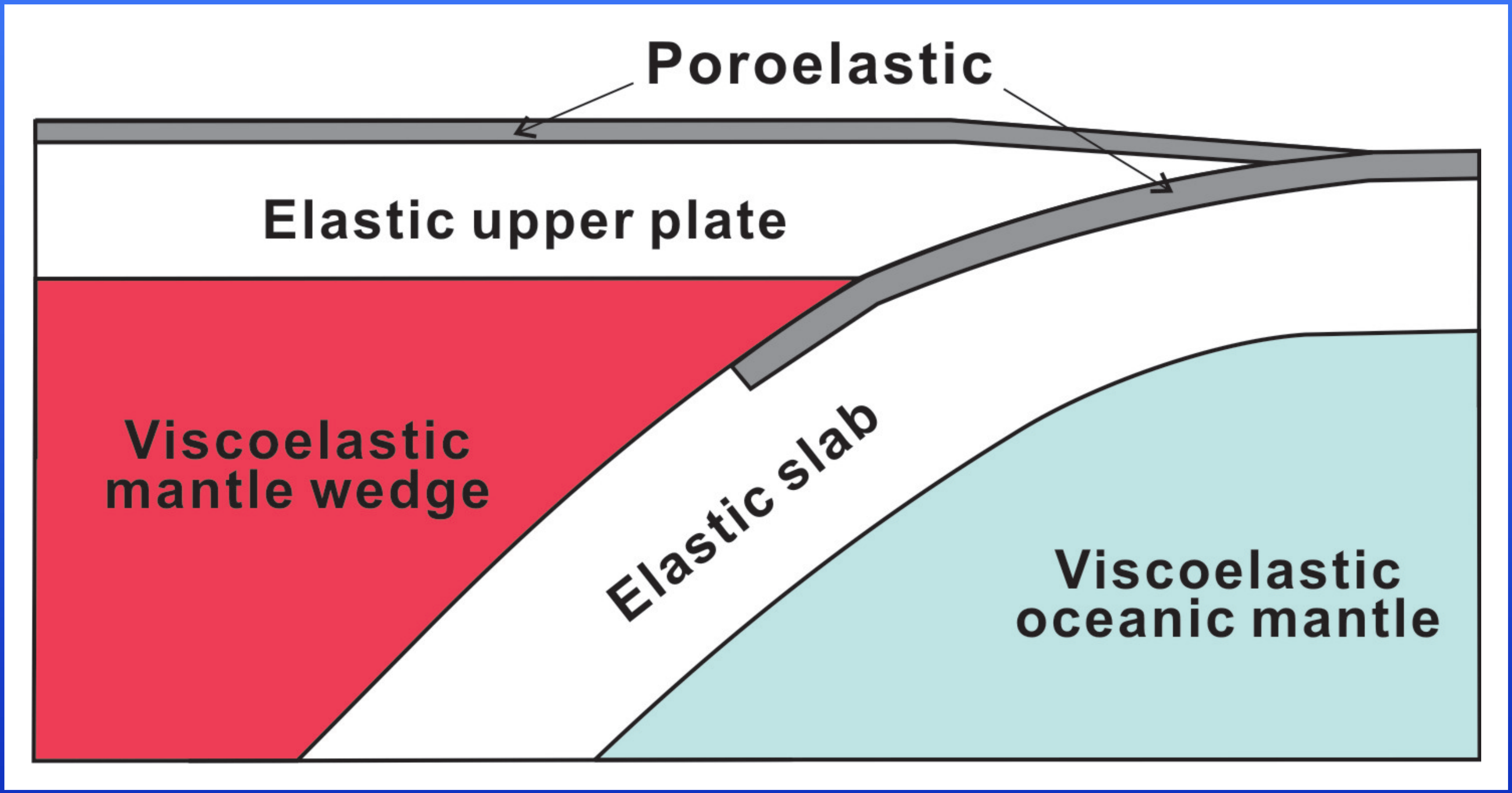

Continental crust:
Shear modulus μ: 15 Gpa
Undrained Poisson's ratio υ_u: 0.34
Drained Poisson's ratio υ: 0.25

Oceanic crust (slab):
μ: 20 Gpa
υ_u: 0.31
υ: 0.25

Poroelastic Rebound

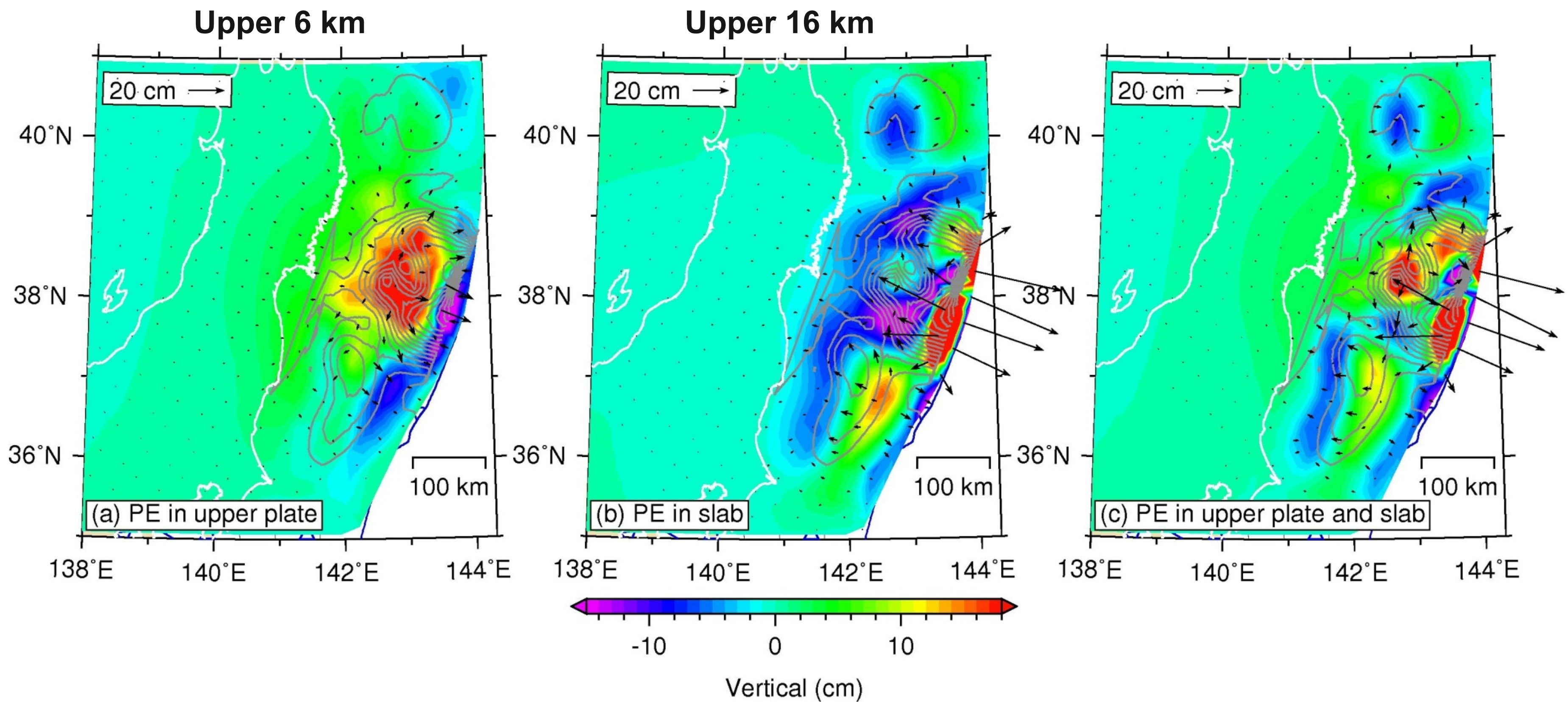

Conclusion

1. Time-dependent, stress-driven afterslip of the fault may be simulated through the viscoelastic relaxation of a weak shear zone attached to the fault.
2. The viscosity of the shallow shear zone (≤50 km) is at orders of 10^{17} Pa s, constrained by the repeating earthquakes. Deeper shear zone has a viscosity of ~10^{18} Pa s.
3. Viscosities of the mantle wedge and oceanic mantle is determined to be 10^{19} Pa s and 10^{20} Pa s, respectively.

Conclusion

4. Contributions of the subducting Philippine Sea plate to the surface deformation is negligible.
5. Weak lower crust beneath the arc improves the fit to GPS observations on land. A weak asthenosphere beneath the oceanic lithosphere produces landward and subsidence motion offshore.
6. Poroelastic rebound in the continental and oceanic crust produces uplift and subsidence in the rupture zone, respectively.

Separating Misfit of Far-field, Land, and Marine GPS

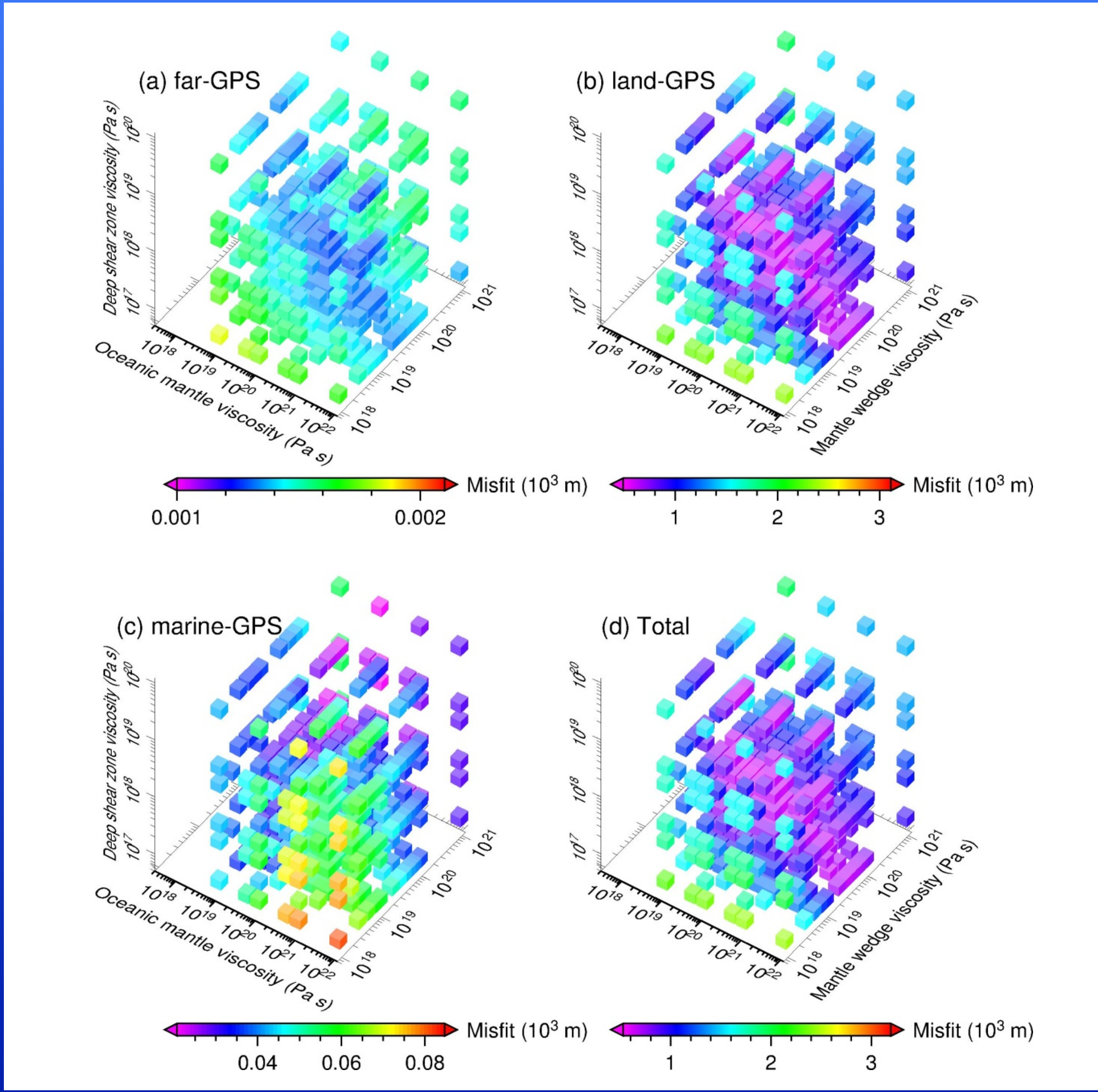

Separating Misfit of Far-field, Land, and Marine GPS

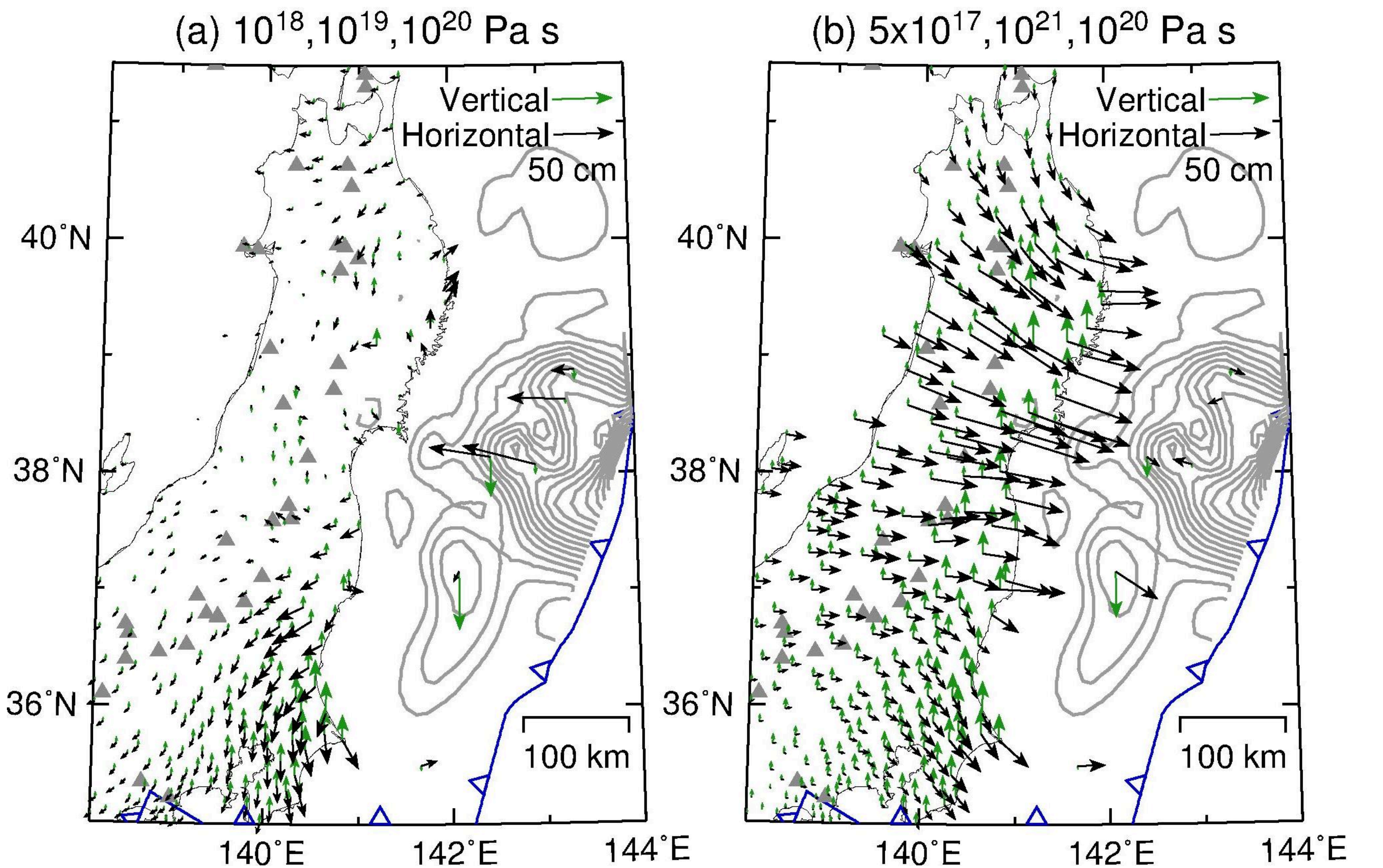

Shallow Shear Zone Viscosities Constrained From Repeating Earthquakes

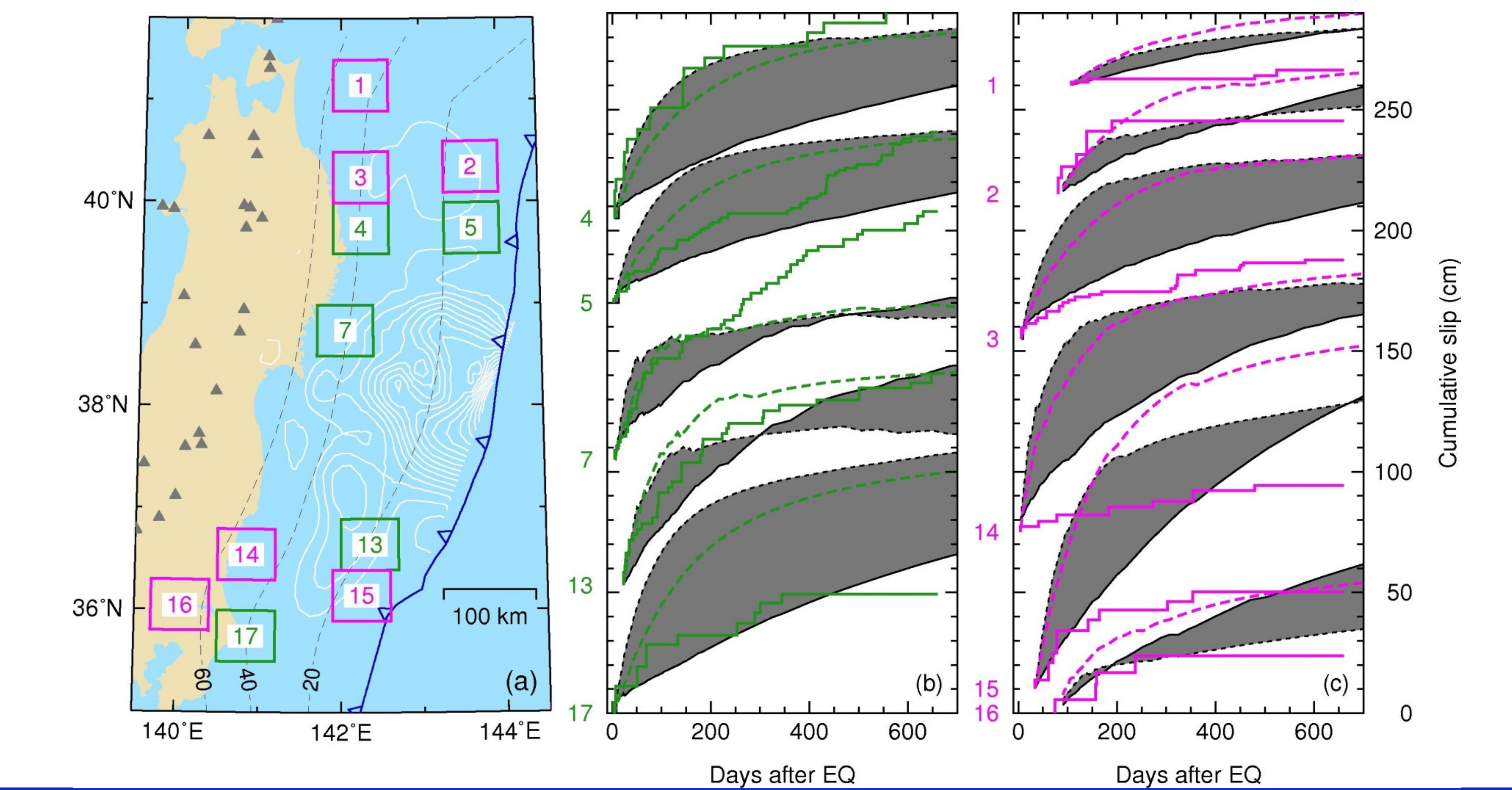

Shallow shear zone (≤50 km):

Steady-state (Maxwell) viscosity: η_M = 10^{17} Pa s (5×10^{16} - 5×10^{17})

Transient (Kelvin) viscosity: η_K = 10^{16} Pa s (5×10^{15} - 5×10^{16})

Giant Earthquakes in Last Century

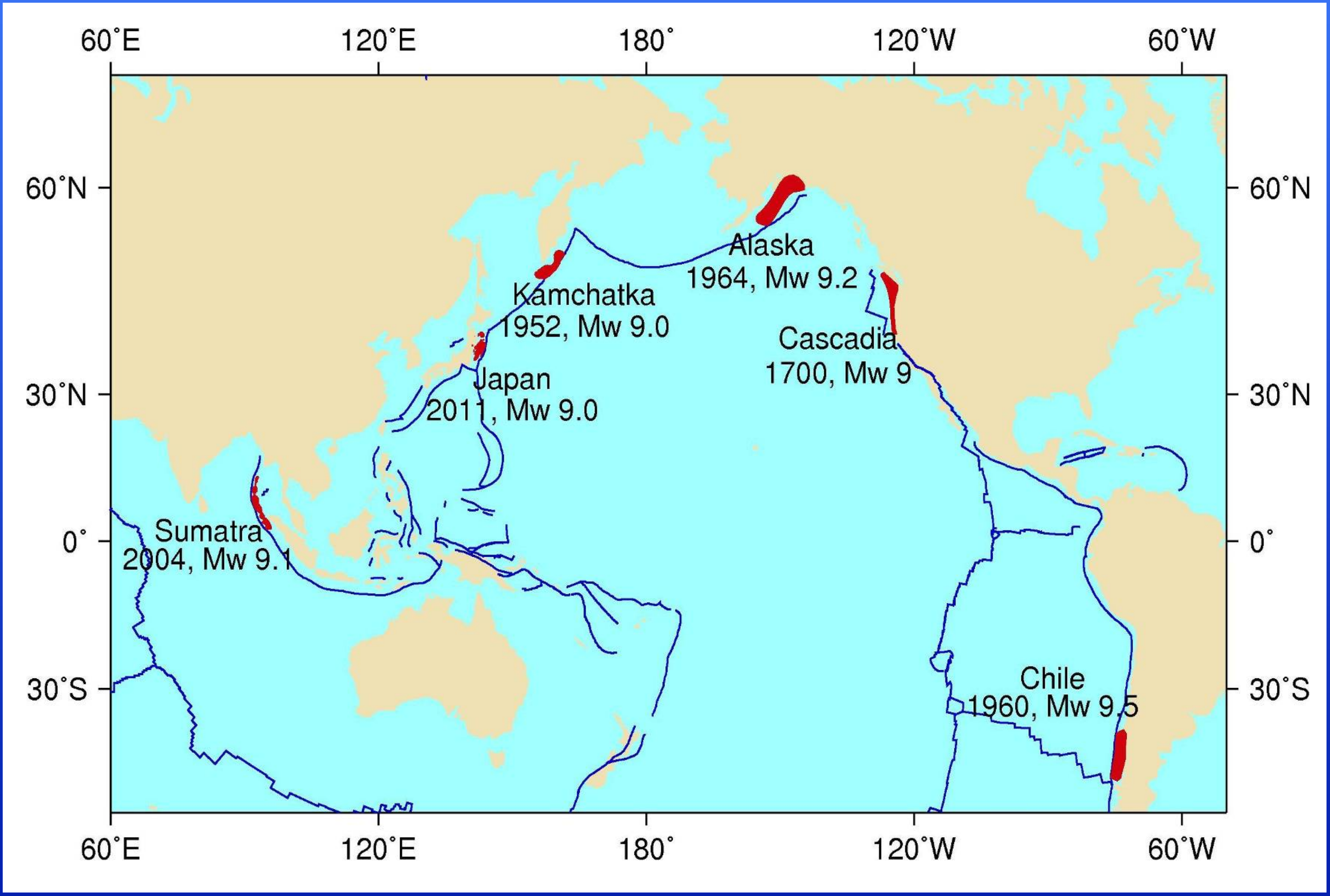

Poroelastic Rebound

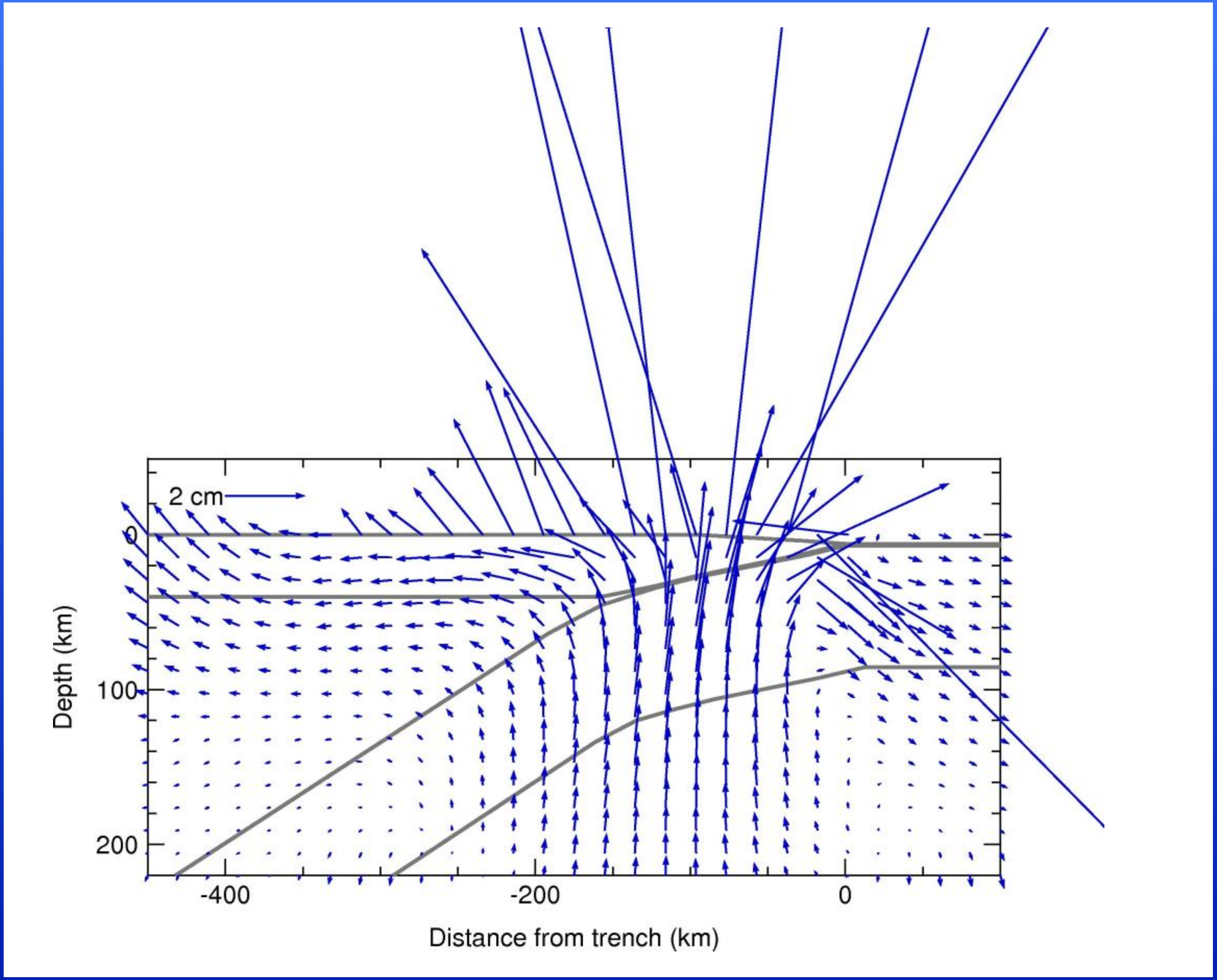

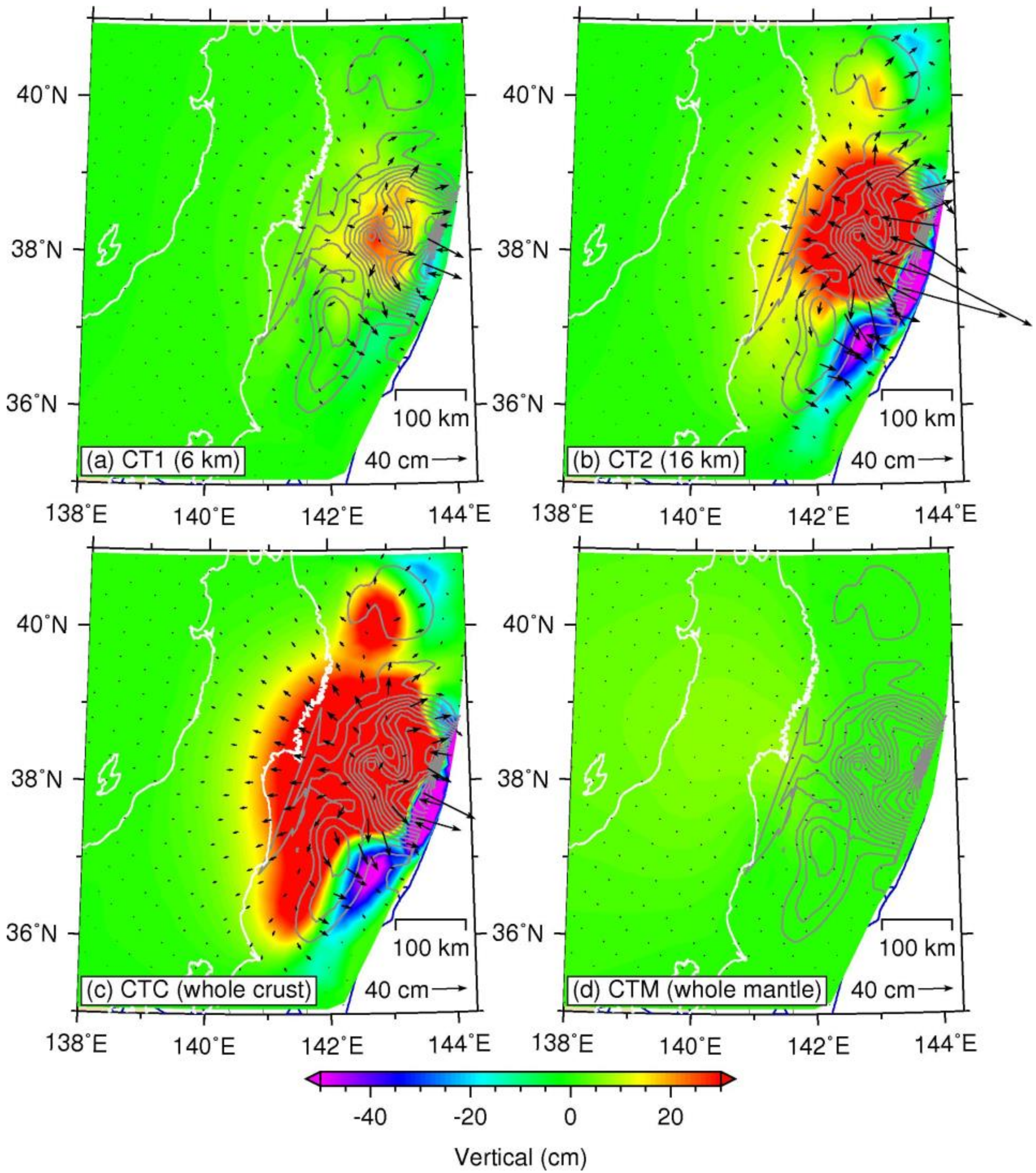

PE at

Continental Side

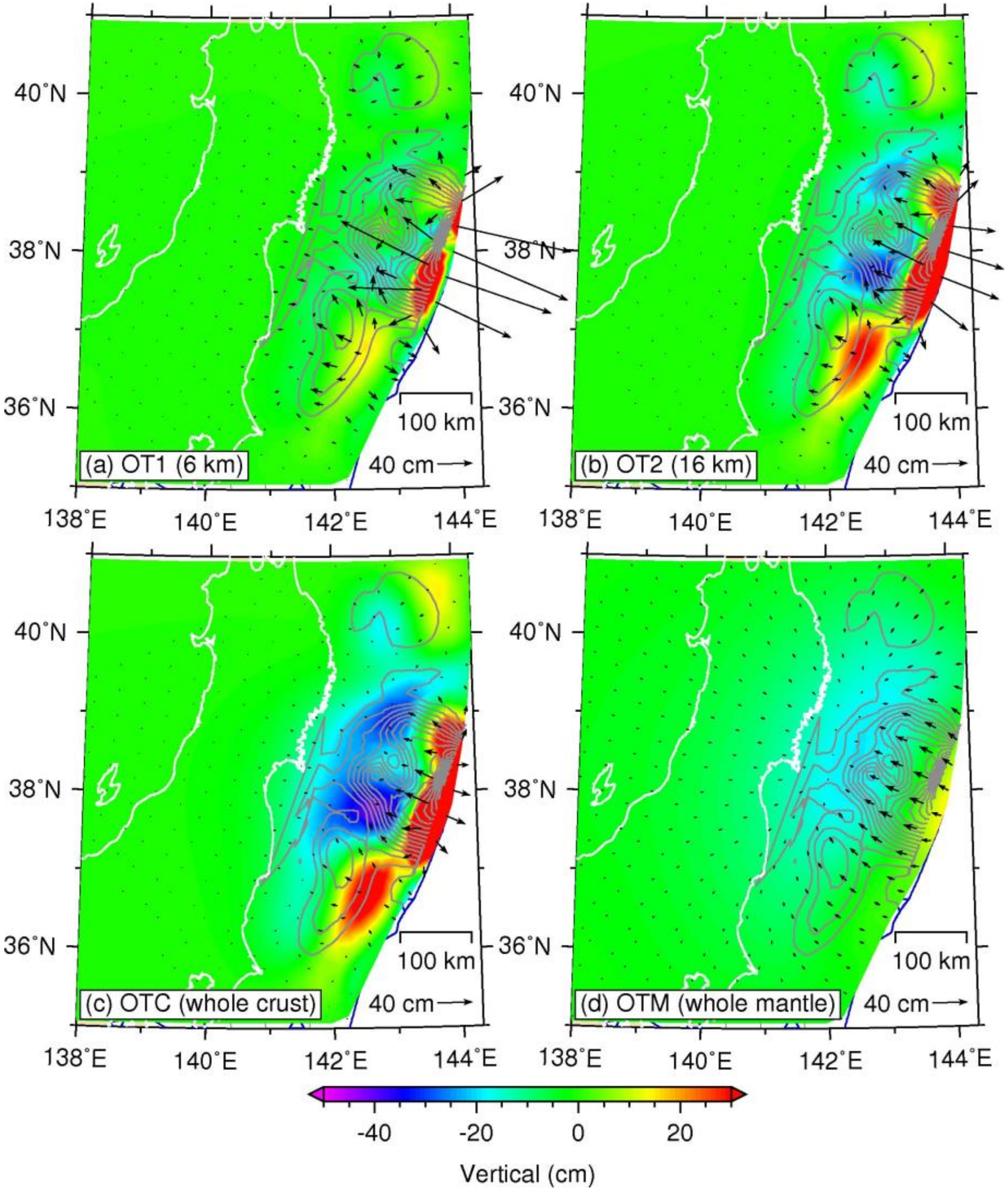

PE at

Oceanic Side

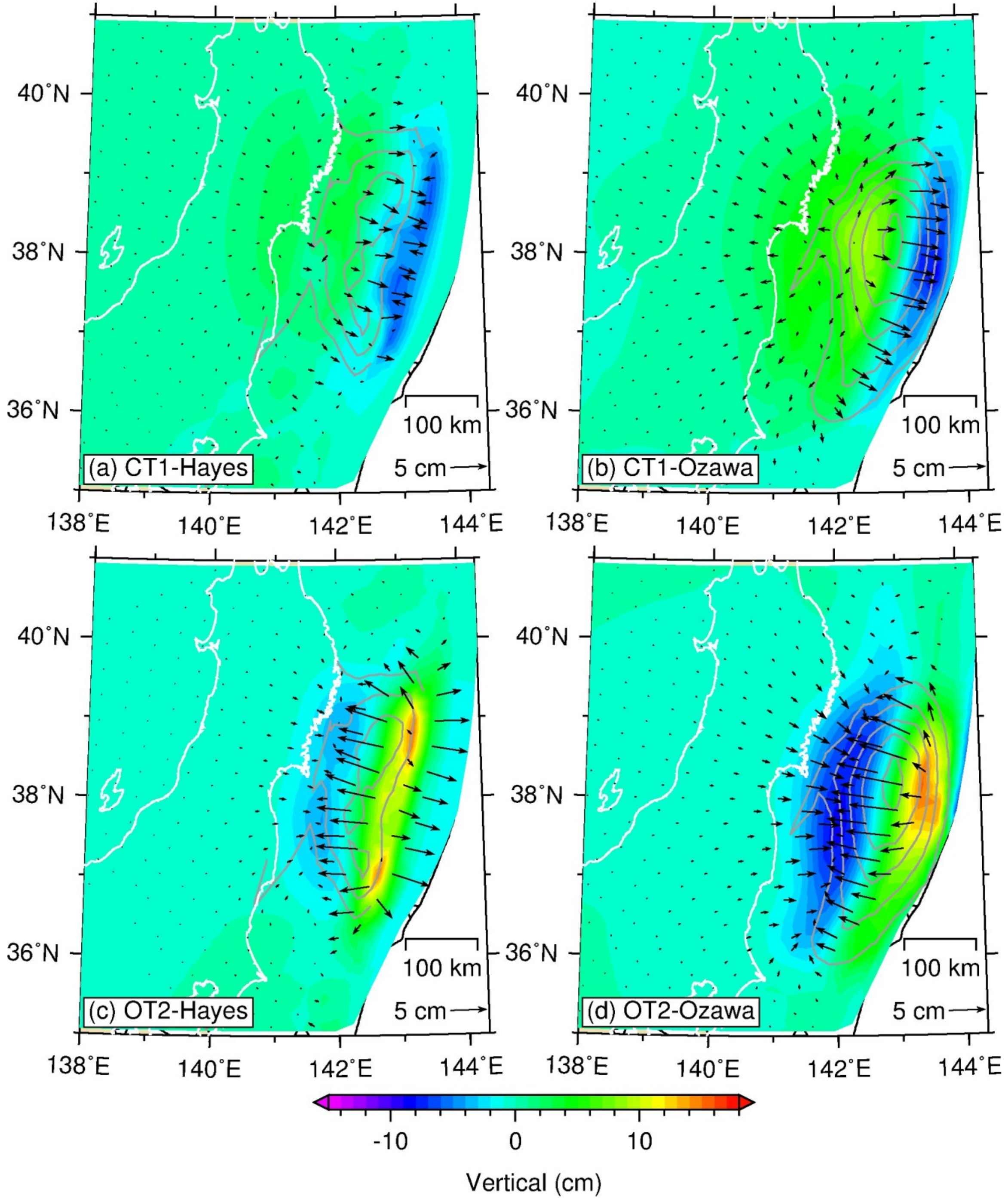

PE in Continental and Oceanic Crust of Different Source Models

Rheology Structure Beneath the Volcanic Arc

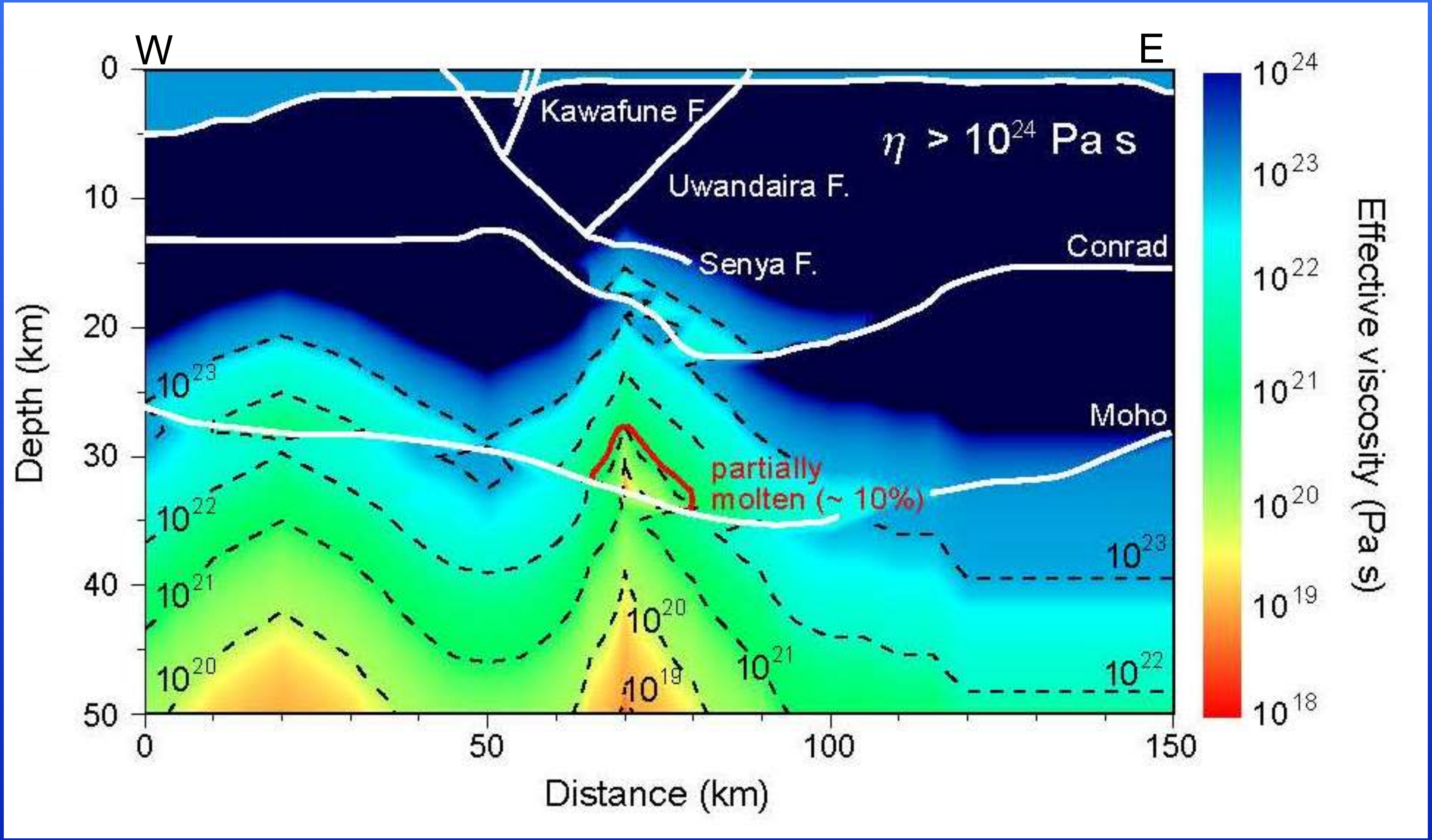

(Muto, 2011; Muto et al., 2013)

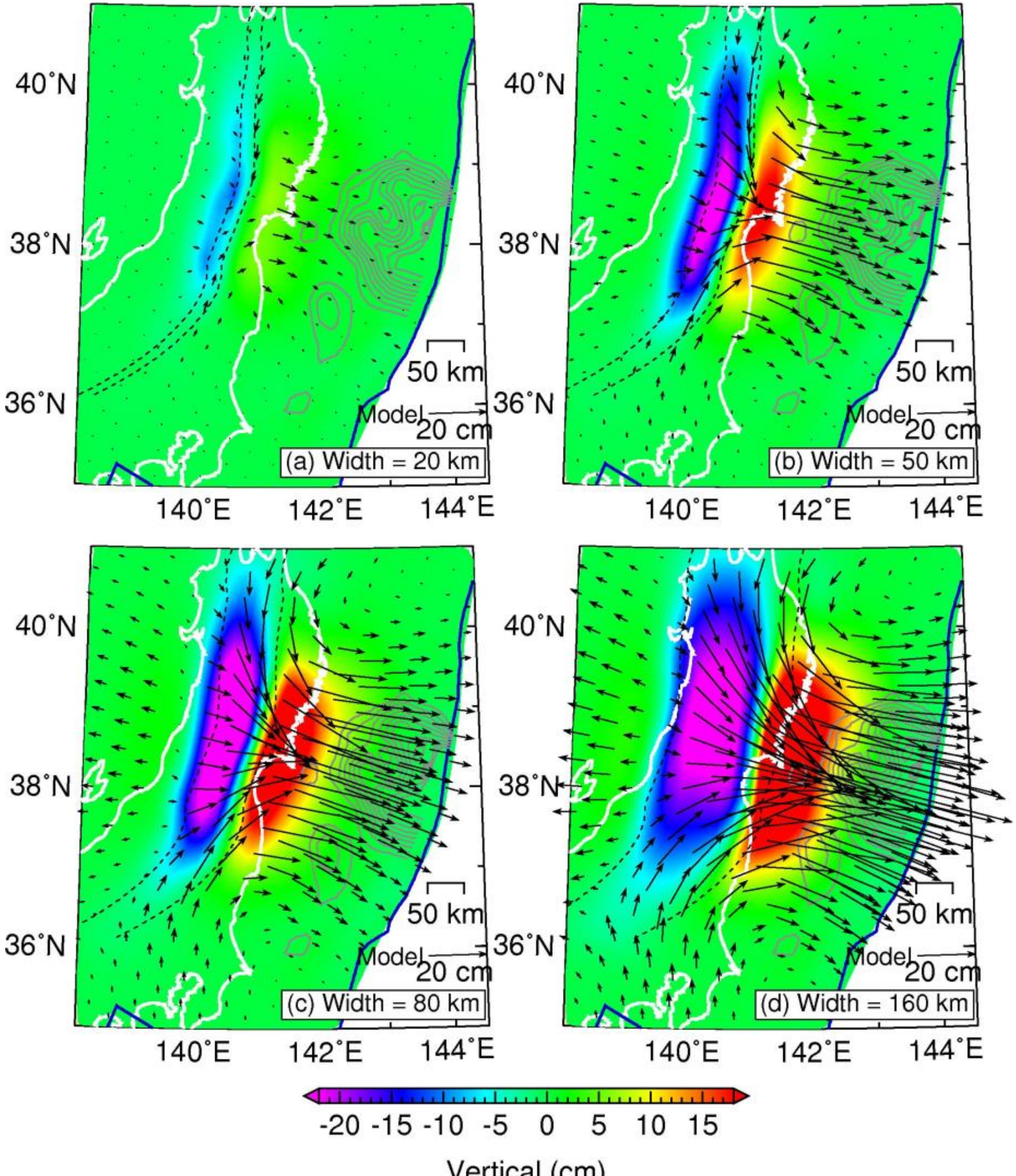

Variation in the plan-view width of the weak zone

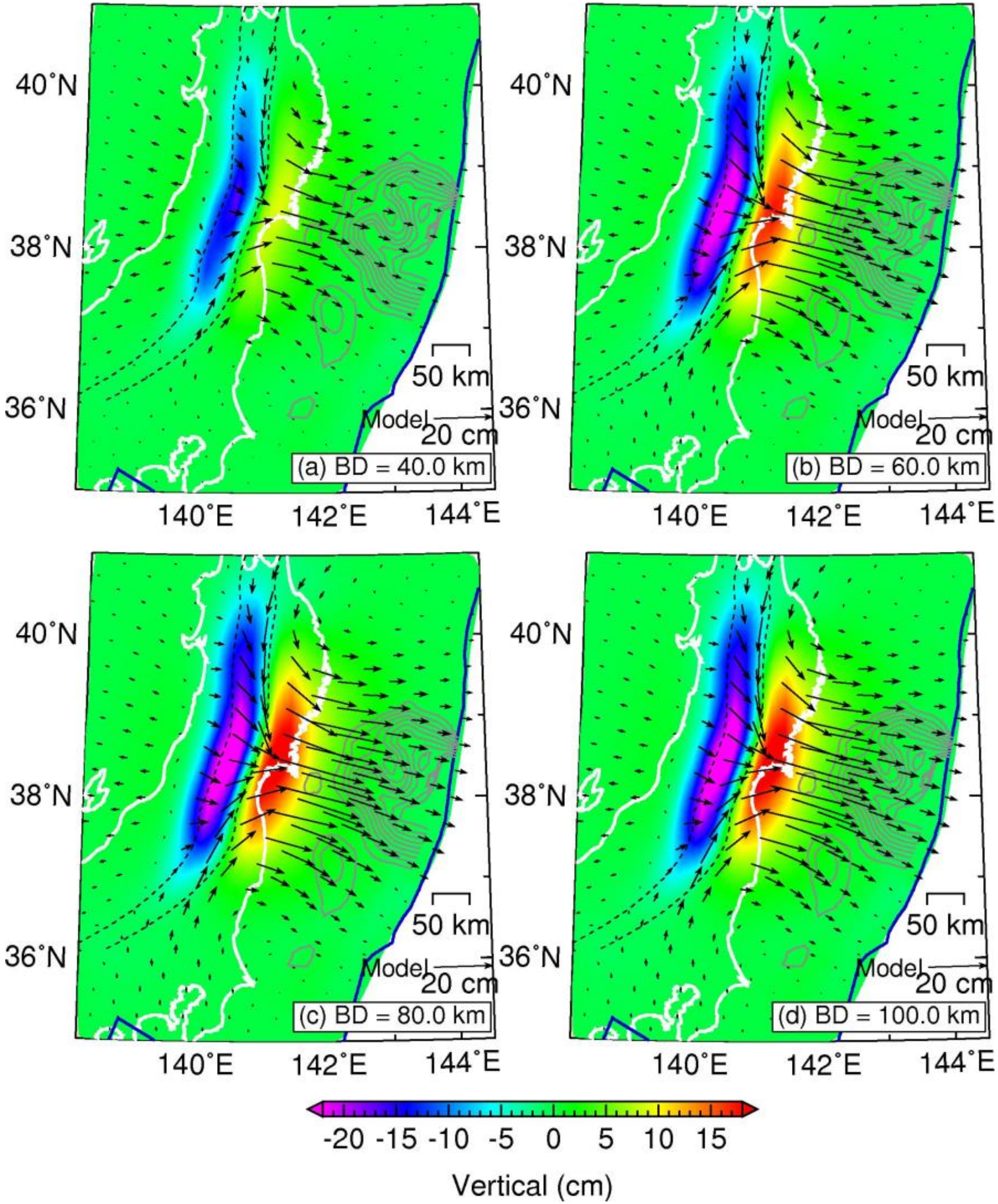

Variation in the bottom depth (BD) of the weak zone

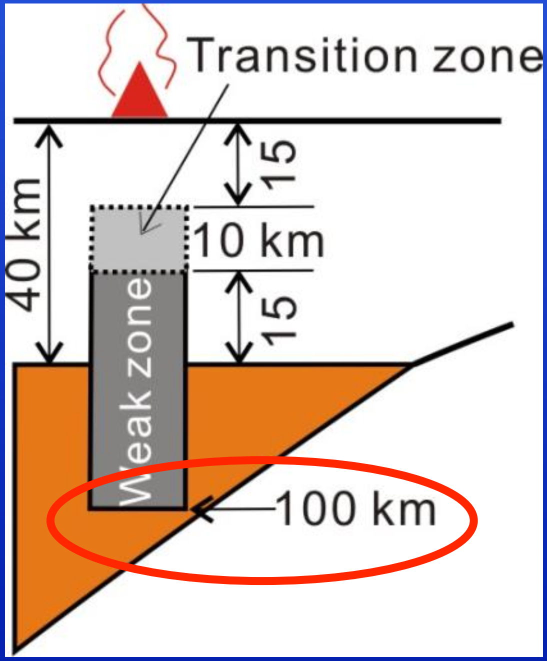

Different Viscosity in the Sub-arc Weak Zone

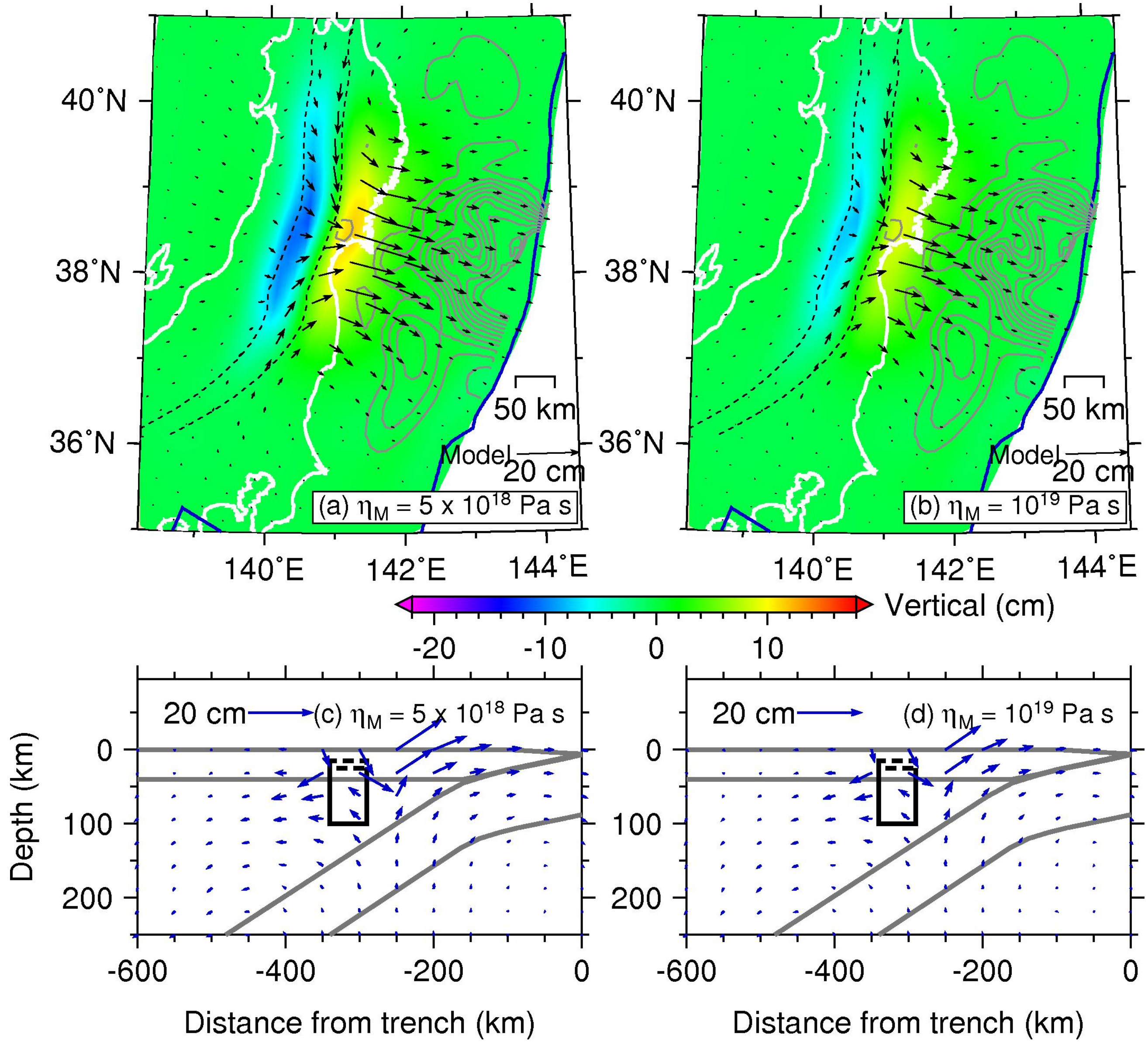

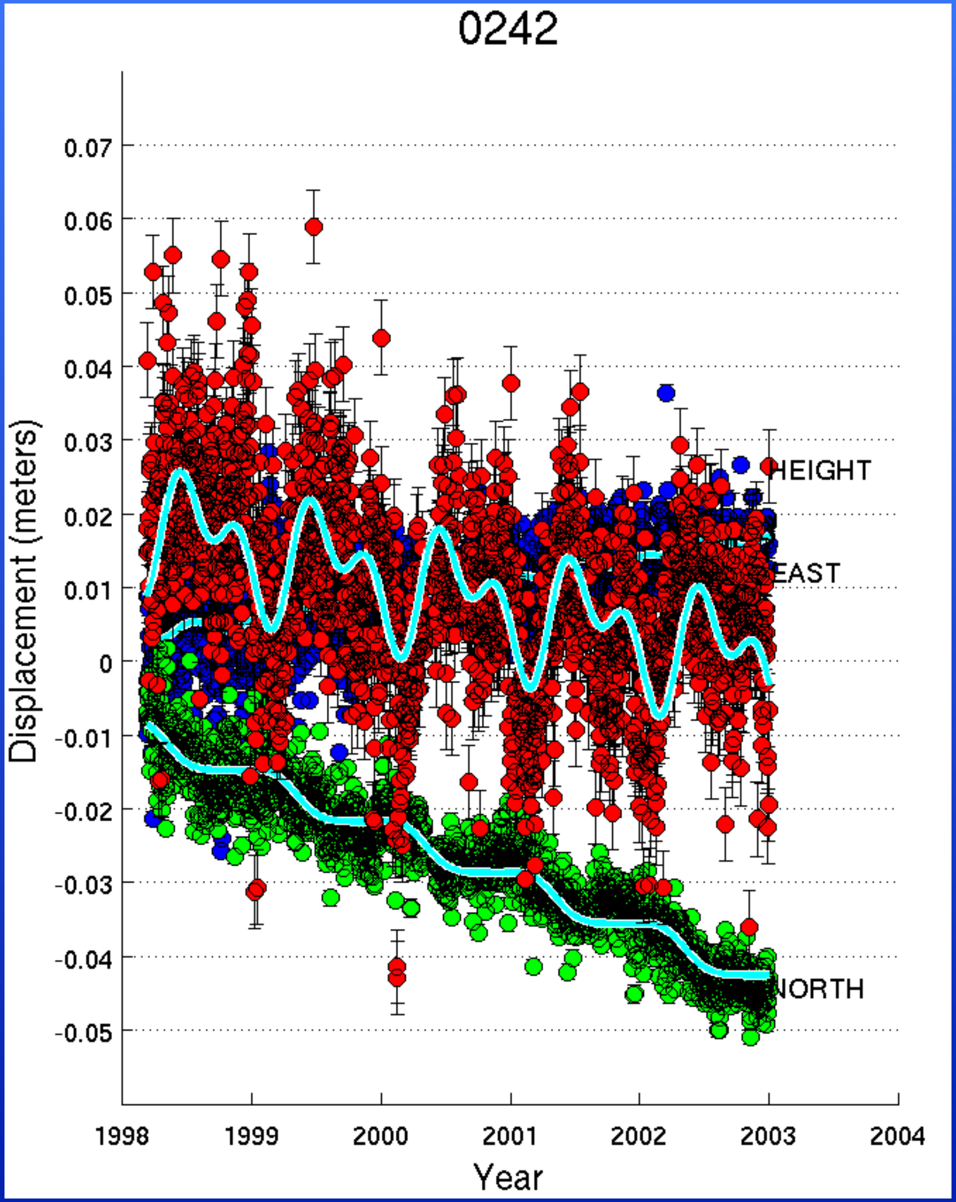

Pre-earthquake linear and seasonal trends

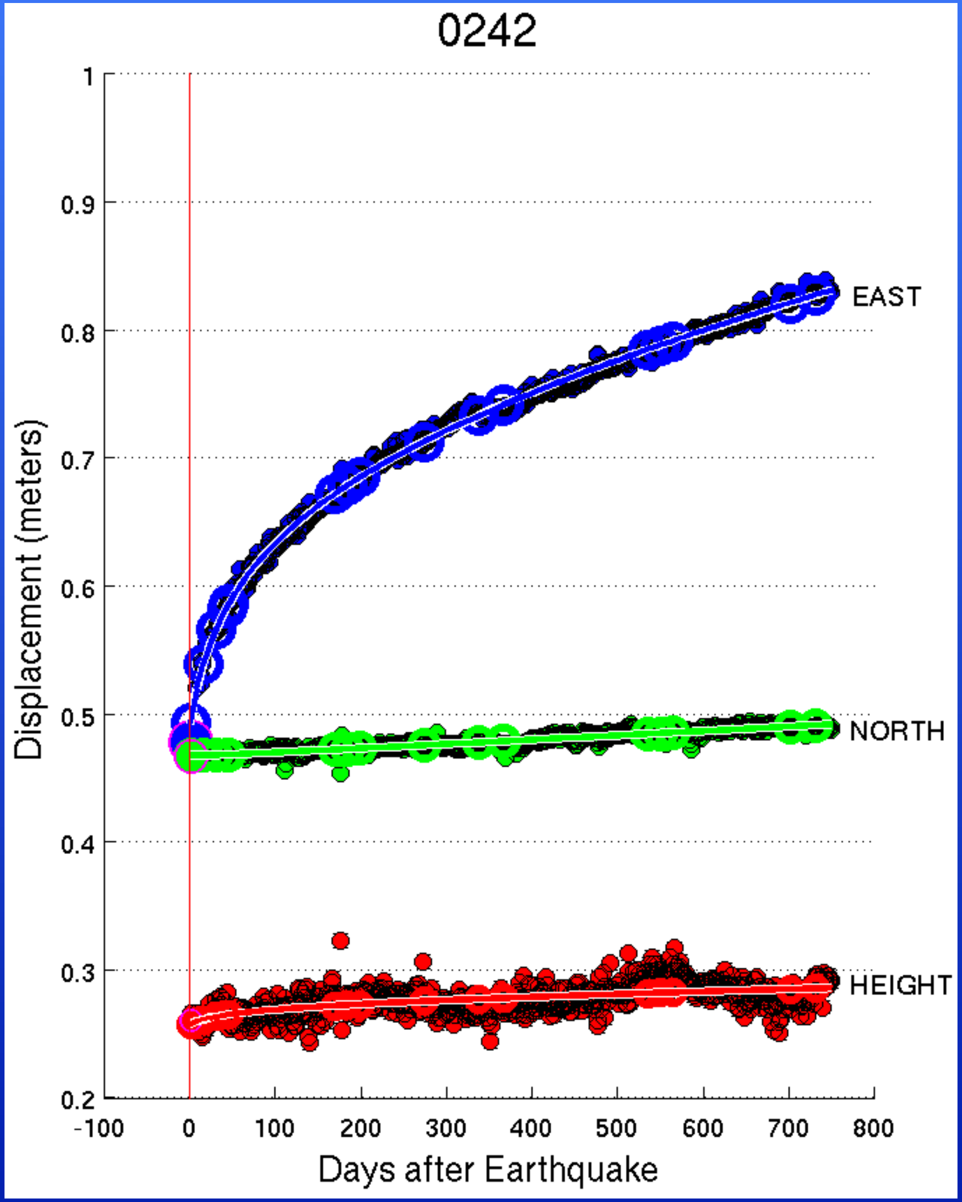

Postseismic deformation corrected for pre-earthquake trends

Cartoon Showing Different Rheologies

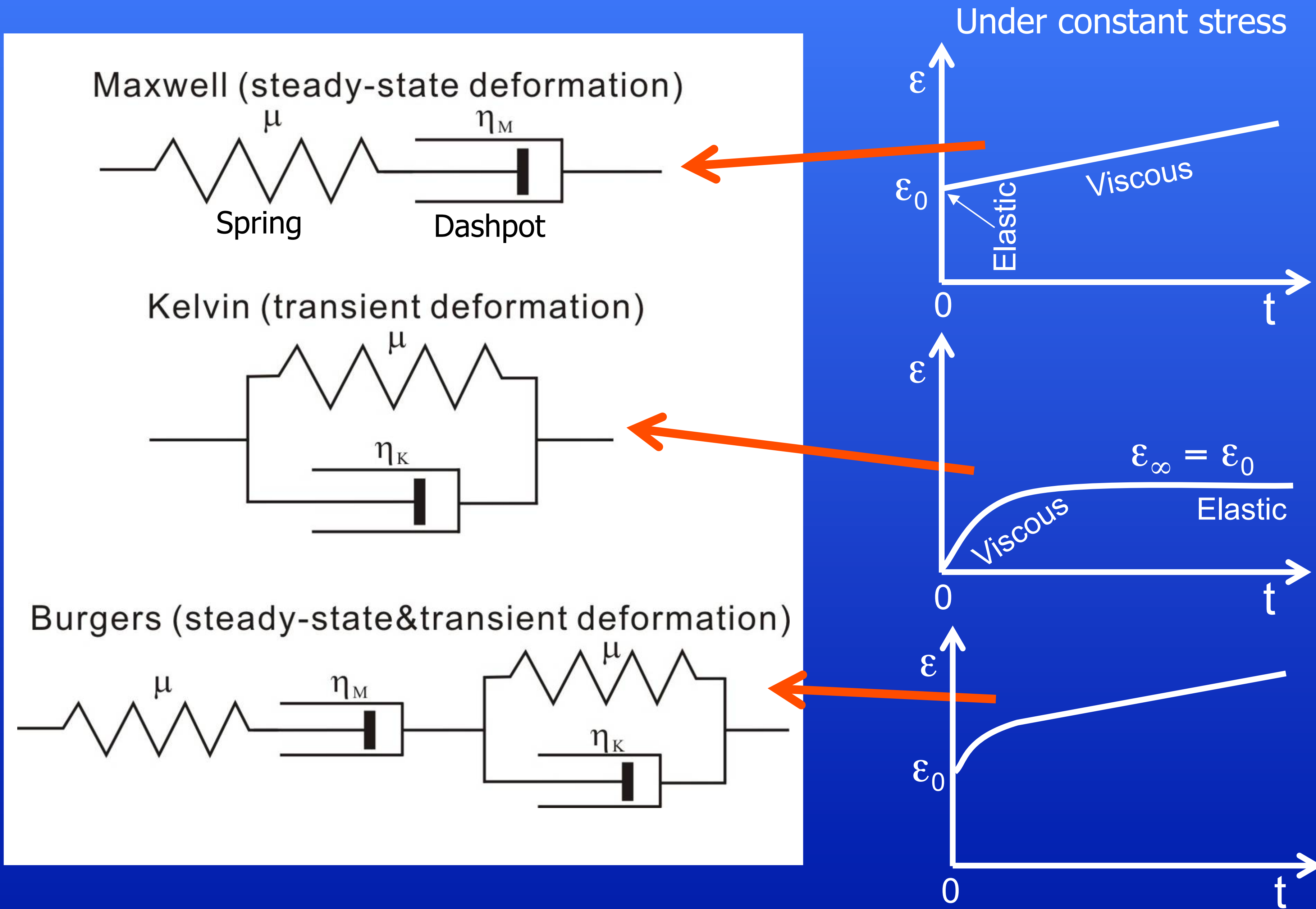

Stress Evolution of the Megathrust

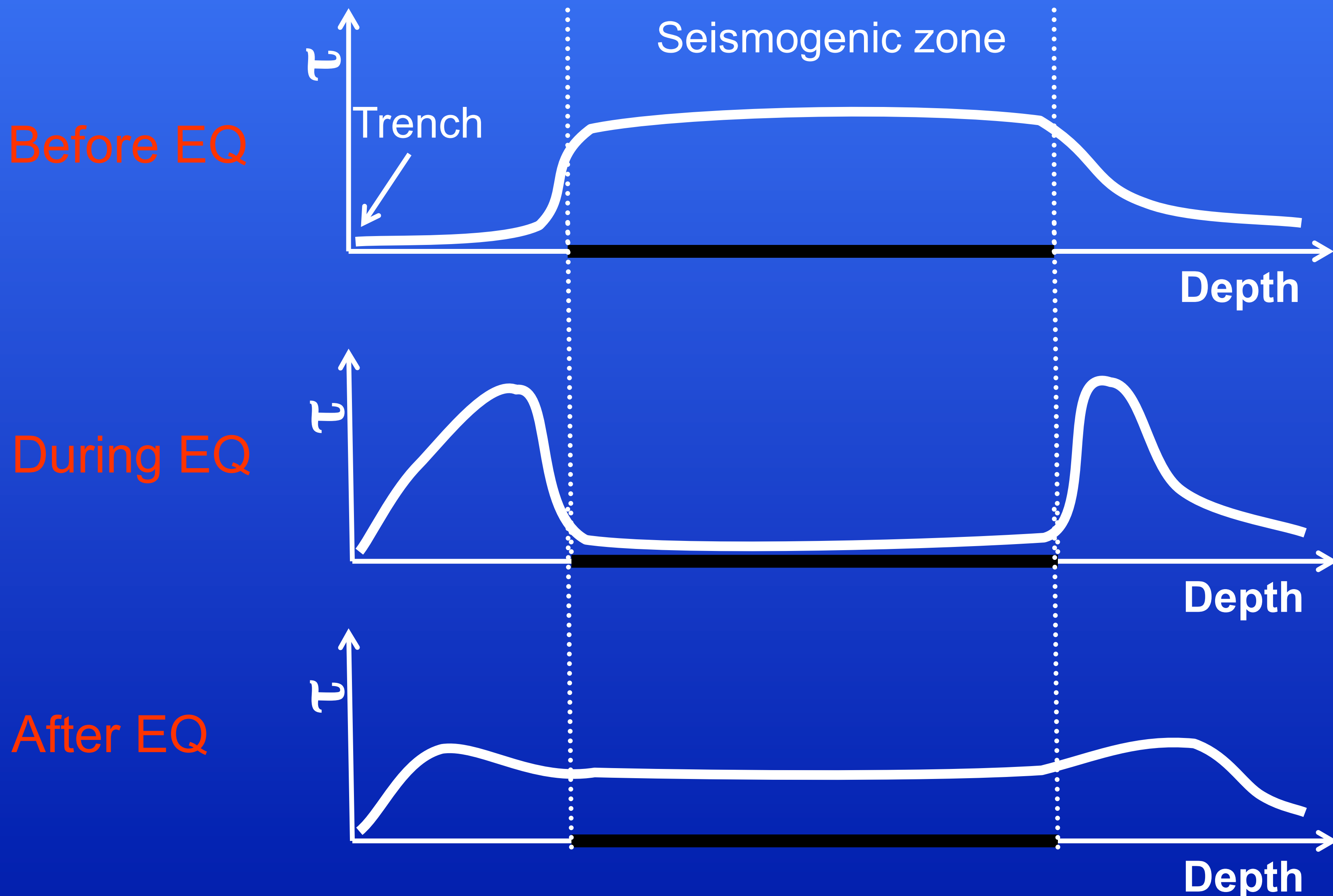

Laboratory-observed Rock Deformation

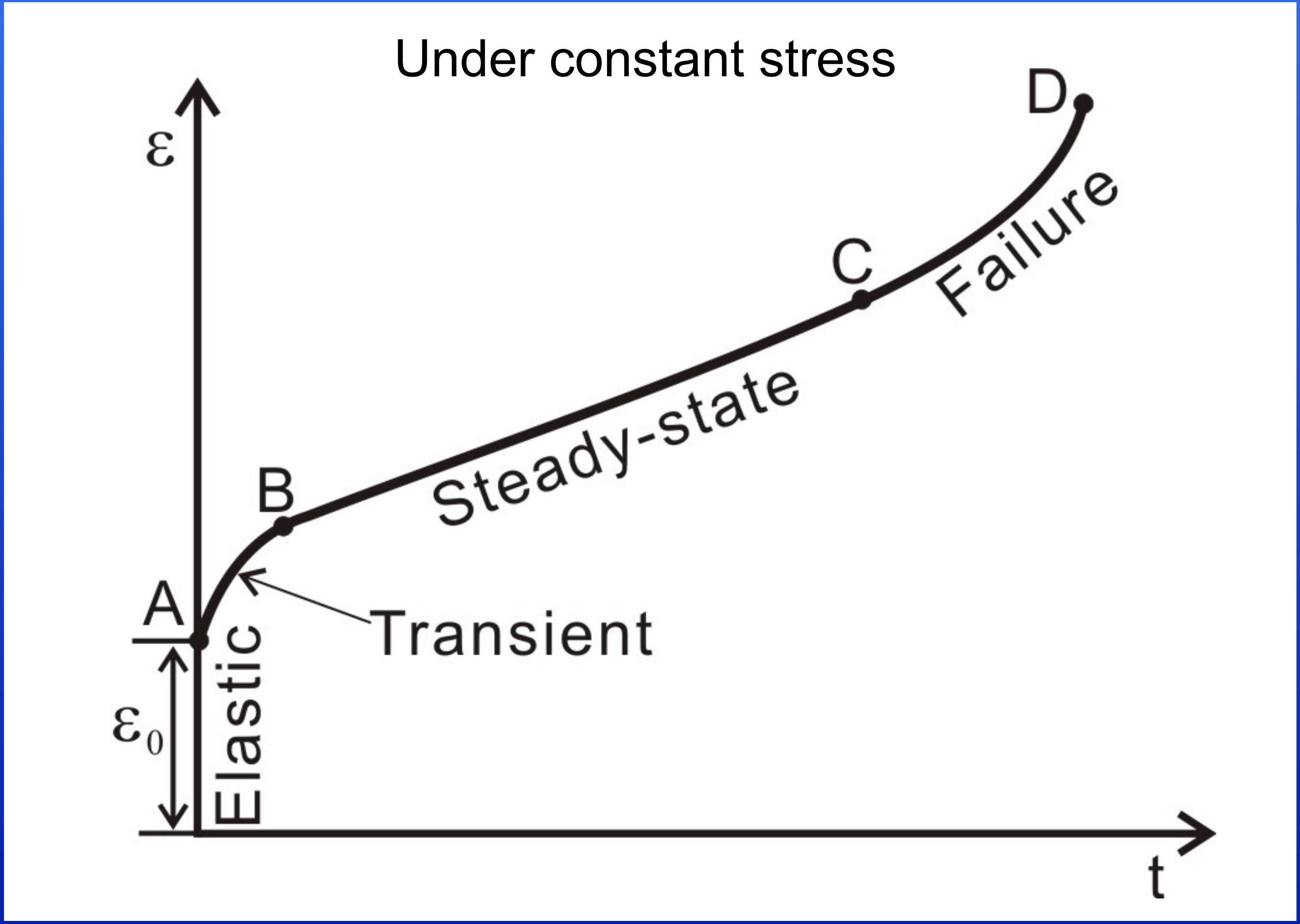

Coseismic Slip Distribution and Assignment of Locking Motion

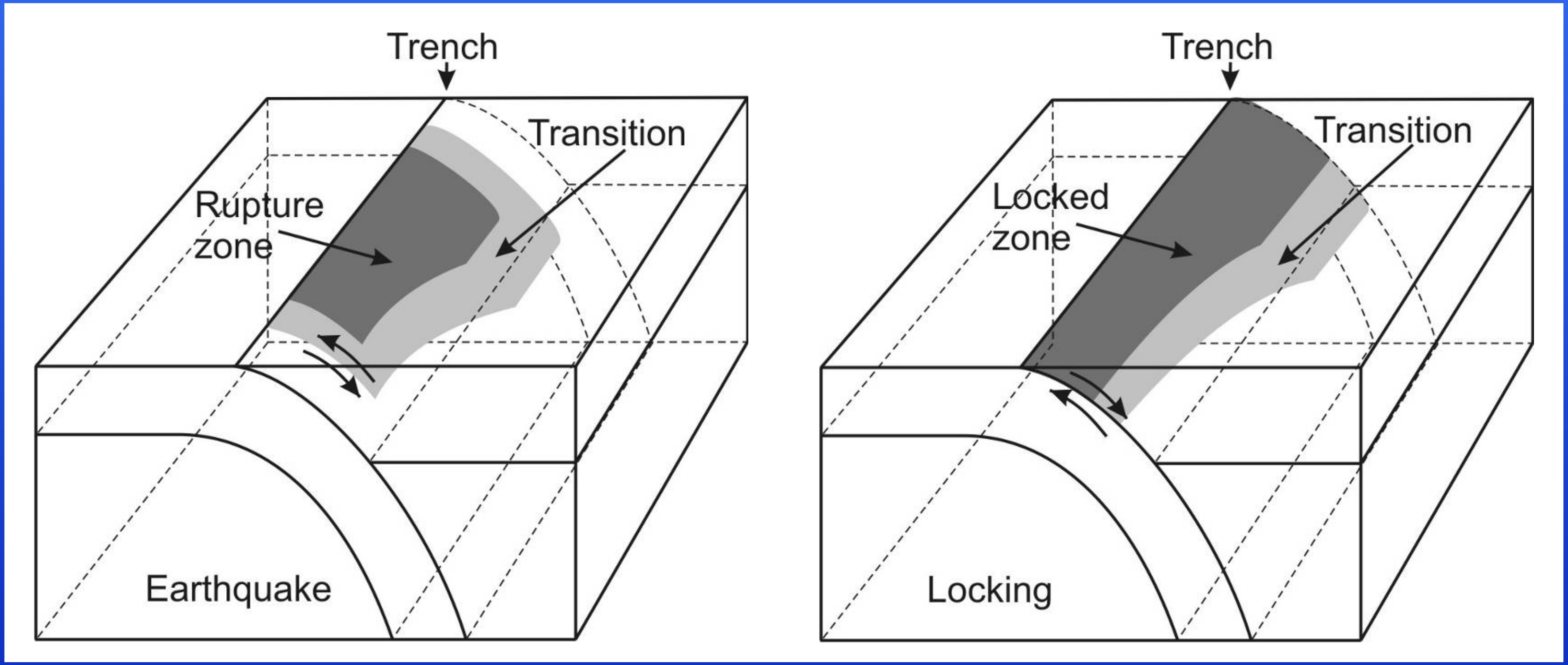

(*Hu et al.*, 2004)